Impact of Demand Response and Battery Energy Storage System on Electricity Markets

by

Haytham Raafat Gamal Ibrahim

A thesis
presented to the University of Waterloo
in fulfillment of the
thesis requirement for the degree of
Master of Applied Science
in
Electrical and Computer Engineering

Waterloo, Ontario, Canada, 2017

AUTHOR'S DECLARATION

I hereby declare that I am the sole author of this thesis. This is a true copy of the thesis, including any required final revisions, as accepted by my examiners.

I understand that my thesis may be made electronically available to the public.

Abstract

The calls for the reduction of carbon dioxide (CO_2) and other greenhouse gases emissions from conventional electricity generation have been dramatically growing in the recent years owing to their negative environmental impact which became evident in climate change. The penetration level of Renewable Energy Sources (RESs) in the electrical power system is promptly increasing as they provide a cleaner and a cheaper solution to generate electricity. The main impediment to the spread of these RESs is that they are not dispatchable due to their intermittent nature. For example, the photovoltaic arrays output depends mainly on the solar insolation level. As for wind generation, the output is primarily affected by the wind blow. Hence, their coincidence with demand is not guaranteed, and this affects system reliability. Distributed Energy Resources (DER), such as Energy Storage Systems (ESSs) and Demand Response (DR) can play a major role to overcome the operational challenges with RESs, especially in the context of Smart Grid (SG).

The main aim of this research is to assess the effect of using DR service and utilizing an existing Battery Energy Storage System (BESS) with the objective of minimizing the costs from the utility point of view. This is carried out by solving a constrained Optimal Power Flow (OPF) problem in three different cases (i.e.: Base Case, DR Case and BESS Case) to get the total incurred costs, conventional generation commitment and Locational Marginal Costs (LMCs) in each case to highlight the impact of DR and BESS on the electricity market.

The results obtained for the IEEE 14-bus system show that either the application of a DR program or the employment of an existing BESS with the objective of cost minimization can be beneficial in terms of reducing the running costs vis-à-vis operating the system with neither.

Acknowledgements

First and foremost, all praises to Allah Almighty for providing me with the opportunity, patience, and guidance to finalize this thesis work and my MASc degree successfully.

I would like to express my deep appreciation and gratitude to my advisors Prof. Magdy Salama and Dr. Mohamed Ahmed for their invaluable guidance, limitless support, and continual encouragement. Throughout my MASc journey, their advice was the key to direct this research on the right path.

Besides, I am grateful to the members of my thesis committee, Dr. Ramadan El-Shatshat and Dr. Tarek Abdel-Galil for sparing the time to review this thesis and their tolerance doing so. Their constructive comments helped me develop the final presentation of this work.

I would also like to acknowledge my colleagues in the Power and Energy Systems Group for their vital discussions and fruitful suggestions.

Furthermore, I would like to extend my cordial gratitude to my beloved parents and siblings for their unconditional support, love, and prayers throughout all my endeavors.

Last but not least, I will always be in debt to my lovely wife, Hoda, for her support, patience, understanding, and belief. She has always been there to uplift me when I felt down. Thanks to my beautiful daughters, Aasiyah and Aaminah, who are the source of my inspiration and strength.

Dedication

To my parents

To my siblings, Amr, Tamer, Rana and Radwa

To my beloved wife, Hoda

To my beautiful daughters, Aasiyah and Aaminah

Table of Contents

List of Figures

List of Tables

Chapter 1
Introduction

1.1 Preface

There are growing calls to reduce carbon dioxide (CO_2) and other greenhouse gases emissions and the dependence on fossil fuels to generate electricity because of their negative environmental impact. In this context, the renewable energy sources (RESs) have highly penetrated the electrical power system as they provide a cleaner and a cheaper solution for electricity generation. However, the integration of these sources into the grid faces a serious challenge which is their stochastic nature. Owing to this intermittent nature, RESs fail to be dispatchable. This increases the uncertainty in supply, especially with the recent high share of renewables in the grid. Also, it results in different power quality issues. Moreover, uncertainty is a characteristic of the system demand by nature. Several means received interest from researchers and were introduced in the literature to handle these problems, namely Demand Side Management (DSM) and Energy Storage Systems (ESSs) which tackle uncertainty from the load side and the supply side respectively to ensure the demand/supply balance [1-8].

One of the main categories of DSM is Demand Response (DR) which can be defined as "The changes in electric usage by end-use customers from their normal consumption patterns in response to changes in the price of electricity over time." Further, DR is defined as "The incentive payments designed to induce lower electricity use at times of high wholesale market prices or when system reliability is jeopardized" [7].

Energy Storage Systems (ESSs) store the electrical energy in another form of energy during low system demand and low generation cost and share the grid load during high system demand and high generation cost (or if no enough generation is available). The electrical energy can be stored in different forms [1-5]:

- As gravitational potential energy with water reservoirs.
- As compressed air.
- As electrochemical energy in batteries and flow batteries.
- As chemical energy in fuel cells.
- As kinetic energy in flywheels.

- As magnetic energy in inductors.
- As electric field in capacitors.

1.2 Motivation

With the output power fluctuations of the solar systems and wind turbines, planning and operational grid problems emerge. Also, some economic concerns might rise such as unit commitment, electricity market settlement, and spinning reserves [9]. One of the means of mitigating for this unpredictability of solar and wind powers is the Demand Response in which the system load is added as an additional degree of freedom. One other way is the Energy Storage Systems (ESSs) widely spread over the grid.

So, applying a DR program or utilizing an existing ESS with the objective of cost minimization will have an influence on the total running costs incurred by the utility as it primarily changes the commitment of the conventional generators. Furthermore, it will have an impact on the electricity prices because of the variation in the costs.

To analyze this effect, three different constrained Optimal Power Flow problems are formulated:

1. Base Case Problem: The system is the IEEE 14-bus system with a solar system and a wind farm.
2. DR Case Problem: The same system of the Base Case with a DR program in which participating customers receive bill credit (incentives) from the utility.
3. BESS Case Problem: The same system of the Base Case with a Battery Energy Storage System (BESS) installed with the solar system.

Three test case are studied, each represents one of the three problems, and the results are compared in order to highlight the impact DR and BESS on utility costs.

1.3 Research Objectives

This research focuses on assessing the influence of applying a DR program or employing an existing BESS with the cost minimization objective on the total costs, conventional generation commitment, and electricity prices. The objectives of this research are as follows:

- Develop mathematical models that represent the stochastic nature of solar and wind powers along with system demand and obtain the profiles of four typical days, each representing a season.

- Formulate three different constrained OPF problems for the three cases mentioned in section 1.2 and obtain the solution for the three test cases.
- Examine the impact of DR and BESS by comparing the results of the three test cases.

1.4 Thesis Outline

The thesis is organized as follows: Chapter-2 discusses the literature review on Optimal Power Flow and its applications, Demand Response programs, and Energy Storage Systems and applications in power system operation.

Chapter-3 presents the modeling of Renewable Energy Sources (RESs) and system demand in which their mathematical models are developed by processing available historical data and fitting them to a Cumulative Distribution Function (CDF). The most probable (expected) values are then obtained by applying a Monte Carlo Simulation (MCS). The profiles of the solar and wind powers in addition to the system demand are obtained.

Chapter-4 presents the formulation of the OPF problem for the three different cases. The objective functions along with their constraints are developed. The expected values obtained in Chapter-3 are used as an input to the OPF model. The models are solved in GAMS environment. The solutions are compared in terms of total costs, conventional generation commitment, and Locational Marginal Costs (LMCs) to show the impact of DR and BESS.

Finally, the thesis summary, conclusions, and suggested future work are presented in Chapter-5.

Chapter 2
Literature Review

2.1 Introduction

The need for renewable energy sources (RESs) has dramatically grown in recent years in order to maintain the environment. This led to the transition to higher fractions of renewable energy generation in current electricity grids. These RESs, however, face an undisputable constraint which is their intermittent availability. This feature presents a great challenge to maintaining energy generations and load balance. Hence, and to overcome this obstacle, researchers paid great attention to search for viable solutions including Energy Storage Systems (ESSs), interconnection with external grids, load shifting through Demand Side Management (DSM) ...etc.

This chapter is divided into three sections. In Section 2.2, the main differences between the Optimal Power Flow (OPF) problem and the classical Economic Load Dispatch (ELD) one are discussed to highlight the superiority of OPF. Some power system applications of OPF are also introduced.

Section 2.3 presents literature review about the definition of Demand Response (DR) as a main category of DSM. The classification of DR programs is also debated along with the basic features of each program. Finally, Section 2.4 introduces the different technologies and applications of ESSs found in the literature. Layouts of the proposed technologies are also illustrated.

2.2 Optimal Power Flow and Applications in Power System

2.2.1 General

Basically, the Economic Load Dispatch (ELD) solution assumes that both supply and demand are aggregated at one node for the entire system. In practice, power flow does not follow such a simple constraint, yet, it is determined by the physical laws of electricity (power flow equations). Also, reactive power generation and demand are ignored, and bus voltages are not considered. Furthermore, the representation of transmission line losses is neglected or approximated. All these deficits are tackled in Optimal Power Flow (OPF), where the demand-supply balance equations are represented by the power flow equations. Hence, the solution yields a set of generation variables that optimize the

objective function while satisfying the physical laws of the flow of electricity. The main features of OPF are:

- The losses representation is exact because of the introduction of system topology and bus-wise demand balance.
- The problem can be formulated with many operating constraints to be satisfied like power flow equations, bus voltage limits, active and reactive power generation limits, transmission line thermal limits, and bounds on bus voltage angles.
- The adjustable variables and controls are numerous like real and reactive power generation, switched capacitors settings, load active and reactive power curtailment, and transformer tap settings.
- Different objective functions can be optimized such as the cost of operation, active power losses, cost of load curtailment, and emissions.

The OPF is a constrained nonlinear optimization problem which can be solved by forming a synthetic function (the Lagrangian) as stated in equation (2.1).

$$F = \sum_{i=1}^{NG} C_i(P_i) + \sum_{i=1}^{N} \lambda_i \left(PD_i - P_i - \sum_j |V_i||V_j|Y_{i,j} \cos\left(\theta_{i,j} + \delta_j - \delta_i\right) \right) + \sum_{i=1}^{N} \gamma_i \left(QD_i - Q_i + \sum_j |V_i||V_j|Y_{i,j} \sin(\theta_{i,j} + \delta_j - \delta_i) \right) \quad (2.1)$$

Where: $\sum_{i=1}^{NG} C_i(P_i)$ is the objective function, PD_i and QD_i are the active and reactive power demands at bus i respectively, P_i and Q_i are the active and reactive power generations at bus i respectively, and λ_i and γ_i are the active and reactive power lagrangian multipliers (dual). The dual λ_i represent the marginal cost of active power supply at a bus or the Locational Marginal Costs (LMCs).

2.2.2 OPF Applications[1]

1. Minimum Cost Operation: this is the most popular application in which the active power commitments of thermal units that satisfy the power flow and other constraints are obtained.

[1] Bhattacharya, K. (2017). *Module 2: Optimal Power Flow* [PowerPoint slides]. Retrieved from University of Waterloo Power System Operation.
Learn: https://learn.uwaterloo.ca

If the only control variable is the active power, it is called Security Constrained Economic Dispatch (SCED) in which the regular load flow equations are replaced by DC load flow ones.

2. Loss Minimization: the solution tries to minimize the circulating reactive power in the system and maintain a good voltage profile in the meantime. The problem becomes a reactive power dispatch one in which reactive power control means are utilized such as transformer taps and switching capacitors.
3. Preventive Scheduling: the security-constrained dispatch is usually implemented by adding other constraints to the economic dispatch problem. These constraints impose additional limits for post-disturbance configurations after some contingencies. The controls calculated ensure security after both pre- and post-contingency conditions [10].
4. Corrective Scheduling: with an outage, the objective is minimizing operating costs or minimum shift from the optimal solution. Corrective rescheduling is carried out to eliminate violations at the earliest and uses only the capabilities whose impact is significant in violation elimination [10].
5. Optimal Capacitor Siting: the solution seeks the best location or a capacitor in the system. It may include post-contingency analysis.
6. Nodal Pricing of Power: the dual obtained in the solution of a cost minimization problem is the LMCs. This introduces the concept of Locational Marginal Prices (LMPs) or the nodal pricing of power. Reactive power pricing is also possible using the same model.

2.3 Demand Response Programs

2.3.1 General

As the evolution of the smart grids goes on with numerous key objectives, the energy-efficient power grid is considered one of the main objectives that led to the transition to the paradigm of smart grids and the interest it continues to receive from researchers and system operators. One of the main crucial aspects of energy efficiency is the balance between demand and supply at all times considering the substantial costs of installing energy storage means in the system. Both the supply and the demand, however, change continuously and in some cases, their changes cannot be predicted because of some incidents such as the forced outage of a generating unit or a transmission line. Moreover, at peak

periods of demand, expensive or less-efficient generating units have to be utilized to meet that demand, and that results in large fluctuations in electricity price in the wholesale markets. At such moments, even a small reduction in demand can lead to a considerable reduction in system marginal cost.

Taking advantage of the modern advancements in the technologies of the smart grids like two-way digital communications, the concept of demand-side management (DSM) emerged which promotes customers' interaction and response by using the load as an additional degree of freedom.

DSM takes several forms as it comprises all the measures applied from the load side of an energy system that target the alteration of consumers' demand profile, in time and/or shape, to match it with the supply and that may include replacing inefficient loads with better ones up to installing an advanced energy management system. One of the main categories of DSM is Demand Response (DR). It embraces all possible modifications to end users' electricity consumption patterns intended to alter the timing, level of instantaneous demand, or the total electricity consumption [6].

Generally, the customers can take any of the following three actions to respond to high electricity prices at peak periods [7]. Firstly, they have the option to reduce their electrical energy consumption during peak periods and keep their off-peak pattern the same. This, however, results in a loss of comfort such as setting the air-conditioning temperature at a higher value in summer. Secondly, customers can respond by shifting some of their activities during peak periods to some other off-peak time. An example of this is changing the operation time of a pool pump. This, however, may create a new peak at some other time if a large number of customers decided to shift their activities to close times of a day. This is called a rebound effect. Also, an industrial customer will be greatly affected by the postponed activities in terms of lost business. Thirdly, customers can use their own local generation and this helps them to maintain their habits to a great extent as their pattern of energy consumption will suffer no or very little alteration on the one hand. On the other hand, the demand seen by the utility will noticeably change.

The most important DR implementation objectives are as follows

- More efficient utilization of the power market
- Reduction of demand from expensive electricity generating units
- Increasing the short-term capacity

- Avoiding or deferring the need for distribution and transmission infrastructure enforcements and upgrades
- Reduction of the price of electricity for all electricity consumers
- Reduction of price volatility in the spot market
- Reduction of power interrupts and energy not supplied
- Reliability, power quality, security, and stability improvement

It is obvious that the above-mentioned objectives have some overlaps and sometimes may conflict with each other. Hence, Independent System Operator (ISO) needs to determine which program best suits their needs. This evaluation should take into consideration not only the load profile characteristics but also the satisfaction of the customers through reduction of their electricity bills or received incentives/payments.

2.3.2 DR Programs Classification

Basically, DR programs can be classified into two classifications as shown in Figure 1. Their common names are Incentive-Based Programs (IBP) and Price-Based Programs (PBP). However, in literature, they are also named as a system- and market-led, emergency- and economic-based, stability- and economic-based DR programs [8].

IBP can be further categorized into classical and market-based programs. The classical programs encompass Direct Load Control Programs (DLC) and Interruptible/Curtailable Programs. In these types of programs, contributing customers receive payments for their participation in these programs usually in the form of a bill credit or rate discount. While the market-based ones are Demand Bidding, Emergency DR, Capacity Market, and Ancillary Services market. Participants in these programs are rewarded with money depending on the level of the reduction in their corresponding load during critical system conditions.

Customers bid on specific load reduction in the electricity wholesale market in the Demand Bidding Programs. If the bid is less than the market price, the bid will be accepted, and hence, customers are obliged to curtail the amount of load in the bid otherwise, they will be subjected to penalties. Or they would identify how much load they are willing to curtail at the posted prices. In Emergency DR Programs, curtailment is voluntary, but when done, customers receive incentives for measured load reduction during emergency conditions.

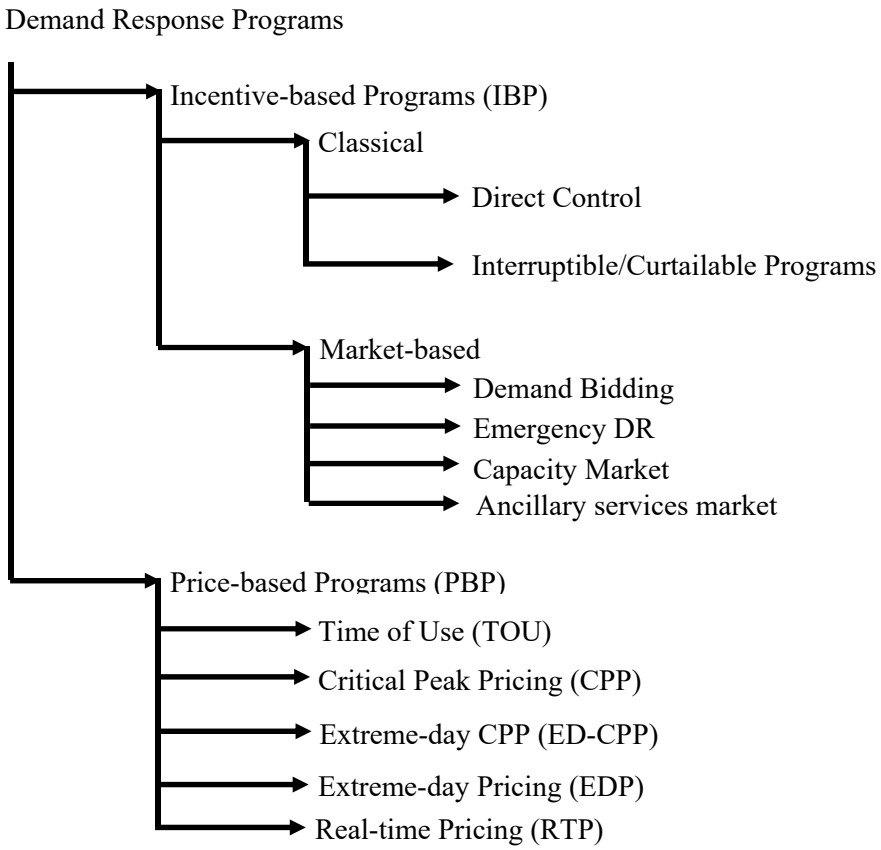

Figure 1 – DR programs classification [8]

In Capacity Market Programs, customers commit to reducing their loads by a predetermined value when the system undergoes contingencies with which the customers are notified one day ahead. Customers will be penalized if they do not respond with load reduction. Capacity Market Programs can be seen as a form of insurance because customers receive guaranteed payments in exchange for being obliged to reduce their consumption when directed. This is because in some years, contingencies will not occur, yet, the customers are paid for being on-call. Customers interested in participating in such programs should demonstrate that load reduction is achievable and sustainable. For example, New York Independent System Operator (NYISO) set the following requirements to receive capacity payments: minimum load reductions of 100 kW, minimum four-hour reduction, two-hour notification, and to be subject to one test or audit per capability period. These requirements are designed to ensure that the reductions can be counted upon when called. Customers partaking in Ancillary Market Programs bid on load reduction in the spot market as an operating reserve.

Customers with accepted bids are paid the spot market price for committing to be on standby and are paid the spot market energy price if load curtailment is required.

Price-based Programs are based on the fact that electricity prices are not flat and that they fluctuate to reflect the real-time cost of electricity. These programs aim at offering high prices during peak periods and lower prices during off-peak times. As shown in Figure 1, they are classified to: Time of use rates (TOU) in which different rates are applied for different blocks of time. The rate design attempts to reflect the average electricity cost during different time periods. Consumers know in advance the price for each period. Such pricing may follow system marginal cost to some extent, but these schemes do not convey the dynamics or resource balance of the system. As an improvement to TOU scheme, Critical Peak Pricing rates (CPP) includes a higher electricity usage price superimposed on the TOU rates or the flat rates and used during system contingencies or high wholesale electricity prices for a limited number of days or hours per year. Consumers know these prices in advance, but they are notified when a pricing event is called usually 24 hours ahead.

Extreme-day Pricing (EDP) is similar to CPP in having a higher price for electricity and differs from CPP in the fact that the price is in effect for the whole 24 hours of the extreme day which is unknown until a day ahead. In ED-CPP rates, flat rates are used for all days but for extreme days in which CPP rates are called. Finally, Real-Time Pricing Programs (RTP) charge customers based on the hourly fluctuating prices that reflect the changes in the real electricity cost in the wholesale market. Customers are informed about the prices a day or hours ahead. Customers need to monitor the prices and adjust their consumption accordingly. RTP is a more directly price-conveying program though it involves additional costs of metering and transactions to customers [8, 11,12].

2.4 Energy Storage System Technologies and Applications in Power Systems

2.4.1 General

There are numerous options for storing energy till it is required for electricity production. With the growing interest in renewables integration in the power systems, the installation of means of energy storage in the power systems will be key to maintain reliable and secure grids. Also, ESSs offer wide varieties of application potentials in the operation of electrical networks as will be debated in the following sections.

2.4.2 Storage Technologies

The energy storage technologies can be mainly classified into four main categories according to the form of the stored energy. These categories are mechanical, electrical, thermal and chemical as illustrated in Figure 2 [13,14]. A brief description of the theory of operation of ESSs found in the literature is further discussed.

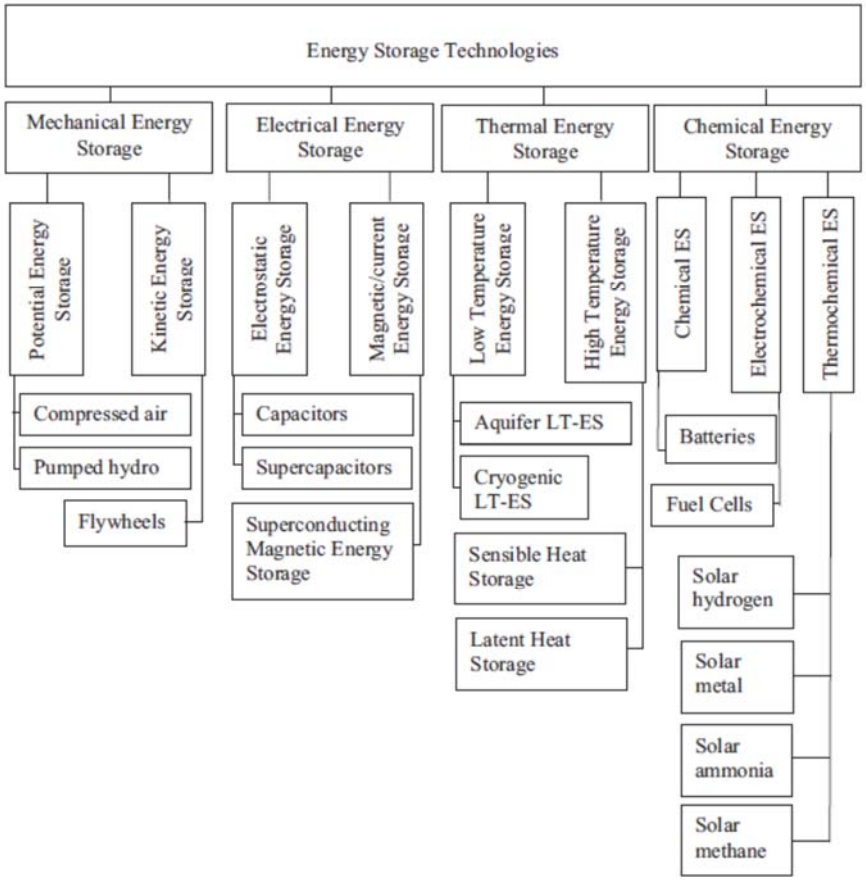

Figure 2 – Main categories of energy storage technologies [13]

2.4.2.1 Mechanical Energy Storage

2.4.2.1.1 Compressed Air Energy Storage (CAES)

The schematic diagram is shown in Figure 3. The basic idea is that the surplus electrical power during low demand requirements is used to run an electric machine in the motor mode to drive a chain of compressors to inject air into a storage vessel either over- or underground. The energy is stored in the form of high-pressure air. When peak periods, the compressed air is released and heated and

introduced to the turbines to run the machine in generator mode and inject electrical energy back into the grid. The recuperator recycles the waste heat from the exhaust [14].

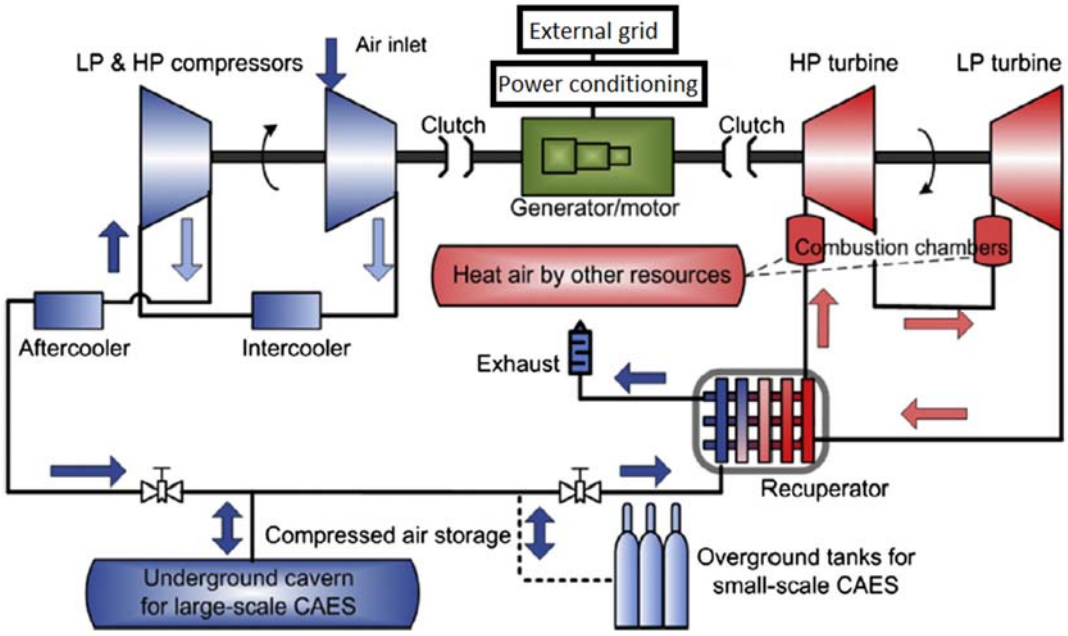

Figure 3 – Schematic Diagram of compresses air energy storage [14]

2.4.2.1.2 Pumped Hydroelectric Storage (PHS)

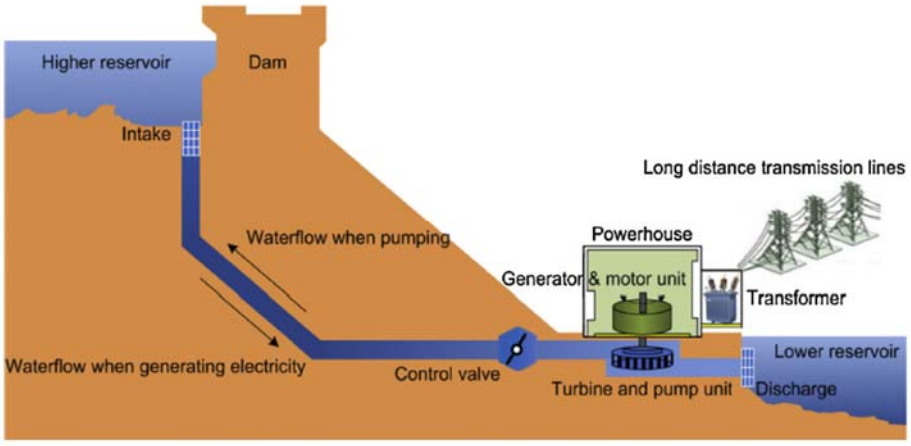

Figure 4 – A pumped hydroelectric storage plant layout [14]

The main concept of this technology is pumping the water from one reservoir to another one at a higher elevation during low demand periods. When the power generation cannot meet the demand

requirements, the water is released from the upper reservoir and introduced to a turbine/pump unit to drive the electrical machine in generator mode. The amount of the stored energy depends on the head difference between the two reservoirs and their capacities. The rated power is a function of the water pressure and its flow rate (discharge) [13,14]. A typical layout of a PHS plant is illustrated in Figure 4.

2.4.2.1.3 Flywheel Energy Storage (FES)

The main components of the Flywheel Energy Storage System are a flywheel, reversible motor/generator unit, vacuum chamber, and power conditioning circuit as presented in Figure 5. The surplus electrical power is used to accelerate the flywheel and hence, store the energy in the form of kinetic energy. The vacuum chamber reduces the air friction to minimize the windage losses. The energy stored in the flywheel is used when it is required to generate electricity. The flywheel decelerates then [13,14].

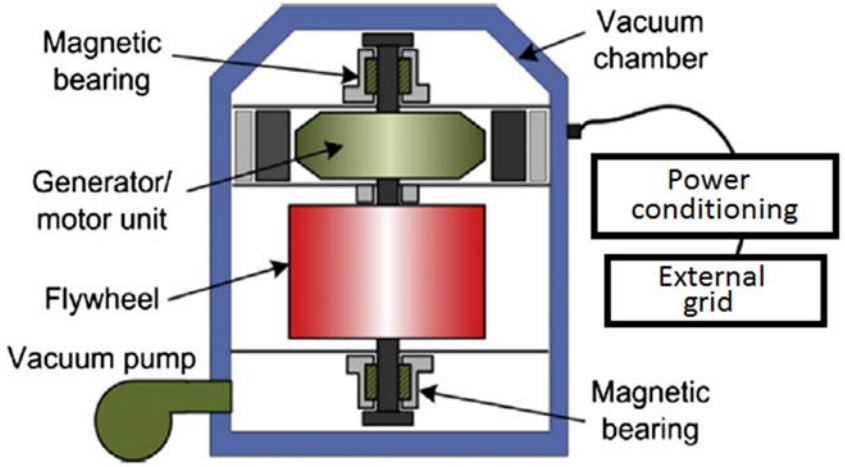

Figure 5 – A flywheel energy storage system [14]

2.4.2.2 Electrical Energy Storage

2.4.2.2.1 Capacitors and Supercapacitors

The capacitor mainly consists of two electrical conductors separated by an insulator. When charged, the capacitor stores energy in the form of the electric field.

The supercapacitors (sometimes called ultracapacitors) consist of two conducting electrodes, an electrolyte, and a porous membrane separating them. Due to their construction, they have common

features with both batteries and capacitors. The energy is stored in the form of static charges on the surfaces between the electrodes and the electrolyte [13,14]. A schematic diagram of the supercapacitor energy storage system is shown in Figure 6.

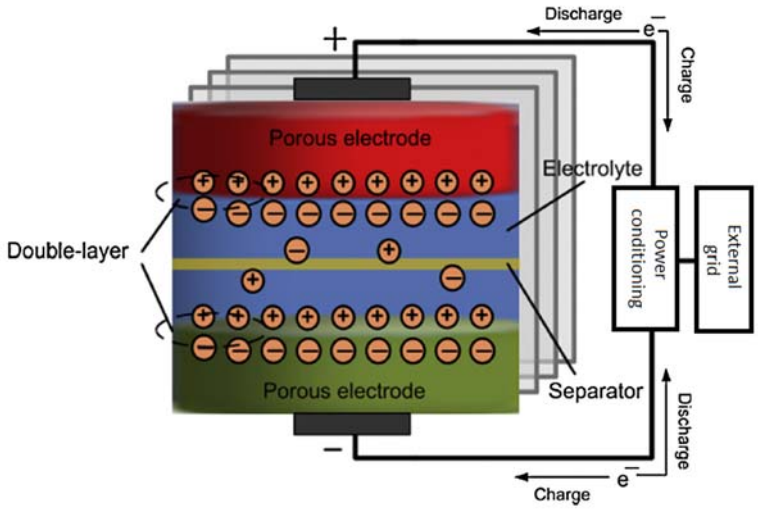

Figure 6 – Schematic diagram of a supercapacitor energy storage system [14]

2.4.2.2.2 Superconducting Magnetic Energy Storage System (SMES)

As shown in Figure 7, the SMES consists of a coil made of a superconducting material, a refrigeration system, and a power conditioning circuit. The surplus energy is stored in the form of the magnetic field produced by a DC current flowing in the coil which is cooled to a temperature lower than its superconducting temperature to assure zero resistance, and consequently, no power dissipation in the form of heat. When required, the energy is supplied back to the grid by the power conditioning circuit.

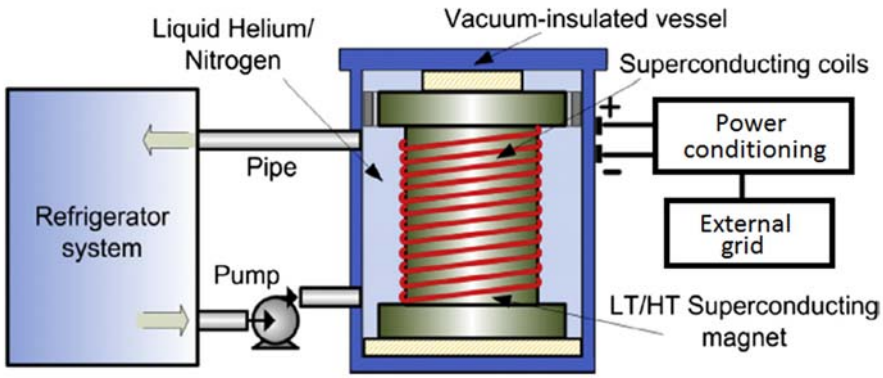

Figure 7 – Schematic diagram of a SMES system [14]

2.4.2.3 Thermal Energy Storage (TES)

This technology uses different approaches to store the available heat energy into available reservoirs. Depending on the operating temperature range they are classified into low-temperature TES and high-temperature TES.

An example of low-temperature TES is the cryogenic energy storage using air which is called Liquid Air Energy Storage (LAES). The air is cooled down with surplus energy to the point where it liquefies. Liquid air occupies a much smaller volume than its gaseous state. When needed to generate electricity, the liquefied air passes through a heat exchanger in which it is subjected to air at the atmospheric conditions and ambient temperature or to hot water produced by an industrial facility. The liquefied air returns back to the gaseous state. The resulting substantial increase in air volume can be introduced to a turbine to generate electrical power.

As for high-temperature TES such as latent heat energy storage, Phase-Changing Materials (PCM) are utilized where the energy is stored at a constant temperature during the transition from one phase to another. Figure 8 describes the storage mechanism. A solid material is heated, and its temperature increases proportionally to the supplied heat till the melting point. Beyond this point, the heat supplied does not raise the temperature. It is, however, used for the transition from solid to liquid (latent heat), this means that the material stores the thermal energy isothermally. When the material is totally liquefied, the temperature rises with the supplied heat till the vaporization temperature beyond which the material stores the thermal heat isothermally again. The same process applied for cooling in which the stored energy as latent heat can be retrieved [13-15].

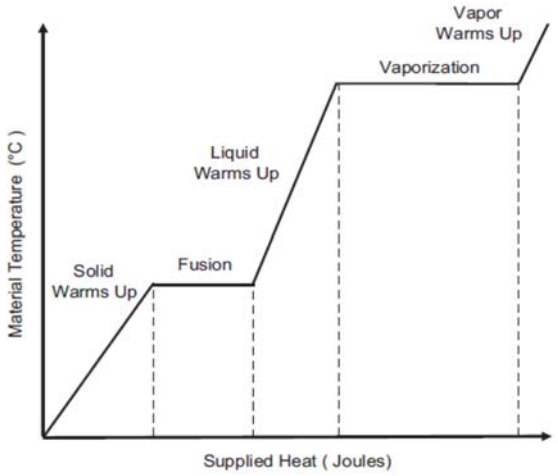

Figure 8 – Temperature increase profile in terms of supplied heat [15]

2.4.2.4 Chemical Energy Storage

These can be classified into electrochemical (mainly batteries and fuel cells) and thermochemical (solar fuels).

2.4.2.4.1 Battery Energy Storage Systems (BESSs)

The rechargeable batteries are considered one of the most widely spread means of energy storage. As illustrated in Figure 9, a battery cell basically consists of two electrodes and an electrolyte in between. In discharge, chemical reactions occur in a certain way at the cathode and the anode causing electrons to emerge from the anode and be collected at the cathode. While charging, the reverse chemical reactions occur at both electrodes with the battery connected to a voltage source. A battery system includes a number of cells connected in series (to increase system voltage rating) and in parallel (to increase current rating) [13,14].

There are several available battery technologies, the main ones are:

1. Lead-acid batteries.
2. Sodium-Sulphur batteries
3. Nickel-Cadmium batteries
4. Lithium-Ion batteries
5. Flow batteries

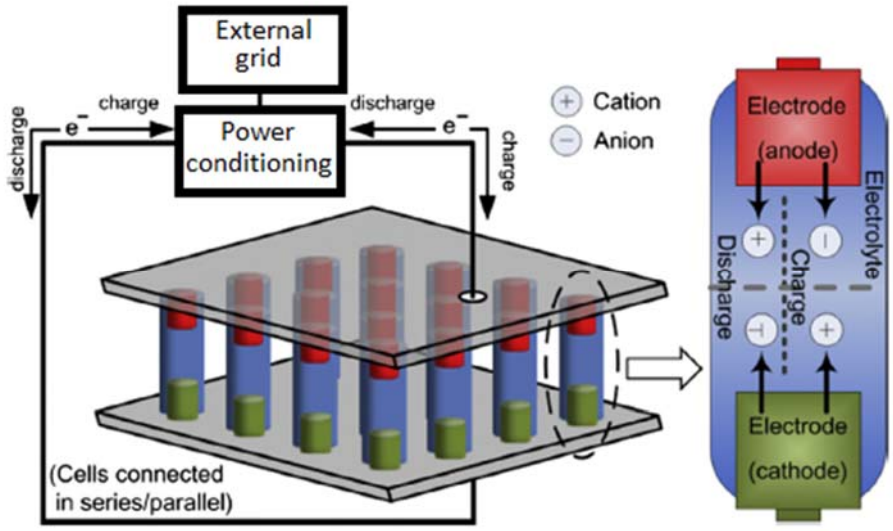

Figure 9 – A typical schematic diagram of a battery energy storage system [14]

2.4.2.4.2 Hydrogen Storage and Fuel Cells

As indicated in Figure 10, the water electrolysis process is responsible for Hydrogen generation which can then be stored in containers. This Hydrogen can then be used to generate electricity by using the fuel cell.

In fuel cells, electricity is generated from the reaction of the fuel (anode) and the oxidant (cathode) with an electrolyte in between. With the continuous flow of reactants, reaction keeps producing energy and forming products. In Hydrogen fuel cells, the reactant and the oxidant are Hydrogen and Oxygen respectively [13,14].

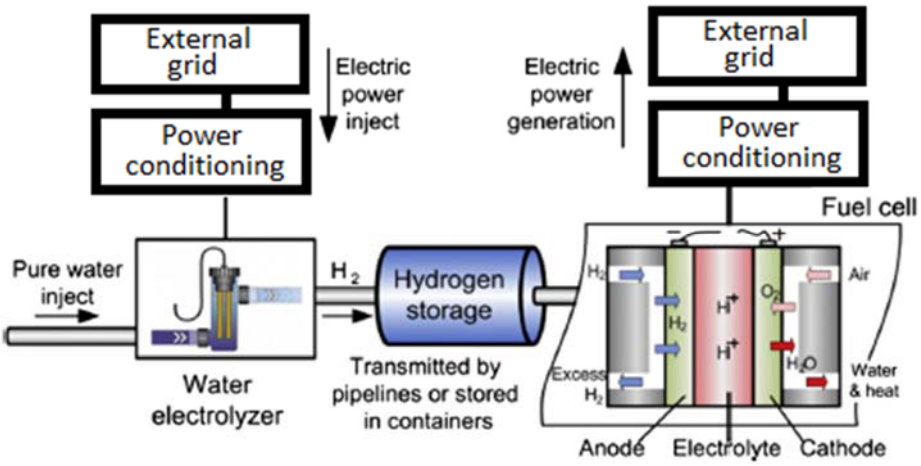

Figure 10 – Hydrogen storage and fuel cell system [14]

2.4.2.4.3 Solar Fuels

Solar energy can produce many types of fuel that can be stored and used for electricity generation at a later stage. The basic process of this phenomenon is the natural photosynthesis. The artificial photosynthesis also utilizes the same concept by absorbing the solar energy by specific elements (such as Ruthenium) as catalysts. This causes the flow of electrons from the Donor (D) to the acceptor as presented in Figure 11 which highlights the basic difference between natural and artificial photosynthesis [13,14].

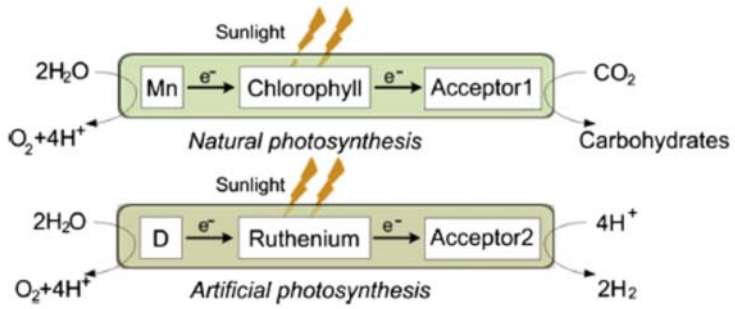

Figure 11 – Difference between natural and artificial photosynthesis [14]

2.4.3 ESSs Applications in Power Systems

The selection of a proper type of energy storage technology depends on the main role it is required to play and the timescale of the response. Mainly, the applications can be divided into three categories: Power Quality, Bridging Power and Energy Management [16]. Figure 12 shows different storage

technologies (with their respective ranges of rated power and discharge time) along with the applications.

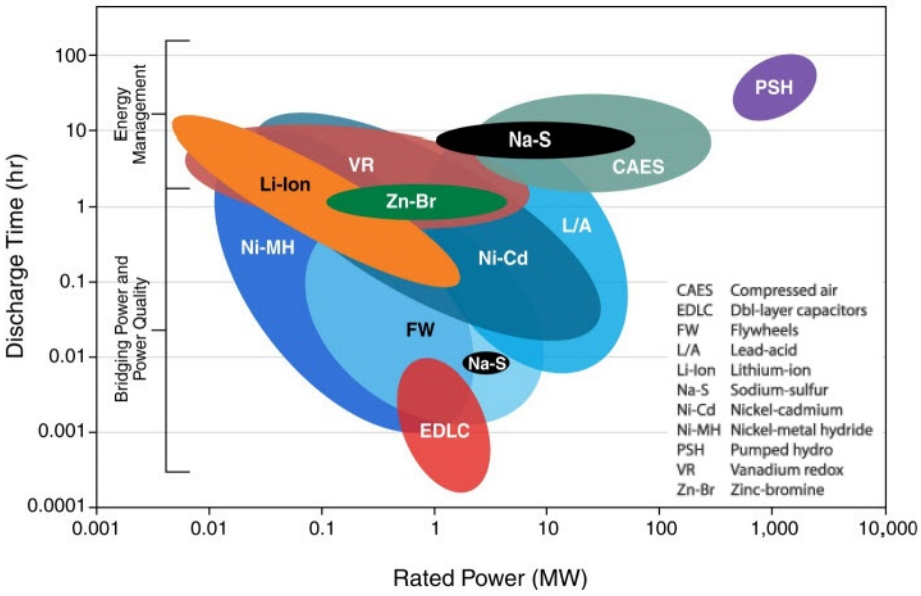

Figure 12 – Energy storage applications and technologies [16,17]

ES can be utilized to perform several functions in power systems such as:

- Load leveling/arbitrage: energy is stored during off-peak periods where prices are low and then used during expensive peak times.

- Firm capacity: ES can be used to provide reliable capacity during peak periods.

- Regulation: some ES technologies with fast response times can be used to respond to random or unpredicted demand variations. This reduces the use of partially-loaded generators and hence, reduces fuel usage and emissions.

- Contingency spinning reserve: the same as regulation but response is in the case of a contingency such as a generator failure.

- Load following: ES can be employed to follow long-term (hourly) variations in demand. This will also reduce the fuel usage and emissions by reducing the operation times of lightly-loaded generators.

- Transmission and distribution replacement and deferral: ES can relieve the transmission and distribution systems by reducing their loading at peak periods. With deploying ES systems near loads,

the costs associated with enforcing or upgrading the grid infrastructure can be deferred or even avoided.

- Black start: ES can be assigned the task of providing energy after a system failure. The ES system, in this case, acts also as a frequency reference for system synchronization. Mainly, pumped-hydro storage systems have been used for this purpose.

- Power quality and system stability: ES can mitigate for power quality problems such as harmonic distortion, and voltage sags. It can also assist in damping frequency oscillations which might affect system stability if not damped.

In this thesis, where the market model is an hourly one as will be discussed in Chapter-4, the response time is a vital factor to be considered in the selection of the storage technology. Systems like PHS and CAES would not be a proper choice for this application. The storage system should have a fast response time, and the technology should also be mature enough such that the operation and maintenance costs are as low as possible to present reasonable competition with DR service. Thus, the storage system in this study is a BESS.

2.5 Summary

In this chapter, the definition of the Optimal Power Flow (OPF) problem is discussed. The main differences between OPF and ELD are also presented. Then, OPF applications in the power system are enumerated.

Furthermore, the literature review on Demand Response (DR) as a main category of DSM is discussed. A detailed classification of DR programs is presented along with the basic features of each program.

Moreover, different energy storage technologies found in the literature are debated highlighting the theory of operation of each. Finally, the potential applications of ES in the power system are introduced with the conclusion to adopt a BESS as the storage system in this research.

Chapter 3
Renewable Energy and System Demand Modeling

3.1 Introduction

In Chapter-2, the classical optimal power flow (OPF) problem is illustrated in details and the differences from the economic load dispatch (ELD) are highlighted. The concept of Demand Response (DR) is also discussed along with its different programs and their impact on the electricity market. Also, the numerous energy storage technologies and applications in the power systems are introduced. In this chapter, the mathematical models that represent the stochastic nature of the Renewable Energy Sources (RESs) and demand are developed. The model is then employed into the OPF problem as an input as debated in Chapter-4. So, the main objective of this chapter is to obtain a typical day data in the four seasons for RESs output power and the system demand based on the available historical data.

3.2 System under Study

The system used in this study is the IEEE 14-bus system [18-20]. The system along with its data are described in Appendix-A. It is considered that the system also includes a solar system at bus 11 and a wind farm at bus 12. The solar module data sheet (in Appendix-B) and wind turbine data are obtained from [21] and [22] respectively. The historical data of solar irradiance and the ambient temperature is obtained from [23] while the load profile is available at [24].

3.3 Assumptions

1. All solar arrays (photovoltaic modules) and wind turbines are subjected to the same profiles of solar irradiance and wind speed respectively.
2. The solar and wind generations are considered to be negative loads.
3. Load buses are operating at constant power factor.

3.4 Data Preparation

The historical data of hourly solar irradiance, wind speed, and load is used with the most suitable distribution function to obtain the most probable (expected) hourly irradiance, speed, and load of a typical day in each of the four seasons. This is done by calculating the parameters of the Beta,

Weibull, and Normal cumulative density functions (CDFs) for each hour from the available data. With these CDFs, a Monte Carlo Simulation (MCS) is employed to get the expected values [25,26]. This is further discussed in the following sections. MATLAB is used to prepare and arrange the typical days data.

3.5 Wind Speed Model and Wind Turbine Output Power Calculation

3.5.1 Wind Speed Model

The available historical data is divided to get the wind speed at each hour in the day for the available time period. The data is then fitted to the most suitable CDF which is the Weibull distribution function [27]. Where the Weibull distribution function is defined by two parameters: the shape index k and the scale index c. Equations (3.1) to (3.3) give the Weibull distribution function and its parameters [28].

$$f(v) = \frac{k}{c} * (\frac{v}{c})^{k-1} * \exp\left[-\left(\frac{v}{c}\right)^{k}\right] \tag{3.1}$$

$$k = (\frac{\sigma}{v_m})^{-1.086} \tag{3.2}$$

$$c = \frac{v_m}{\Gamma(1 + \frac{1}{k})} \tag{3.3}$$

Where: $f(v)$ is the Weibull distribution function of v, v is the wind speed in m/s, k and c are the shape and the scale factors respectively, v_m is the average wind speed, and σ is the standard deviation. Figure 13 shows the Weibull CDF that fits the data of wind speeds at a certain hour in a day in the winter season.

These CDFs generated are used in Monte Carlo Simulation (MCS) in order to obtain the most probable value of wind speed of each hour in the day in each season. These expected wind speed values are then employed to calculate the output power of a wind turbine.

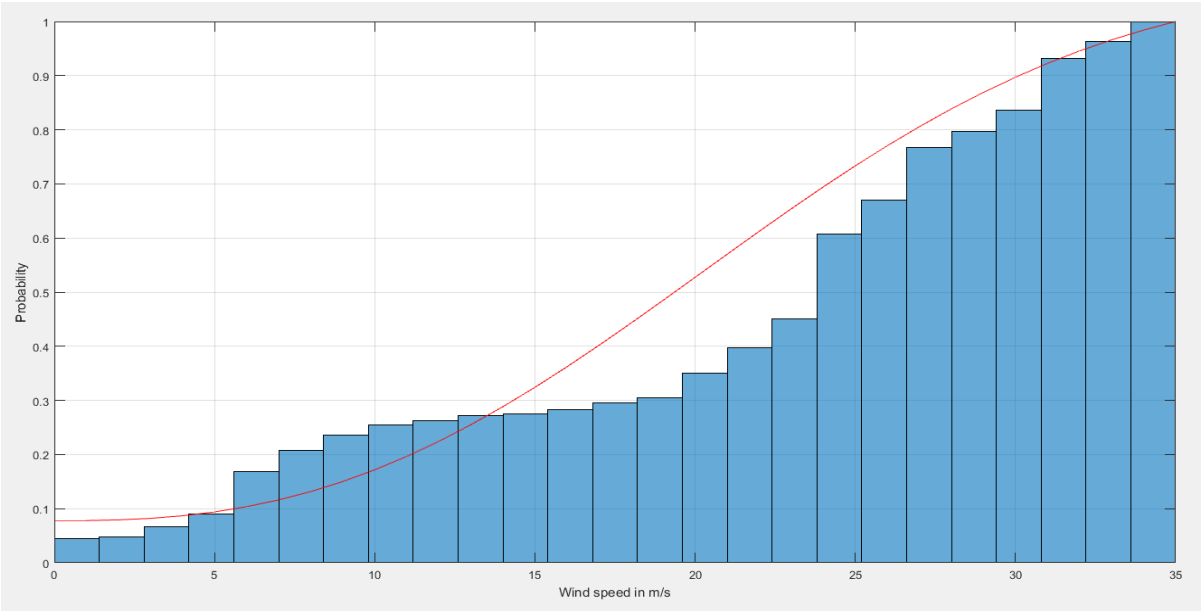

Figure 13 – Weibull CDF for wind speeds of an hour in the typical winter day

3.5.2 Wind Turbine Output Power Calculation

The output power of a wind turbine is a function of the wind speed. Below the turbine cut-in speed, the output power is equal to zero. In the range between the cut-in speed and the turbine rated speed, the output power is proportional to the wind speed. The turbine delivers its rated power in the region between the rated and the cut-out speeds. The turbine is shut down for mechanical protection of the rotor against forces generated at high speeds when the speed goes beyond the cut-out speed. In this region, the output power is equal to zero as described in equation (3.4) and Figure 14.

$$P_w(v) = \begin{cases} 0 & ,0 \le v \le v_{ci} \\ P_r * \dfrac{v - v_{ci}}{v_r - v_{ci}} & ,v_{ci} < v \le v_r \\ P_r & ,v_r \le v \le v_{co} \\ 0 & ,v > v_{co} \end{cases} \qquad (3.4)$$

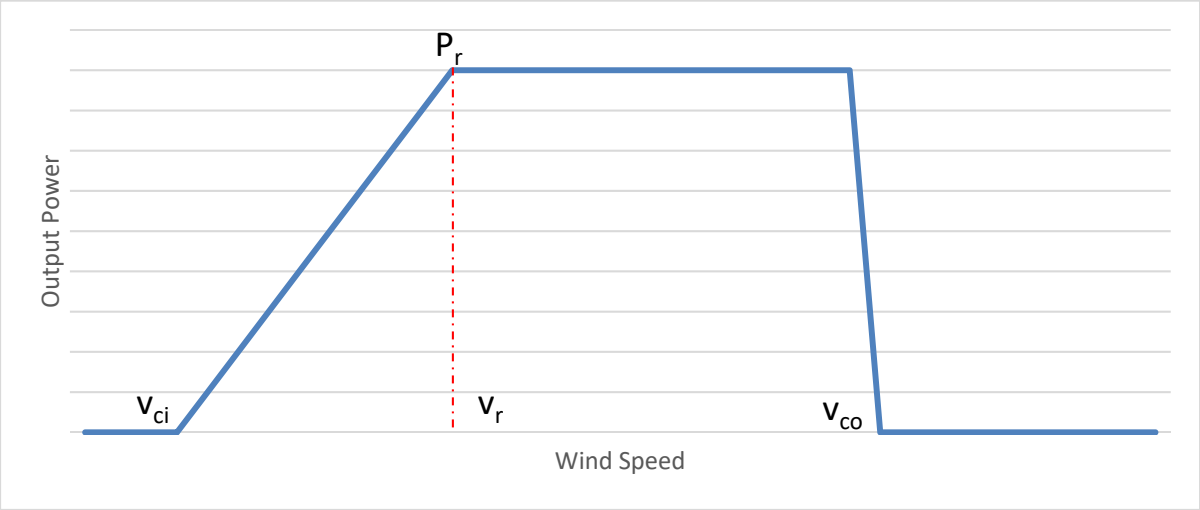

Figure 14 – Wind turbine output power as a function of wind speed

Where: $P_w(v)$ is the wind turbine output power at speed v, P_r is the wind turbine rated power, v_{ci} is the turbine cut-in speed, v_r is the turbine rated speed, v_{co} is the turbine cut-out speed, and v is the simulated wind speed (expected speed) obtained from the MCS.

3.6 Solar Irradiance Model and Solar System Output Power Calculation

3.6.1 Solar Irradiance Model

The available historical data includes the solar irradiance and the ambient temperature. The same procedures applied to model the wind speed are used to model the solar irradiance. However, the most appropriate CDF that fits the distribution of solar irradiance is the Beta distribution function [27]. Equations (3.5) to (3.7) give the Weibull distribution function and its parameters [28].

$$f(S) = \begin{cases} \dfrac{\Gamma(\alpha+\beta)}{\Gamma(\alpha)*\Gamma(\beta)} * S^{\alpha-1} * (1-S)^{\beta-1} & ,0 \le S \le 1, \alpha \ge 0, \beta \ge 0 \\ 0 & ,Otherwise \end{cases} \tag{3.5}$$

$$\beta = (1-\mu) * \left(\frac{\mu * (1+\mu)}{\sigma^2} - 1 \right) \tag{3.6}$$

$$\alpha = \frac{\mu * \beta}{1-\mu} \tag{3.7}$$

Where: $f(S)$ is the Beta distribution function of S, S is the solar irradiance in kW/m^2, α and β are the parameters of the Beta distribution function, and μ and σ are the mean and the standard deviation

of the solar irradiance data respectively. Figure 15 shows the Beta CDF that fits the data of solar irradiance at a certain hour in a day in the winter season.

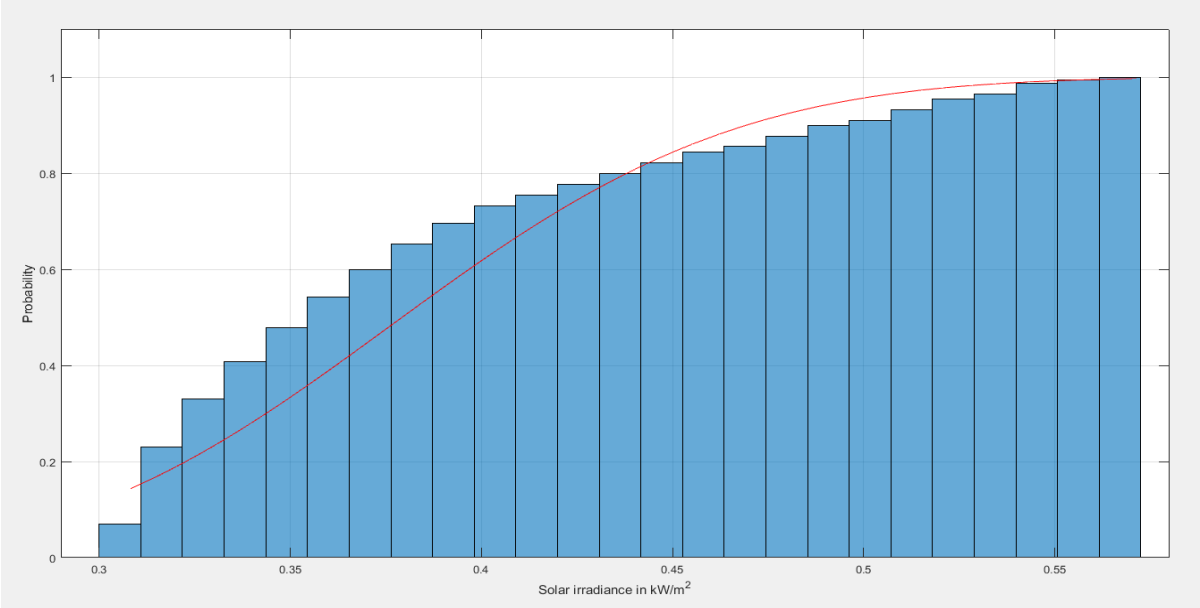

Figure 15 – Beta CDF for solar irradiance of an hour in the typical winter day

Also, the CDFs are utilized with MCS to get the expected solar irradiance in each hour of the typical day in each season. These values are then employed to calculate the output power of a photovoltaic (PV) module.

3.6.2 Solar System Output Power Calculation

The PV module converts the solar radiation into DC current through its photoelectric effect. The main parameters to calculate the module output power are the solar irradiance and the ambient temperature. Typical I-V characteristics of the PV module are shown in Figure 16.

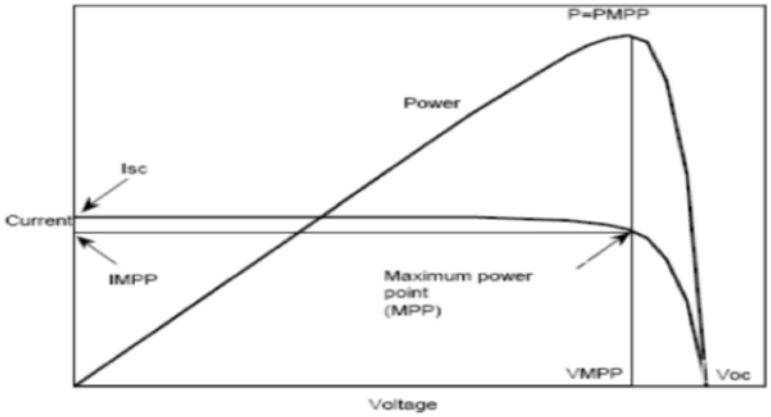

Figure 16 – A typical I-V characteristics of a PV module [29]

The output power of a PV module can be calculated using equations (3.8) to (3.12).

$$T_c = T_a + S * \left(\frac{T_{nom}-20}{0.8}\right) \tag{3.8}$$

$$I = S * [I_{sc} + k_i * (T_c - 25)] \tag{3.9}$$

$$V = V_{oc} - k_v * T_c \tag{3.10}$$

$$FF = \frac{V_{MPP} * I_{MPP}}{V_{oc} * I_{sc}} \tag{3.11}$$

$$P_s = FF * V * I \tag{3.12}$$

Where: T_c is the cell temperature in ºC, T_a is the ambient temperature in ºC, T_{nom} is the cell nominal operating temperature in ºC, k_i is the current temperature coefficient in A/ ºC, k_v is the voltage temperature coefficient in V/ ºC, I_{sc} is the short-circuit current in A, I_{MPP} is the current at maximum power point in A, I is the module current in A, , V_{oc} is the open-circuit voltage in V, V_{MPP} is the voltage at maximum power point in V, V is the module voltage in V, FF is the fill factor, and S is the simulated solar irradiance obtained from the MCS in kW/m^2.

3.7 Load Model

The same steps to model the load are also applied. The available data is the active power demand over a number of years. The most suitable distribution function to model the load is the Normal distribution function presented in equation (3.13).

$$F(P_l) = \frac{1}{\sigma\sqrt{2\pi}} e^{-\left(\frac{P_l - \mu}{2\sigma^2}\right)} \tag{3.13}$$

Where: μ is the mean of the data and σ is the standard deviation. Figure 17 shows the Normal CDF that fits the data of load active power demand at a certain hour in a day in the winter season.

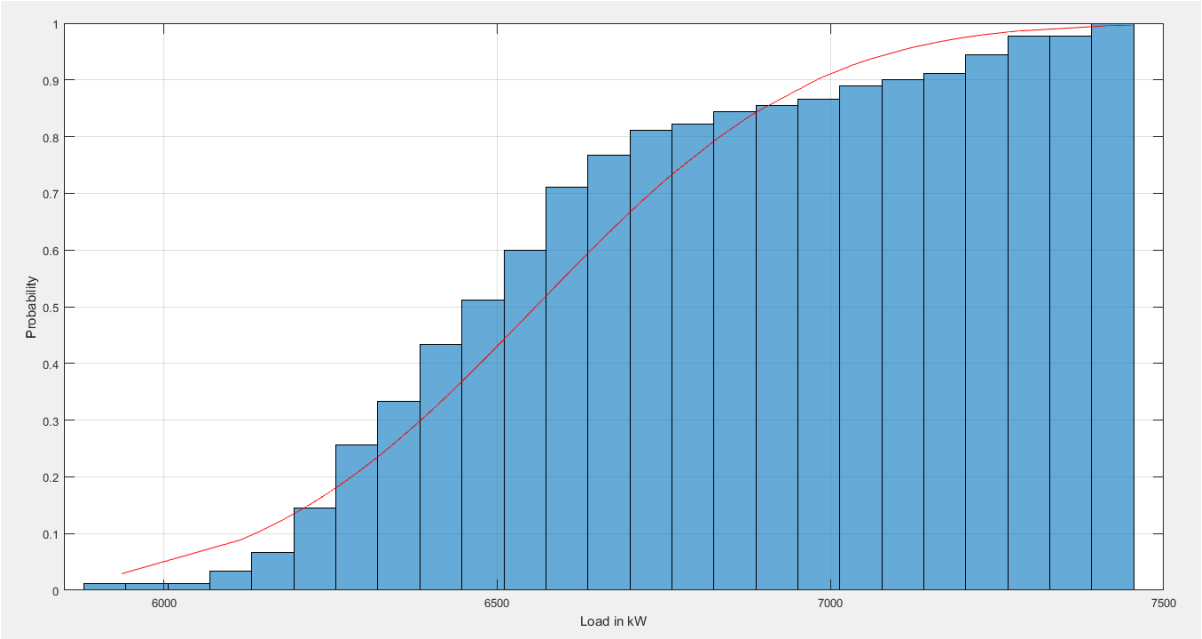

Figure 17 – Normal CDF for load active power demand of an hour in the typical winter day

After obtaining these CDFs. MCS is performed to get the most probable active power load at each hour of the typical four days. This 24-hour profile of loading is normalized and multiplied by the active power load at each bus provided in Table 2 in Appendix-A in order to get different load profiles at the load buses of the system. For the calculation of reactive power load at different buses/hours, it is assumed that each bus is operating at a constant power factor. So, the power factor (pf in equation 3.14) at each bus is calculated using the values in Table 2 in Appendix-A and then the reactive power load at each hour of the typical four days is calculated using equation (3.14).

$$Q_l = P_l \tan\left(\cos^{-1} pf\right) \tag{3.14}$$

3.8 Results

3.8.1 Solar System Output Power

The results of the solar system output power of the typical days of the four seasons are presented in Figures 18-21.

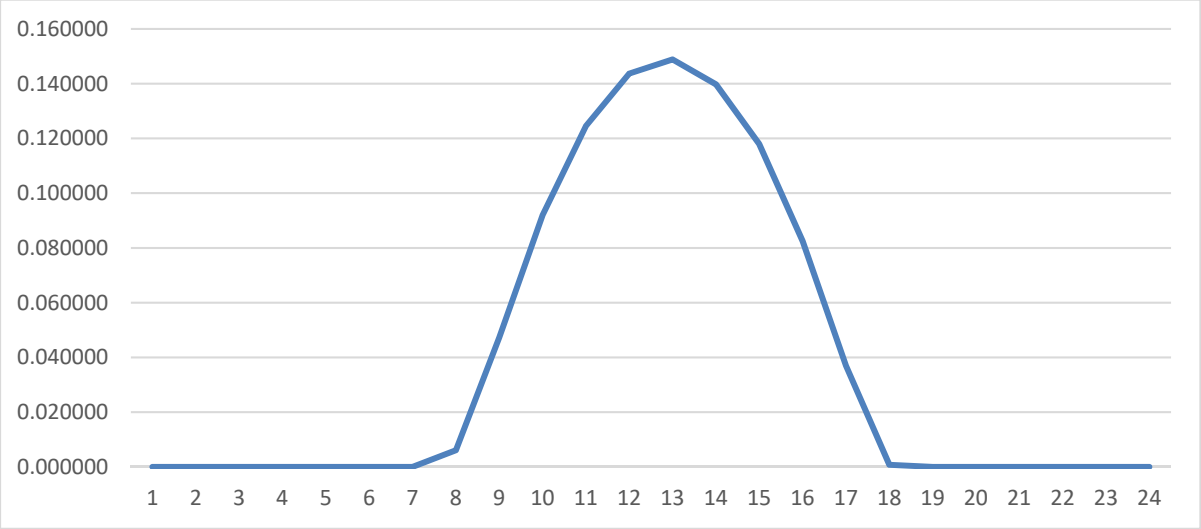

Figure 18 – Solar system output power of the typical winter day

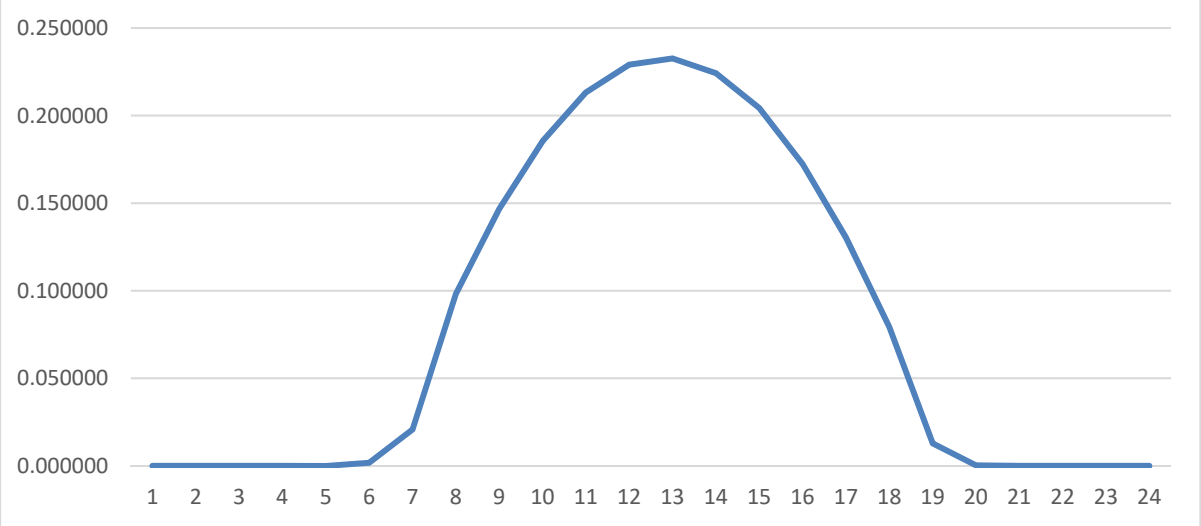

Figure 19 – Solar system output power of the typical spring day

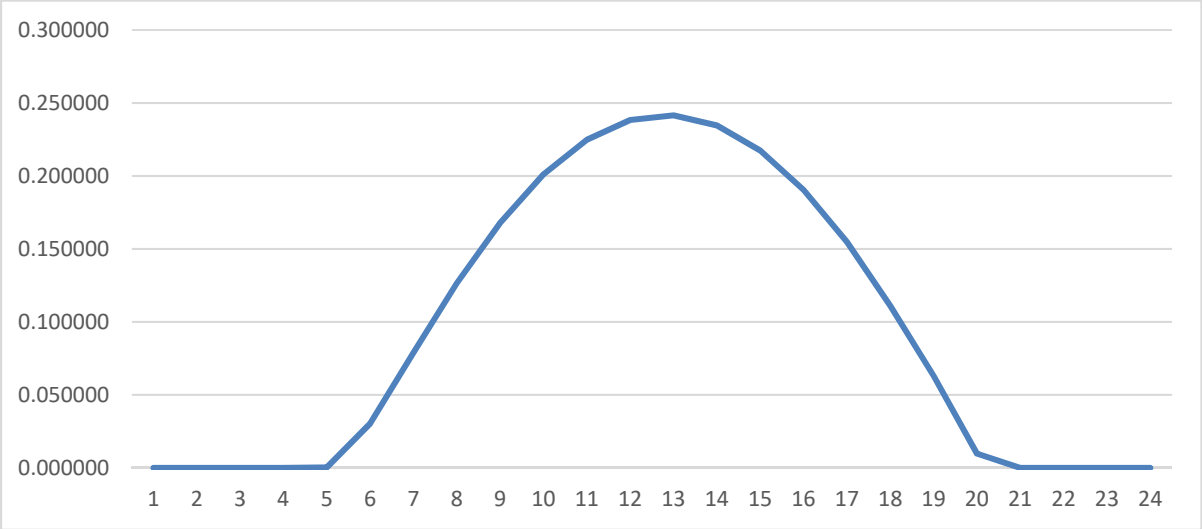

Figure 20 – Solar system output power of the typical summer day

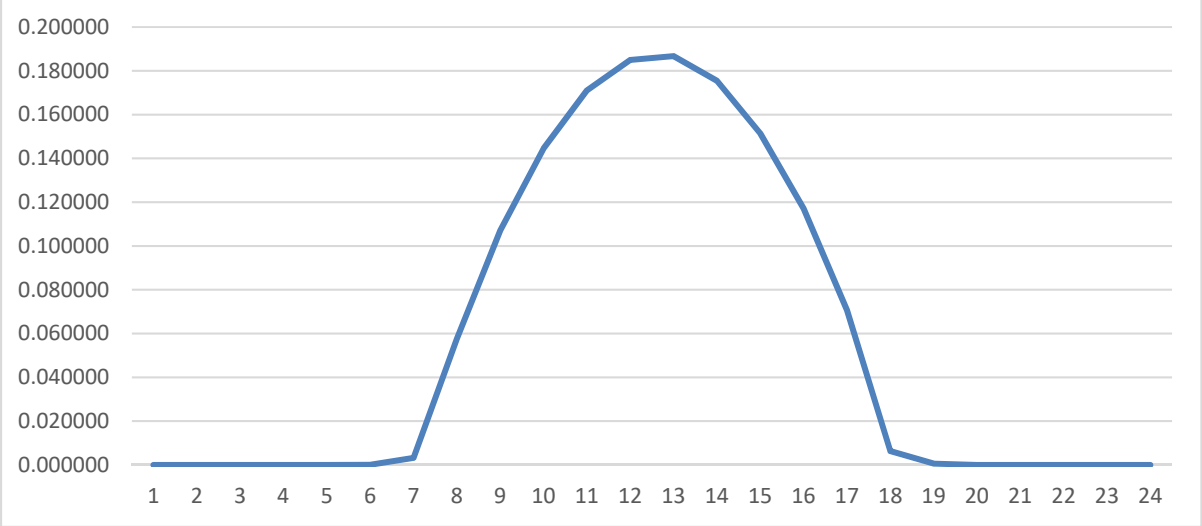

Figure 21 – Solar system output power of the typical fall day

3.8.2 Wind Turbines Output Power

The results of the wind turbines output power in the typical days of the four seasons are presented in Figures 22-25.

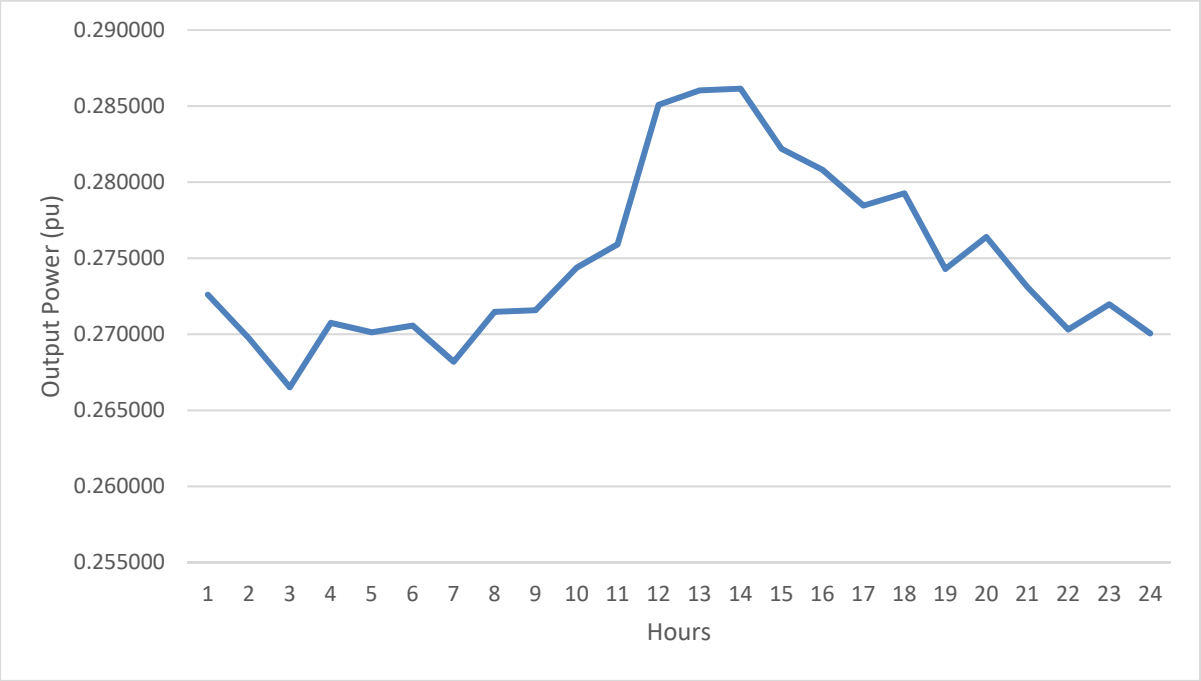

Figure 22 – Wind turbines output power of the typical winter day

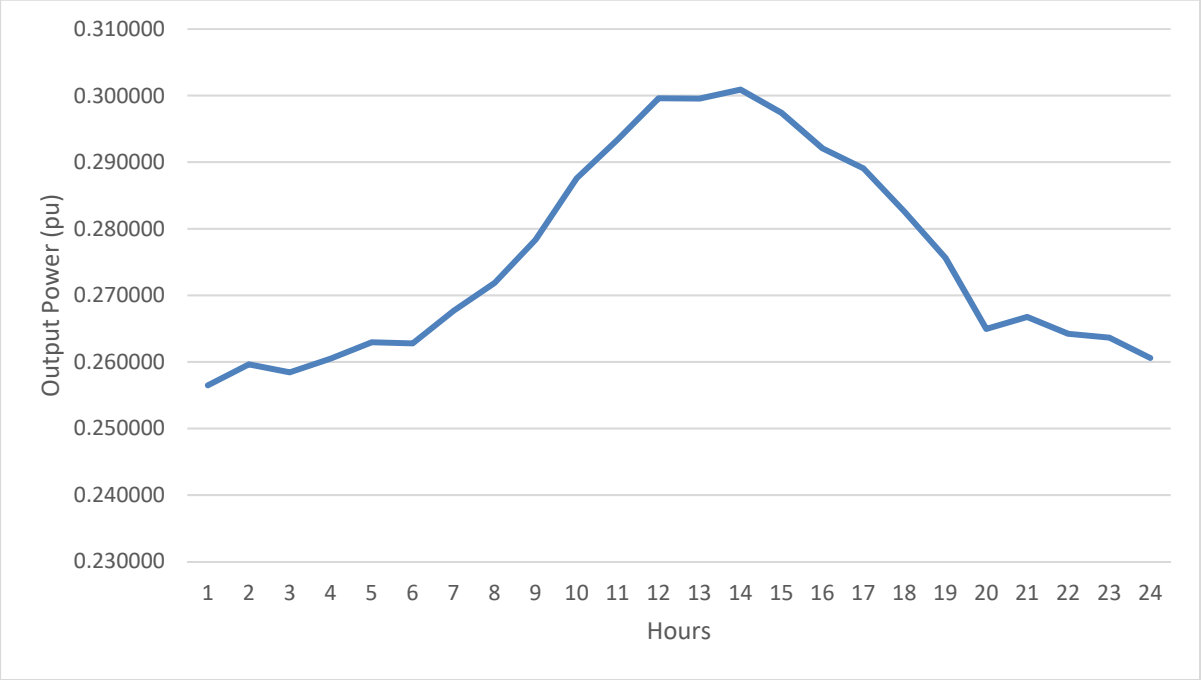

Figure 23 – Wind turbines output power of the typical spring day

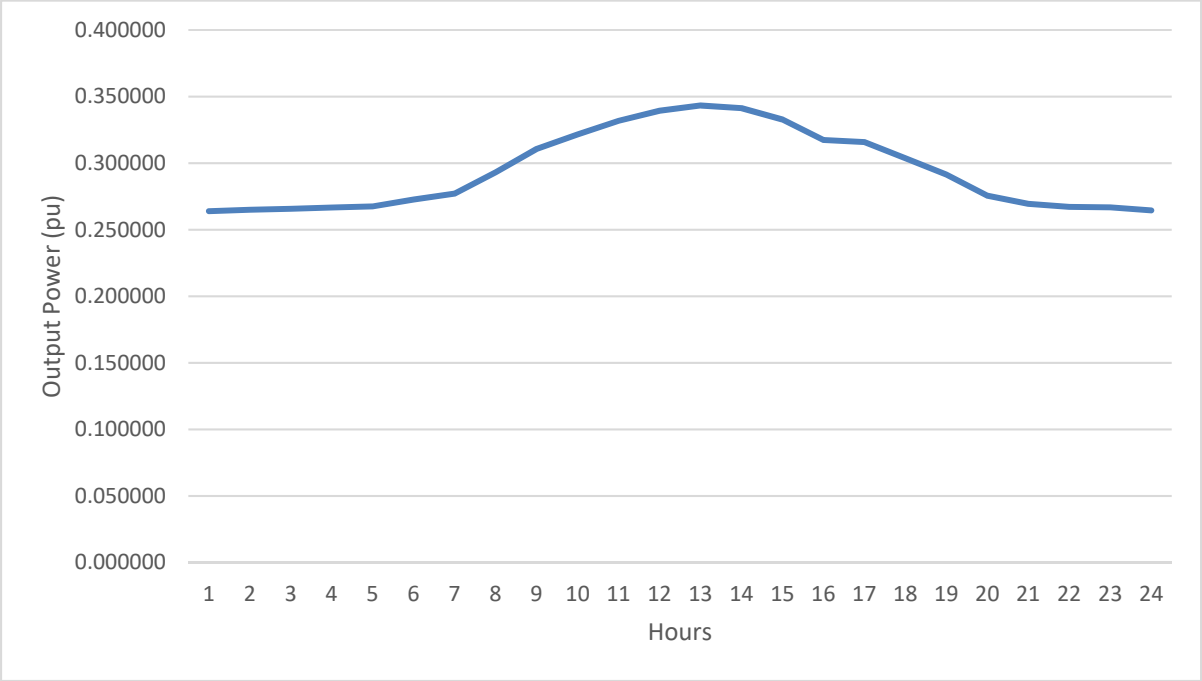

Figure 24 – Wind turbines output power of the typical summer day

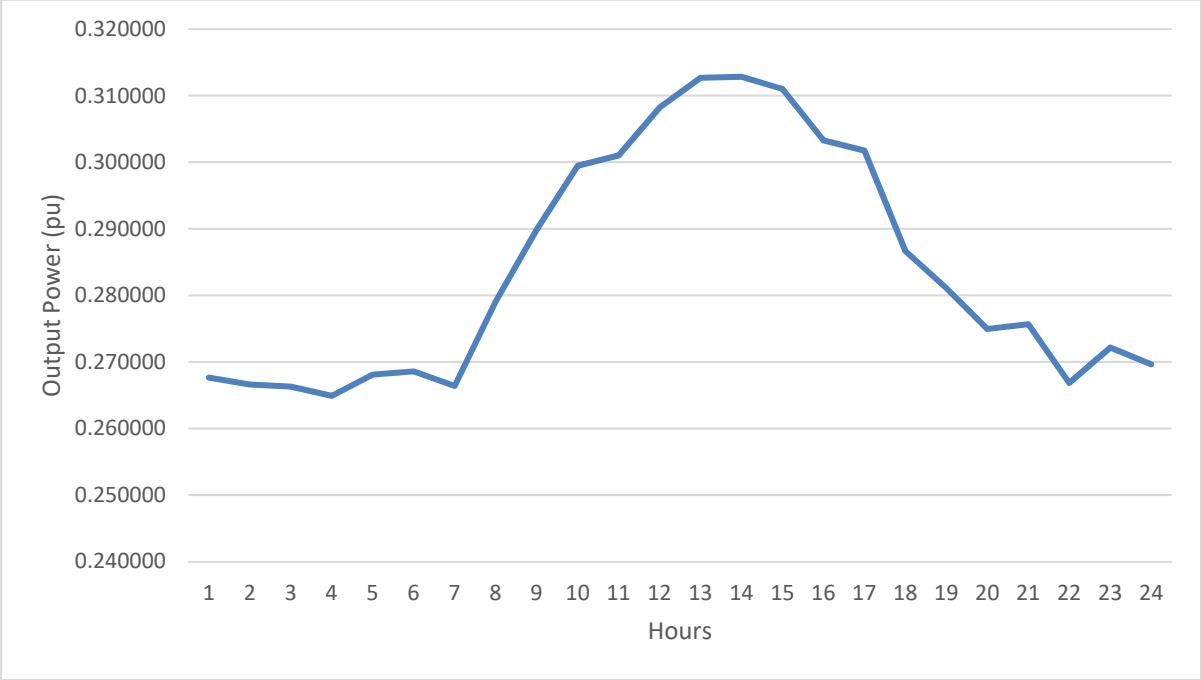

Figure 25 – Wind turbines output power of the typical fall day

3.8.3 System Load at Different Buses

The results of the active and reactive power loads at the load buses in the typical days of the four seasons are presented in Tables 4-11 in Appendix-C.

3.9 Summary

In this chapter, the available historical data of solar irradiance, wind speed, and load is processed to develop a mathematical model for each one that reflects their probabilistic nature. This is carried out by fitting the available data into proper cumulative distribution functions (CDFs) and applying Monte Carlo Simulation (MCS) to get the most probable value of the solar irradiance, wind speed, and load. These expected values are used to calculate the solar system and wind turbine output powers. Finally, profiles of four typical days that represent the different seasons are obtained.

Chapter 4
Impact of Demand Response and Battery Energy Storage System on Electricity Markets

4.1 Introduction

In this chapter, the mathematical model of assessing the impact of applying a DR program and utilizing a battery energy storage system (BESS) on the OPF solution (the running costs and the locational marginal costs at system buses) is developed. The solution is then compared with OPF solution of a system with neither DR nor BESS. Therefore, this chapter aims at examining the merits of using a DR program and operating a BESS in order to minimize the running cost of the system as compared to regular OPF solution.

4.2 Assumptions

1. The OPF solution is preceded by solving a Unit Commitment (UC) problem such that generators at buses-1, 2 and 3 along with the synchronous condensers at buses-6 and 8 are the committed generators in the OPF model.
2. The incentive amount received by customers participating in the DR program is directly proportional to the curtailed load (linear relationship).
3. The BESS was already installed in the system and was operating with some objective other than cost minimization. This means that the capital (initial) costs are not considered in the objective function of the BESS Case Problem.
4. The BESS technology is mature enough such that the operating (running) costs are relatively low.
5. The BESS is owned by the same utility that possesses the conventional generators.
6. The BESS is initially fully-charged (before solving the first hour $h = 1$) and the state of charge (SoC) after solving the last hour ($h = 24$) returns to the same initial value (full charge). This is because of the typical day analysis adopted.

4.3 Problem Formulation

The problem is a classical OPF problem with some modifications introduced. As discussed previously, the target is to assess the influence of DR or BESS on the solution of the OPF. Hence, the following three problems are proposed:

4. Base Case Problem: The system is the IEEE 14-bus system with a solar system at bus 11 and a wind farm at bus 12 as stated in section 3.2.
5. DR Case Problem: The same system of the Base Case with a typical IBP DR program in which participating customers receive bill credit (incentives) from the utility as debated in Chapter-2.
6. BESS Case Problem: The same system of the Base Case with a BESS installed with the solar system at bus 11. In this OPF model, the operation (charge/discharge) pattern of the battery that fulfills the new objective of cost minimization is obtained as part of the solution.

As discussed in Chapter-2, the OPF model is solved as a constrained non-linear optimization problem which is solved in GAMS environment [30]. This is illustrated in more details in the following sections.

4.3.1 Base Case Problem

4.3.1.1 Objective Function

In this case, the costs incurred by the utility are the generators running costs (mainly fuel costs) over the 24 hours of the typical day. The cost functions are usually represented by a quadratic function of the generator output active power as presented in equations (4.1) and (4.2).

$$Minimize \qquad J = \sum_{h=1}^{24} \sum_{i=1}^{NG} C_{i,h}\left(P_{Gi,h}\right) \tag{4.1}$$

$$C_{i,h}\left(P_{Gi,h}\right) = a_i * P_{Gi,h}^2 + b_i * P_{Gi,h} + c_i \tag{4.2}$$

Where: J is the total costs incurred by the utility, NG is the total number of conventional generators, and $P_{Gi,h}$ is the active power generated at generator bus i and hour h.

4.3.1.2 Constraints

1. Power Flow Equations:

$$P_{injk,h} - \sum_{l=1}^{N} V_{k,h} * V_{l,h} * \left[G_{kl} * \cos\left(\delta_{l,h} - \delta_{k,h}\right) + B_{kl} * \sin\left(\delta_{l,h} - \delta_{k,h}\right)\right] = 0 \quad (4.3)$$

$$Q_{injk,h} - \sum_{l=1}^{N} V_{k,h} * V_{l,h} * \left[G_{kl} * \sin\left(\delta_{l,h} - \delta_{k,h}\right) - B_{kl} * \cos\left(\delta_{l,h} - \delta_{k,h}\right)\right] = 0 \quad (4.4)$$

Where: $P_{injk,h}$ is the total active power injected into the system at bus k and hour h, $Q_{injk,h}$ is the total reactive power injected into the system at bus k and hour h, $V_{k,h}$ and $V_{l,h}$ are the magnitudes of the voltages at buses k and l at hour h respectively, G_{kl} and B_{kl} is the real and imaginary parts of the element Y_{kl} in the bus admittance matrix of the system respectively, and $\delta_{l,h}$ and $\delta_{k,h}$ are the voltage angles at buses k and l at hour h respectively.

2. Generators Maximum and Minimum Active Power Limits:

$$P_{Gmin} \leq P_{Gi,h} \leq P_{Gmax},\ i = 1,2,\dots,NG \text{ and } h = 1,2,\dots,24 \quad (4.5)$$

3. Generators Maximum and Minimum Reactive Power Limits:

$$Q_{Gmin} \leq Q_{Gi,h} \leq Q_{Gmax},\ i = 1,2,\dots,NG \text{ and } h = 1,2,\dots,24 \quad (4.6)$$

4. Bus Voltage Magnitude Upper and Lower Limits:

$$V_{imin} \leq V_{i,h} \leq V_{imax},\ i = 1,2,\dots,N \text{ and } h = 1,2,\dots,24 \quad (4.7)$$

5. Bus Voltage Angle Upper and Lower Limits:

$$-\pi \leq \delta_{i,h} \leq \pi,\ i = 1,2,\dots,N \text{ and } h = 1,2,\dots,24 \quad (4.8)$$

6. Line Flow Limits:

$$\left|V_{k,h} * V_{l,h} * \left[G_{kl} * \cos\left(\delta_{l,h} - \delta_{k,h}\right) + B_{kl} * \sin\left(\delta_{l,h} - \delta_{k,h}\right)\right]\right| \leq P_{limkl},\ k,l = 1,2,\dots,N \quad (4.9)$$

Where: P_{limkl} is the active power flow limit (thermal limit) of the line connecting bus k and bus l.

4.3.2 DR Case Problem

4.3.2.1 Objective Function

In this case, the costs incurred by the utility are the generators running costs, in addition to the incentives paid to the load curtailing customers according to their bilateral contract agreement with the utility as stated in equation (4.10).

$$Minimize \qquad J = \sum_{h=1}^{24}\left(\sum_{i=1}^{NG} C_{i,h}\left(P_{Gi,h}\right) + \sum_{j=1}^{N} A_{j,h} * \left(1 - LSF_{j,h}\right) * P_{Lj,h}\right) \tag{4.10}$$

Where: J is the total costs incurred by the utility, NG is the total number of conventional generators, $P_{Gi,h}$ is the active power generated at generator bus i and hour h, N is the total number of buses, $A_{j,h}$ is the incentive paid by the utility to the consumers for the curtailed load at bus j and hour h, $LSF_{j,h}$ is the load scaling factor which is used to represent the reduction in the load (load curtailment) at certain bus j and hour h, and $P_{Lj,h}$ is the active power load at load bus j and hour h.

The variable LSF is defined such that to enable the utility to determine the load curtailed at each bus and each hour which corresponds to the optimal solution. This means that in the case of $LSF_{j,h} = 1$, then there should be no load curtailment at bus j and hour h in order to reach the optimal point. Also, the values of the incentives $A_{j,h}$ paid to the contributing customers are based on the locational marginal costs of the middle cost generator in the Base Case Problem solution and increasing it by some percentage for longer distances between the load bus and the generator bus. This suggests that load buses close to generators will receive lower incentive than the buses far away from the generating stations in case of load curtailment. This is due to the fact that delivering the required power demand to the distant load buses is more costly. Hence, they should be entitled for higher incentives.

4.3.2.2 Constraints

The same constraints of the Base Case Problem are also valid in the DR Case. However, the following additional constraints are added.

1. Load Scaling Factor Limits:

$$0.75 \leq LSF_{j,h} \leq 1, j = 1,2,\dots,N \text{ and } h = 1,2,\dots,24 \tag{4.11}$$

The LSF of any bus j at any hour h is limited between 0.75 and 1.

2. Minimum Active Power Loading:

$$\sum_{j=1}^{N} LSF_{j,h} * P_{Lj,h} \geq P_{GU}, h = 1,2, \dots, 24 \tag{4.12}$$

Where: P_{GU} is the minimum value of active power loading in the system.

These two constraints are introduced in order for the utility to guarantee a minimum loading and that - in turn - guarantees a certain minimum profit from energy selling.

4.3.3 BESS Case Problem

4.3.3.1 Objective Function

Equation (4.13) gives the total costs incurred by the utility in this case which are the generators running costs, in addition to the running costs of the BESS.

$$Minimize \qquad J = \sum_{h=1}^{24} \left(\sum_{i=1}^{NG} C_{i,h}\left(P_{Gi,h}\right) + B * P_{batth} \right) \tag{4.13}$$

Where: J is the total costs incurred by the utility, NG is the total number of conventional generators, $P_{Gi,h}$ is the active power generated at bus i and hour h, B is the running cost of the BESS, and P_{batth} is the battery power at hour h (charging or discharging).

4.3.3.2 Constraints

The Base Case constraints are applicable in this case in addition to the following ones.

1. Initial SoC Limit:

$$E_i = E_b \tag{4.14}$$

2. Final SoC Limit:

$$E_f = E_b \tag{4.15}$$

3. Inter-hour Battery Stored Energy Limit [31]:

$$E_h = E_{h-1} - \frac{P_{dchh}}{\eta_{dch}} + \eta_{ch} * P_{chh} \tag{4.16}$$

4. Battery Power Capacity Limit:

$$P_{batth} \leq P_b \tag{4.17}$$

Where: E_i is the battery initial stored energy, E_b is the battery energy capacity, E_f is the battery final stored energy, E_h is the energy stored in the battery at hour h, E_{h-1} is the energy stored in the battery at hour $h-1$, P_{dchh} is the power discharged from the battery at hour h, P_{chh} is the charging power of the battery at hour h, η_{dch} is the battery discharging efficiency, η_{ch} is the battery charging efficiency, and P_b is the battery power capacity. P_{batth} is defined in equation (4.13).

4.4 Test Cases and Results

4.4.1 Test Case #1

In test case #1, the OPF model is solved using the objective function and the constraints of the Base Case Problem. For the typical winter day, the commitments of generators at buses 1, 2 and 3 are shown in Figures 26-28 respectively. The annual cost incurred by the utility, in this case, is $33,593,826.

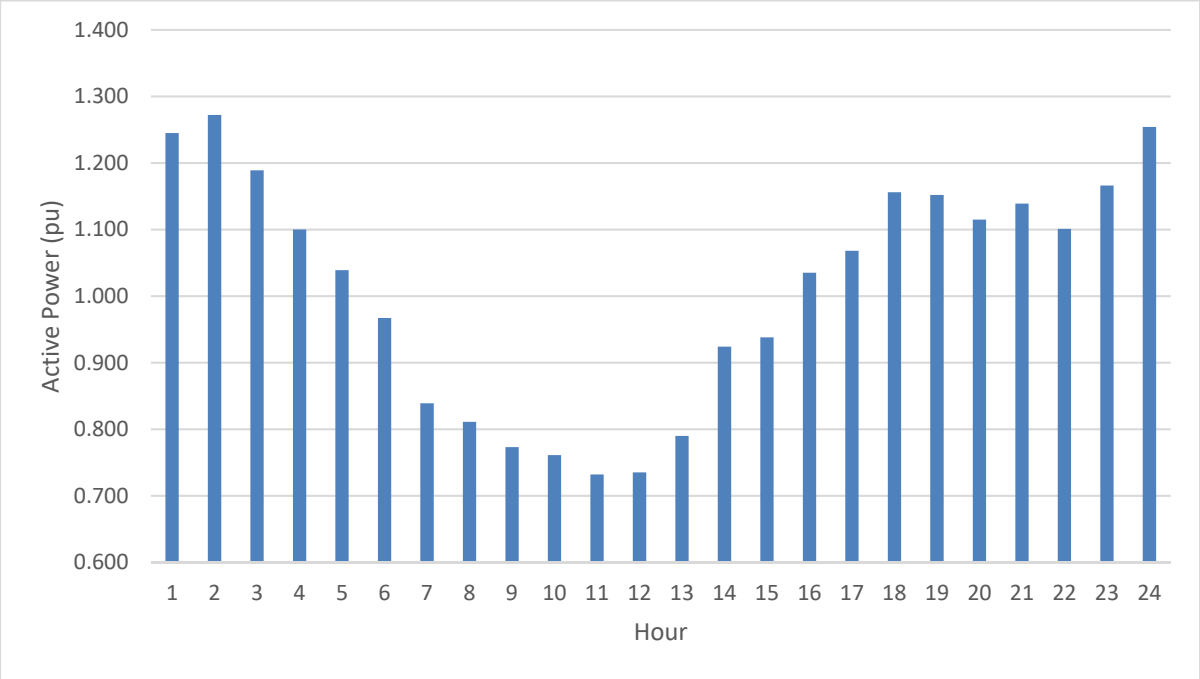

Figure 26 – Commitment of bus-1 generator in Base Case Problem (on the typical winter day)

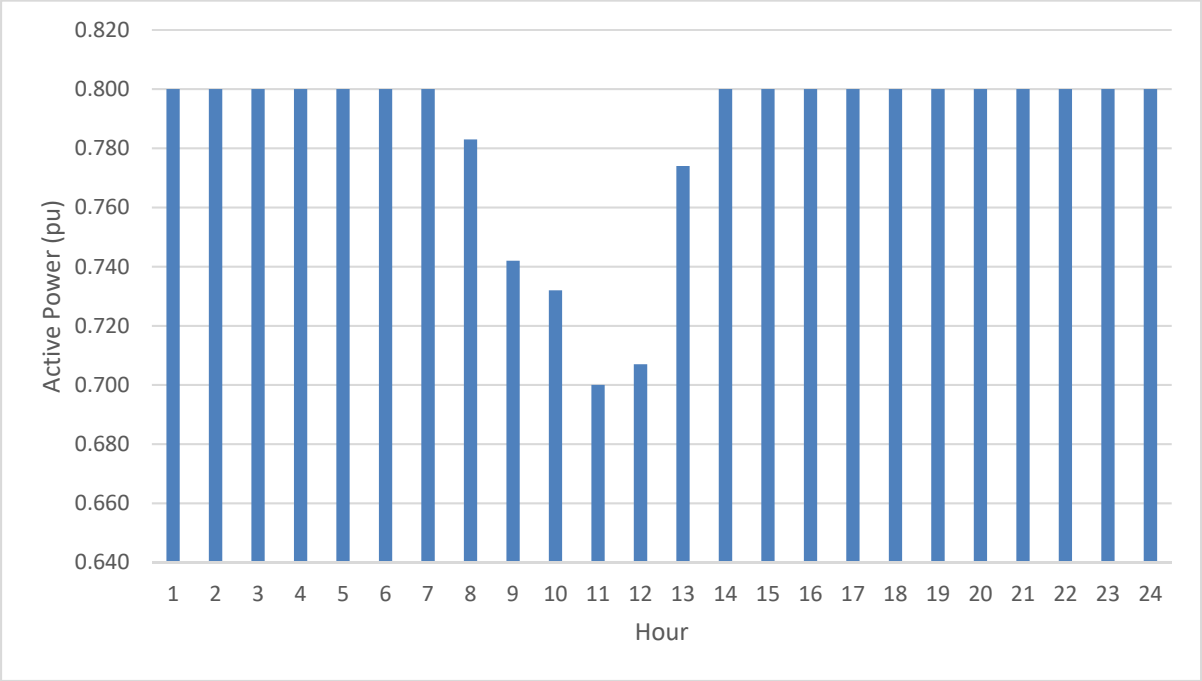

Figure 27 – Commitment of bus-2 generator in Base Case Problem (on the typical winter day)

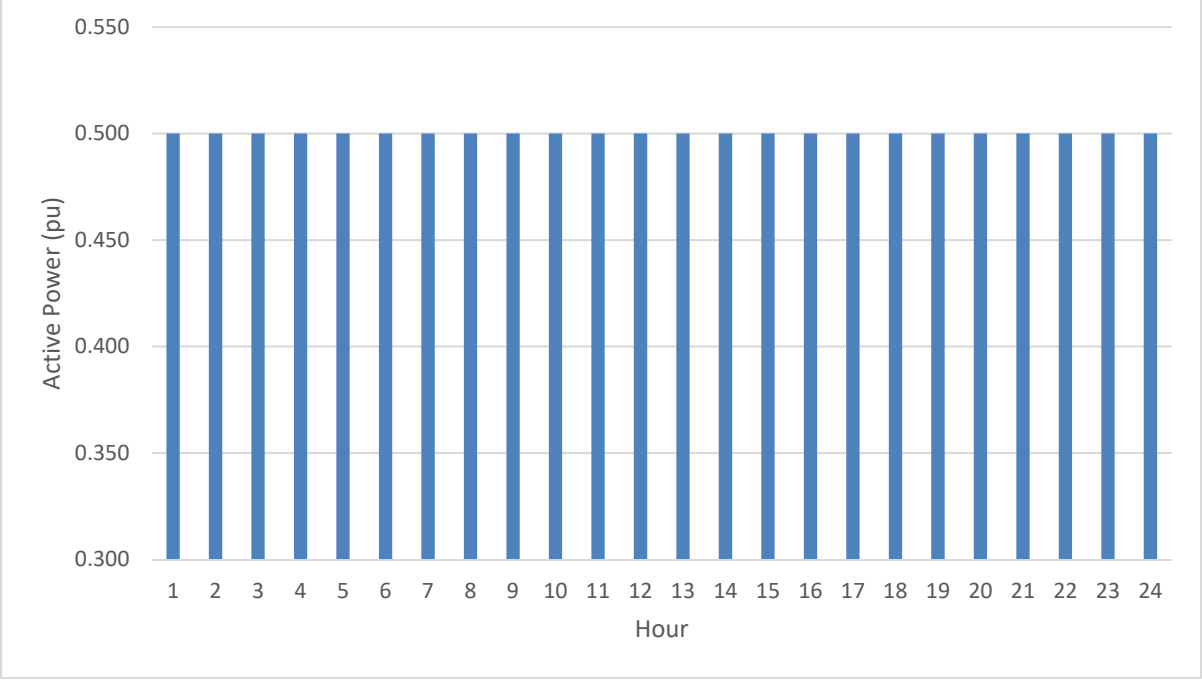

Figure 28 – Commitment of bus-3 generator in Base Case Problem (on the typical winter day)

The generator at bus-3 is the cheapest one. Hence, this generator is loaded with its maximum available power (0.5 pu) as indicated in the results in Figures 26-28. Also, bus-2 generator is the second cheapest in this system demand range. So, it delivers its maximum available power (0.8 pu) most of the hours of the typical winter day. However, for hours 8-13, the commitment of bus-2 generator drops below the maximum value as the system loading in this period is relatively lower than the rest of the typical winter day. In this interval, the optimal solution is to load bus-3 generator with its maximum possible loading and generators at buses-1, and 2 will share the remaining system demand such that the cost is minimum.

4.4.2 Test Case #2

In test case #2, the OPF model is solved using the objective function and constraints of the DR Case Problem. For the typical winter day, the commitments of generators at buses 1, 2 and 3 are shown in Figures 29-31 respectively. Also, the load scaling factor (LSF) at different buses is shown in Figures 32-36. The annual cost incurred by the utility, in this case, is $33,487,100.

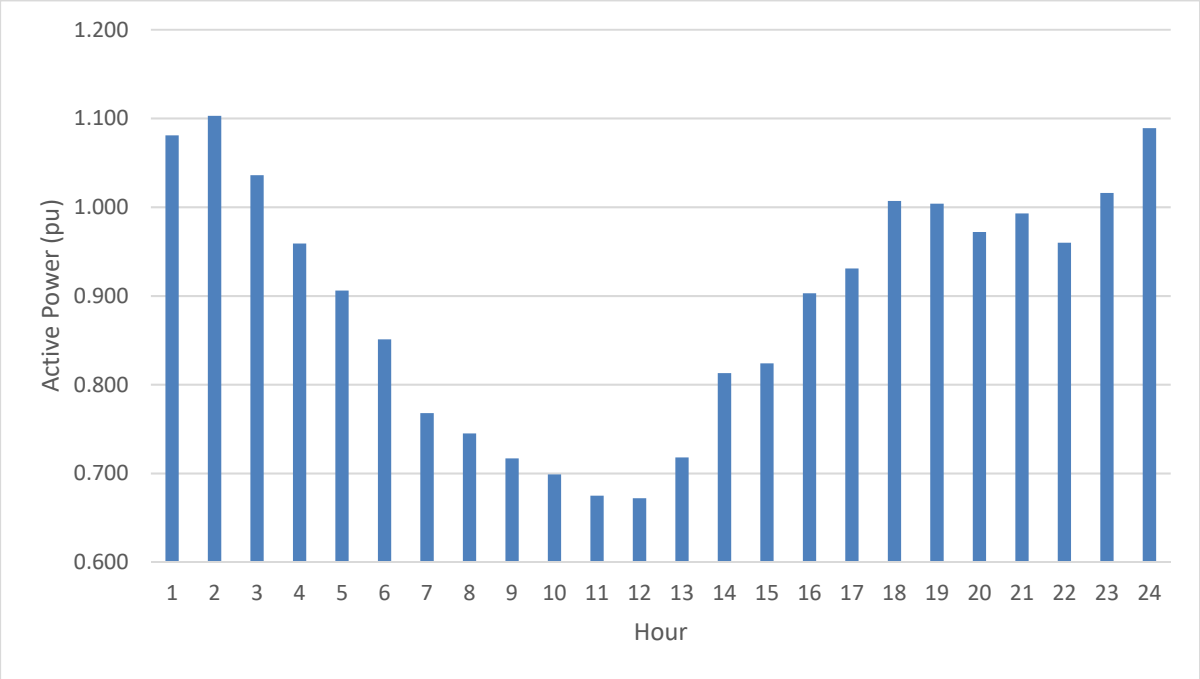

Figure 29 – Commitment of bus-1 generator in DR Case Problem (on the typical winter day)

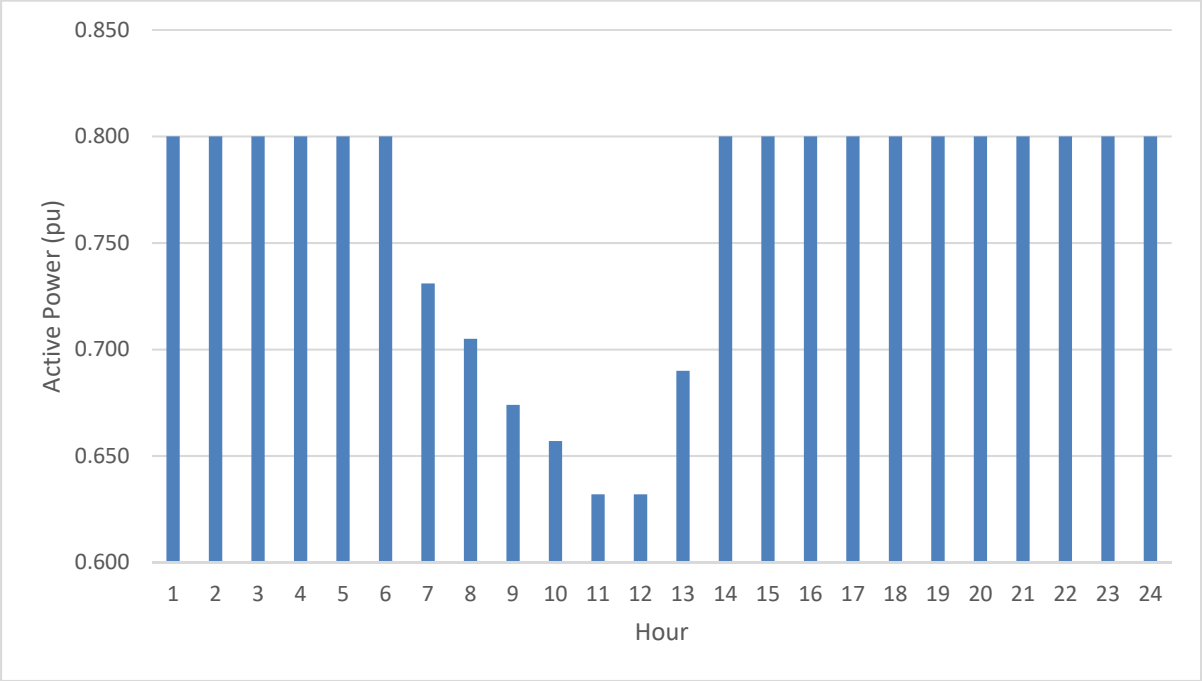

Figure 30 – Commitment of bus-2 generator in DR Case Problem (on the typical winter day)

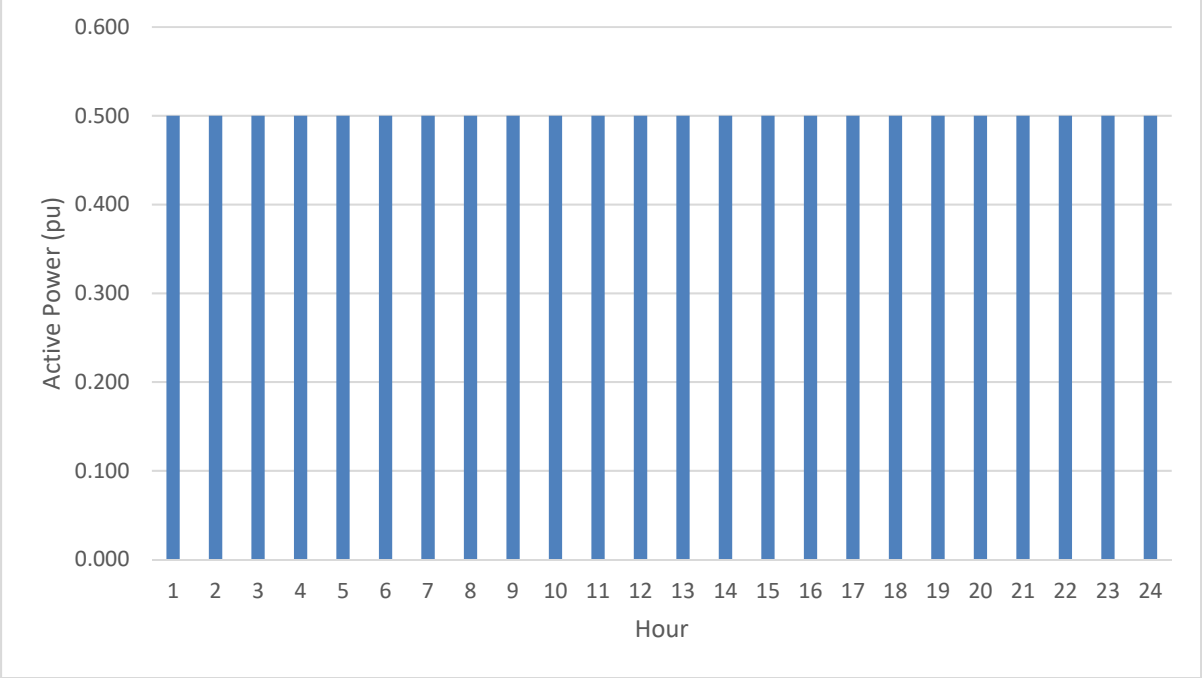

Figure 31 – Commitment of bus-3 generator in DR Case Problem (on the typical winter day)

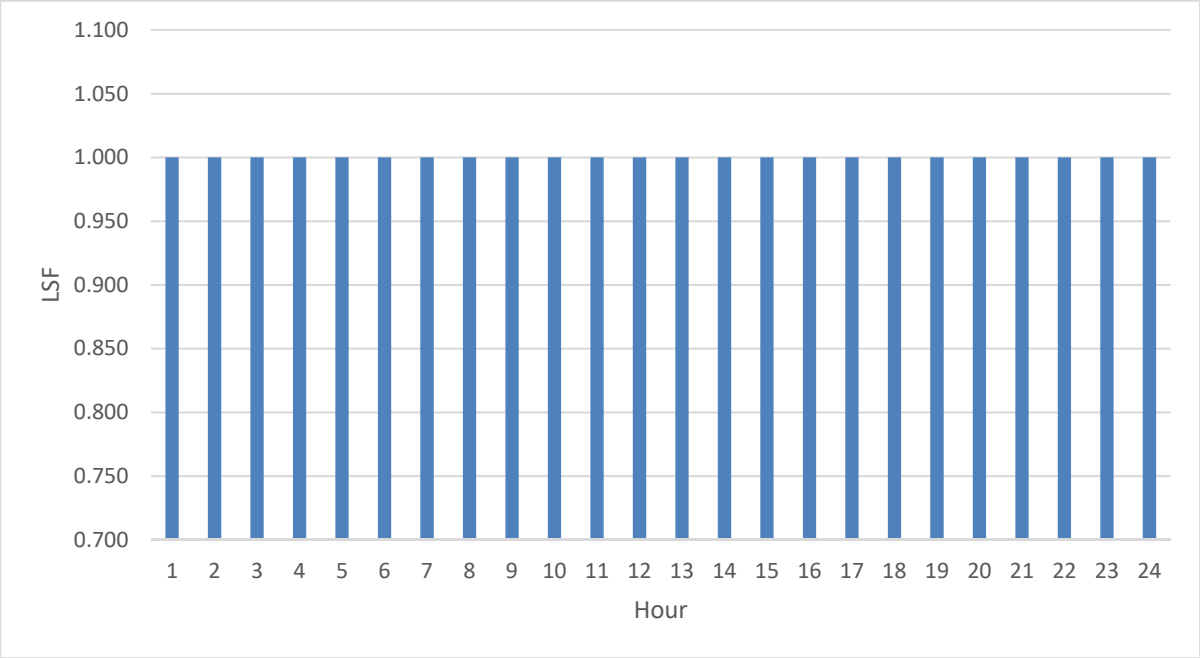

Figure 32 – Load scaling factor of buses-2, 6, 9, 10, 11, 12 and 13 in DR Case Problem (on the typical winter day)

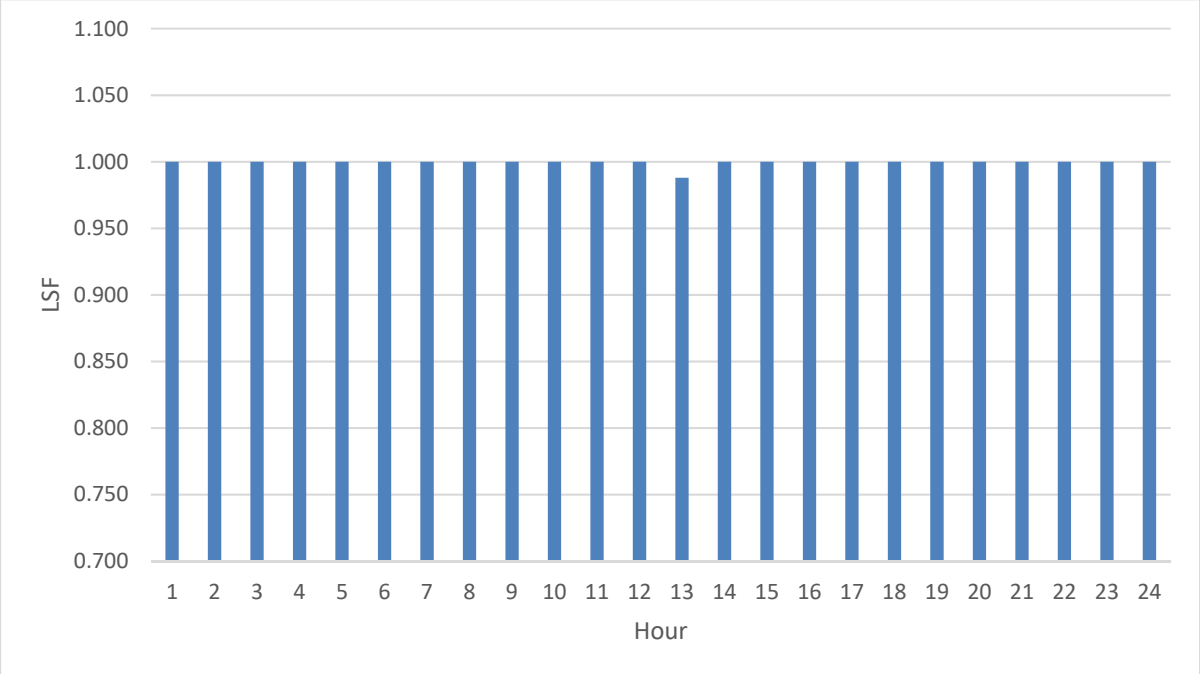

Figure 33 – Load scaling factor of bus-3 in DR Case Problem (on the typical winter day)

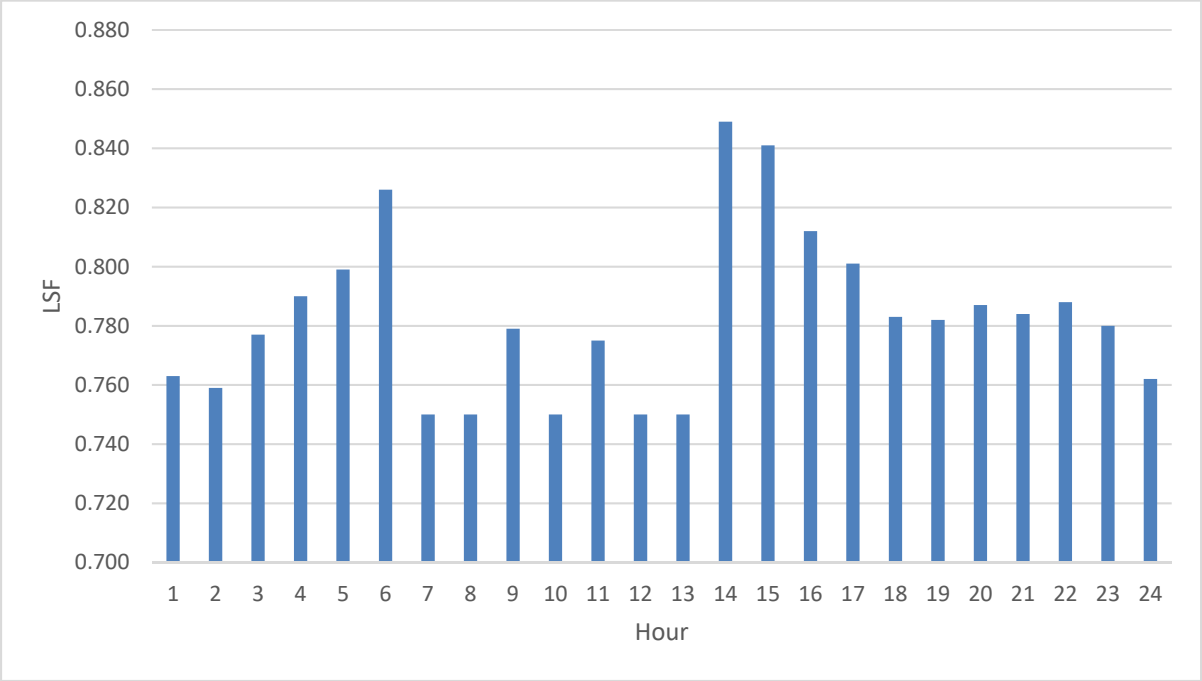

Figure 34 – Load scaling factor of bus-4 in DR Case Problem (on the typical winter day)

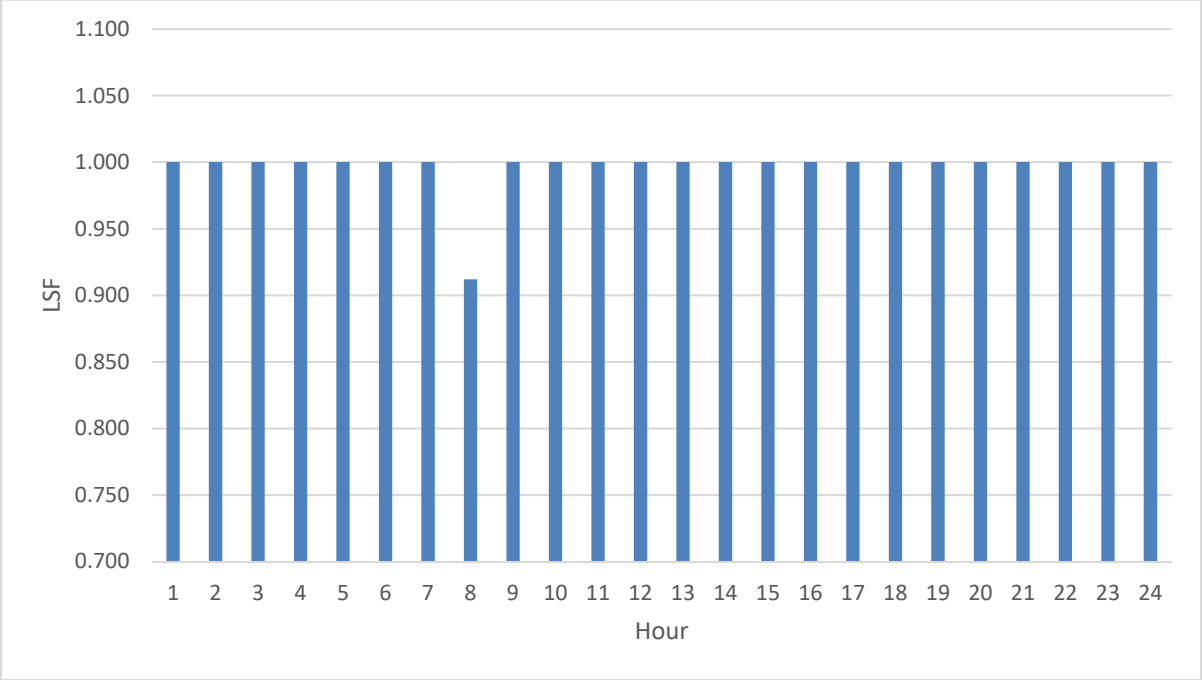

Figure 35 – Load scaling factor of bus-5 in DR Case Problem (on the typical winter day)

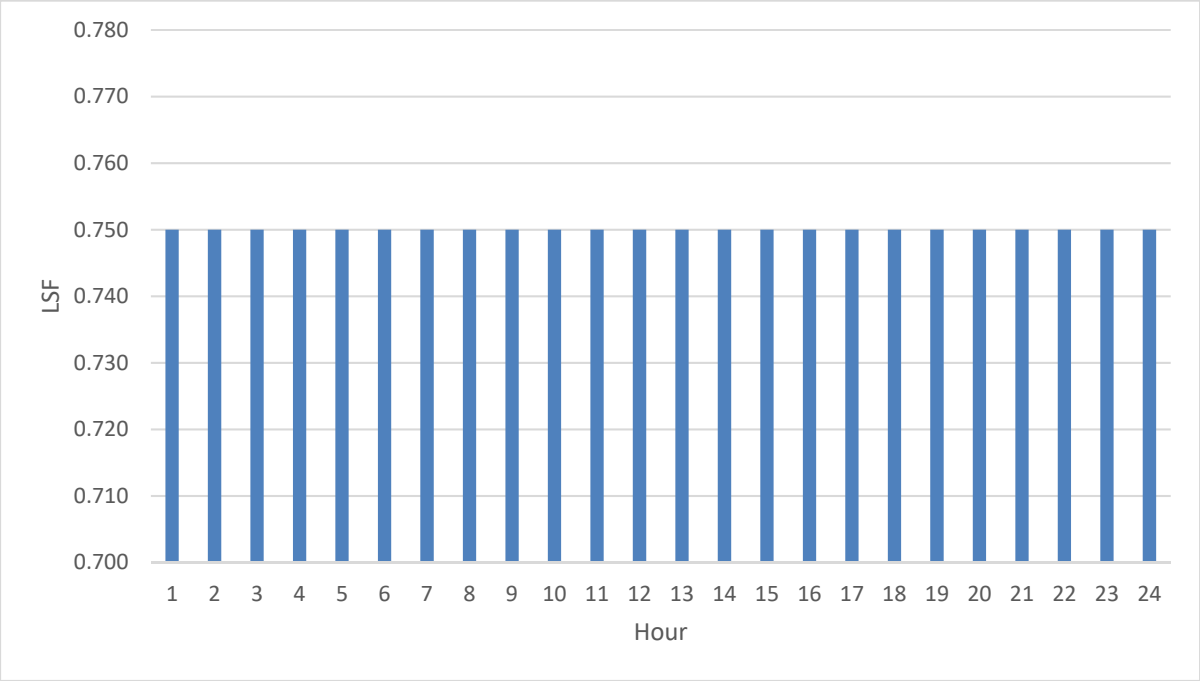

Figure 36 – Load scaling factor of bus-14 in DR Case Problem (on the typical winter day)

Generally, system demand, in this case, will be lower than the Base Case because of the load curtailment. Hence, the expensive generator commitment (generator at bus-1) will be lower as compared to its commitment in the Base Case. Bus-3 generator delivers its maximum available power (0.5 pu) as it is the cheapest. The generator at bus-2 is loaded with its maximum possible power (0.8 pu) most of the time except between hours 7-13 when it shares the system demand with bus-1 generator such that the operating costs are minimal.

As for the LSF, it is equal to 1 at some buses for the whole day. This means that in order to reach the optimal solution of minimum operating costs, these buses should not curtail any load and this is because their consumption of power is cheaper than the incentives they would receive in the case of load curtailment. Another example is bus-14, where the solution shows that, at the optimal point, bus-14 LSF is at its minimum value of 0.75 all the time. This is mainly because paying the maximum incentives to the customers contributing in the DR program (corresponding to maximum load curtailment) is more economical for the utility than generating enough power to cover the demand at this bus. The key reason for this is that this bus is distant from the generating stations at buses-1, 2 and 3.

4.4.3 Test Case #3

In test case #3, the OPF model is solved using the objective function and constraints of the BESS Case Problem. For the typical winter day, the commitments of generators at buses 1, 2 and 3 are shown in Figures 37-39 respectively. Also, the battery power and stored energy are shown in Figures 40 and 41 respectively. The annual cost incurred by the utility, in this case, is $33,589,662.

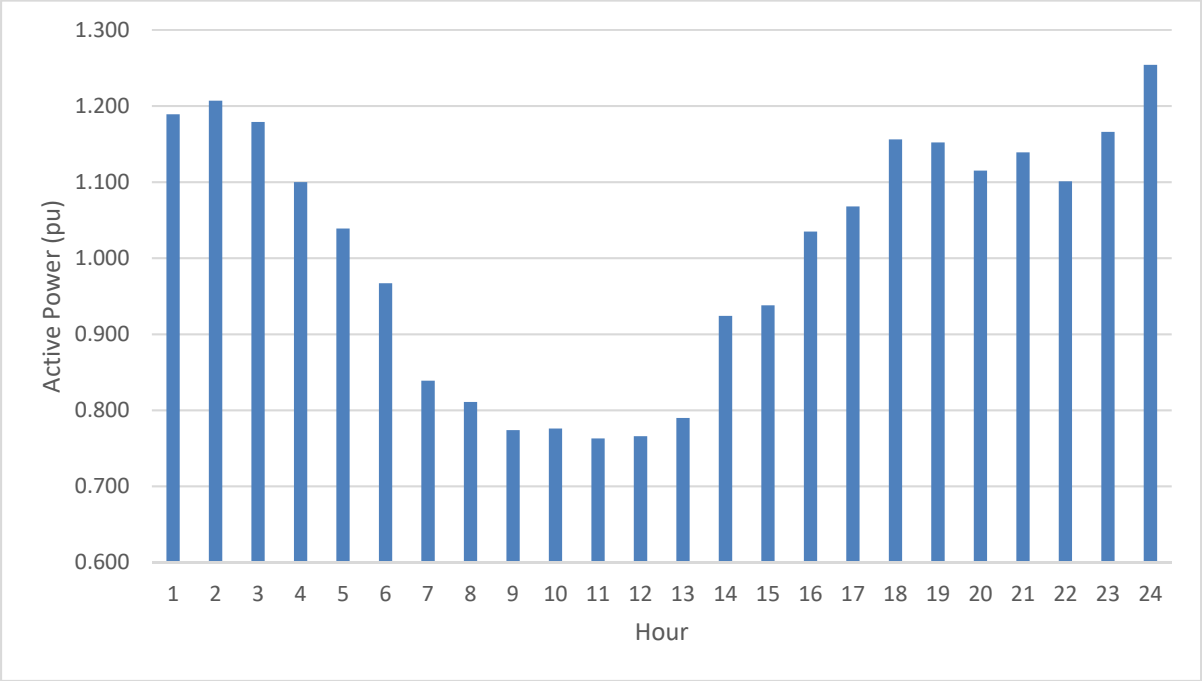

Figure 37 – Commitment of bus-1 generator in BESS Case Problem (on the typical winter day)

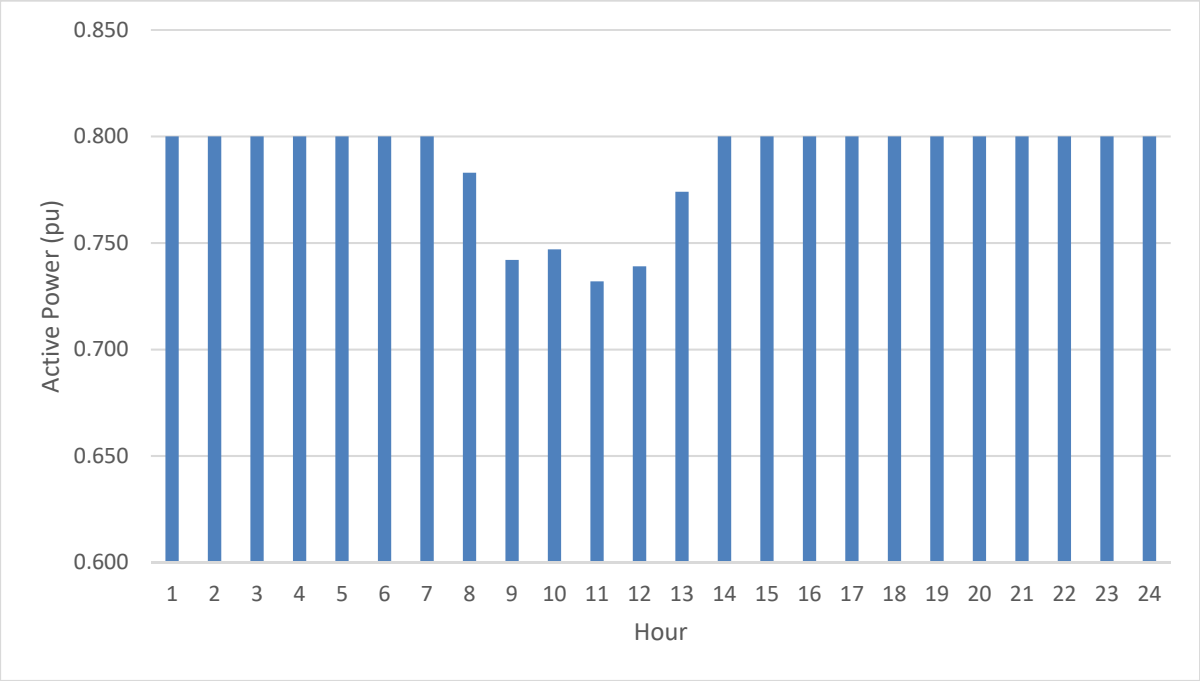

Figure 38 – Commitment of bus-2 generator in BESS Case Problem (on the typical winter day)

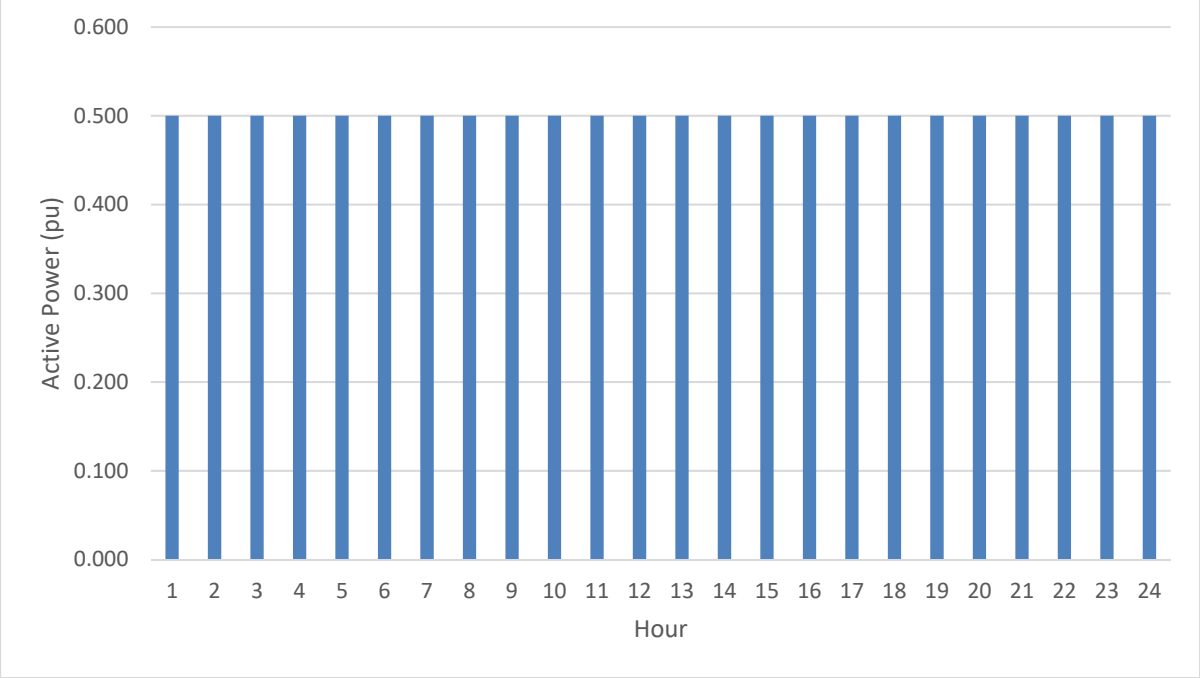

Figure 39 – Commitment of bus-3 generator in BESS Case Problem (on the typical winter day)

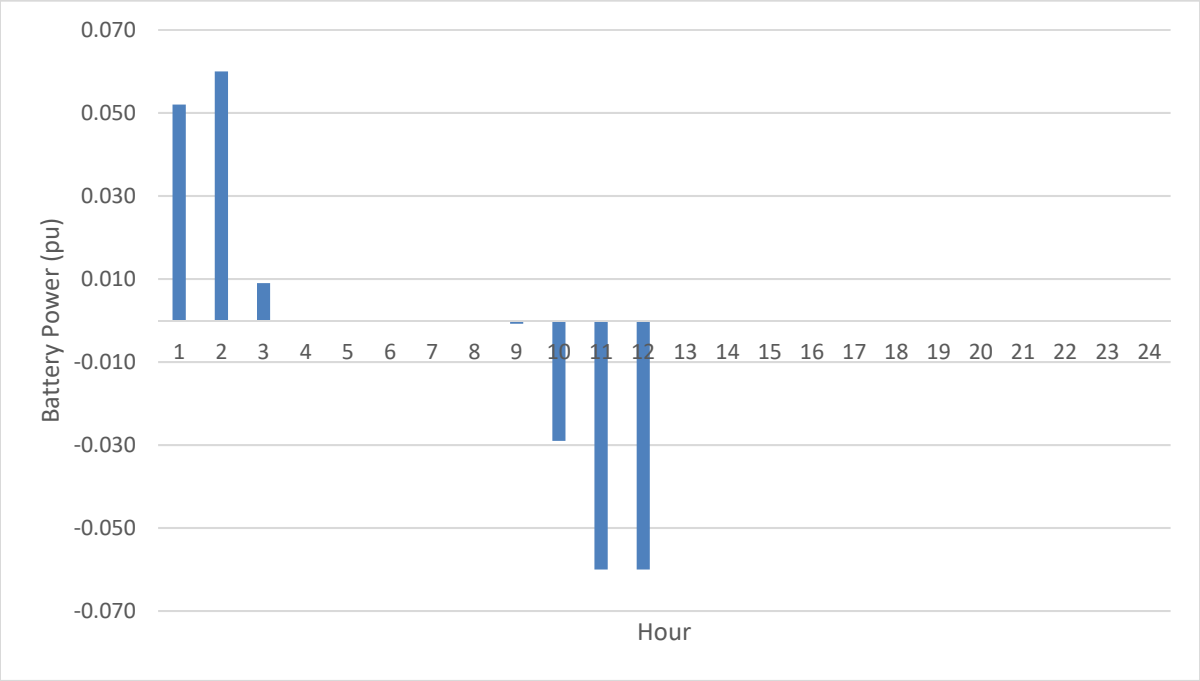

Figure 40 – Battery power in BESS Case Problem (on the typical winter day)

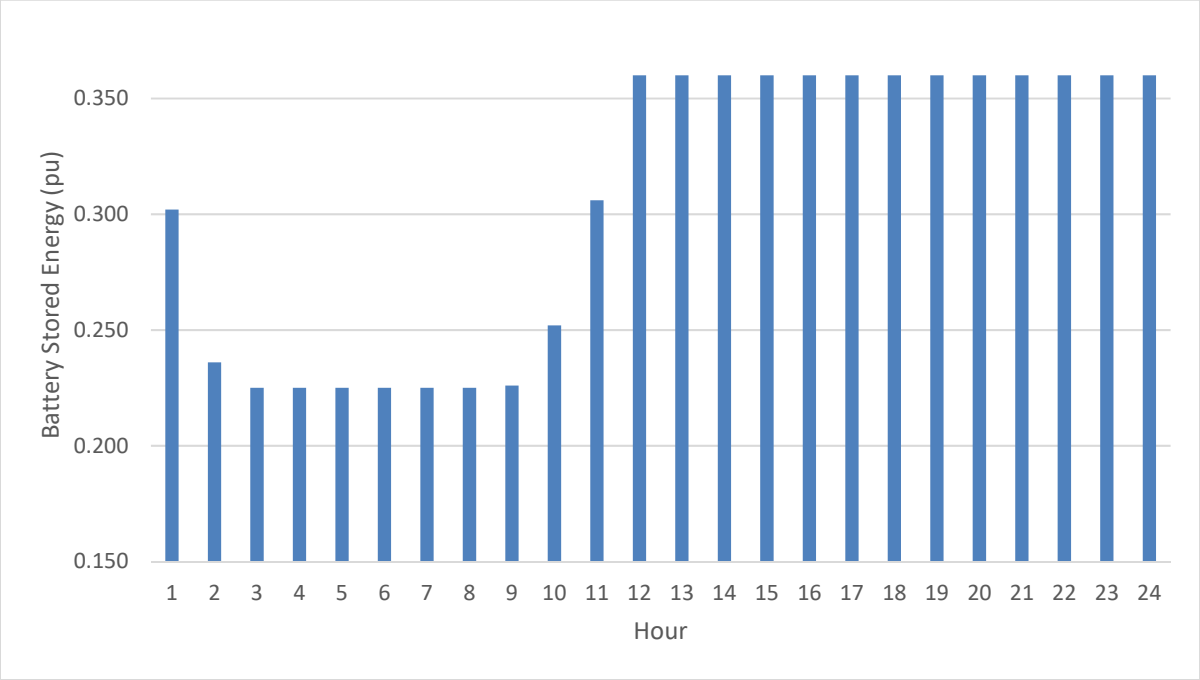

Figure 41 – Battery stored energy in BESS Case Problem (on the typical winter day)

Figure 40 shows the optimal operation pattern of the BESS if it is operated with the objective of cost minimization.

The commitment of the generators, in this case, are exactly the same as in the Base Case except for the hours where the battery is operational. When the battery is discharging, the generators commitment will be lower as they will be relieved from supplying some amount of power handled by the battery. This happens in hours 1-3. The commitment of the conventional generators increases beyond the corresponding values in the Base Case when the battery is charging. In this period, generators have to cover both the system demand and the battery charging power. This happens at hours 9-12.

When the battery is not operating, bus-3 generator delivers its maximum available power (0.5 pu) as it is the cheapest. The generator at bus-2 is loaded with its maximum possible power (0.8 pu) most of the time except between hours 8-13 when it shares the system demand with bus-1 generator such that the costs are minimal.

4.4.4 Locational Marginal Costs Comparison

For the typical winter day, Figures 42-54 show the comparison between the Locational Marginal Costs (LMCs) at the system buses in the three different test cases. Bus-7 is a fictitious bus (not a real one) which is introduced only for the analysis of the three-winding transformer connecting buses-4, 8 and 9; hence, this bus has no LMC.

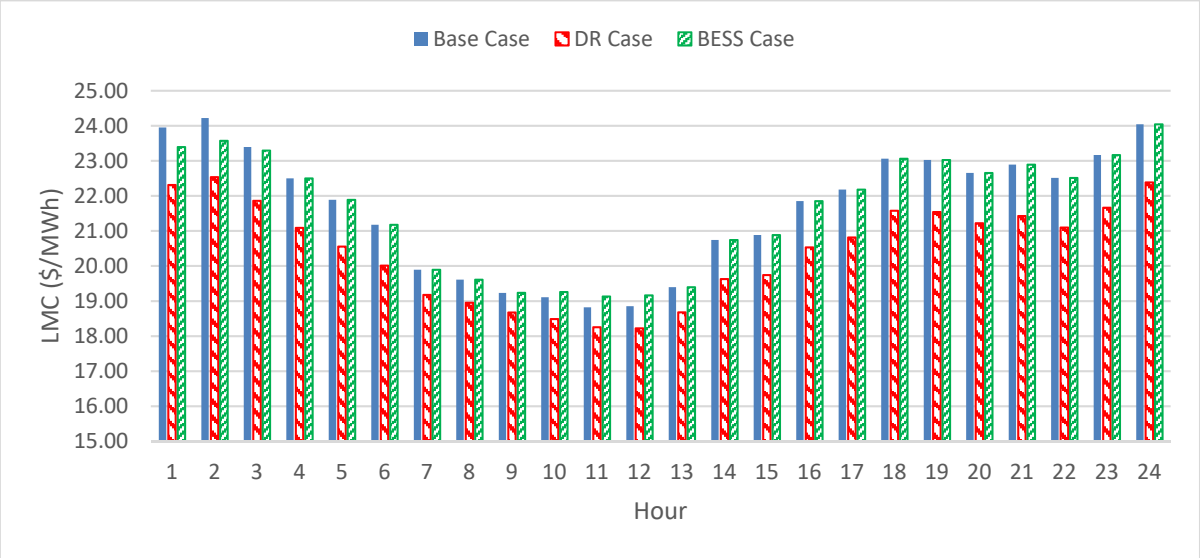

Figure 42 – LMCs at bus-1 (on the typical winter day)

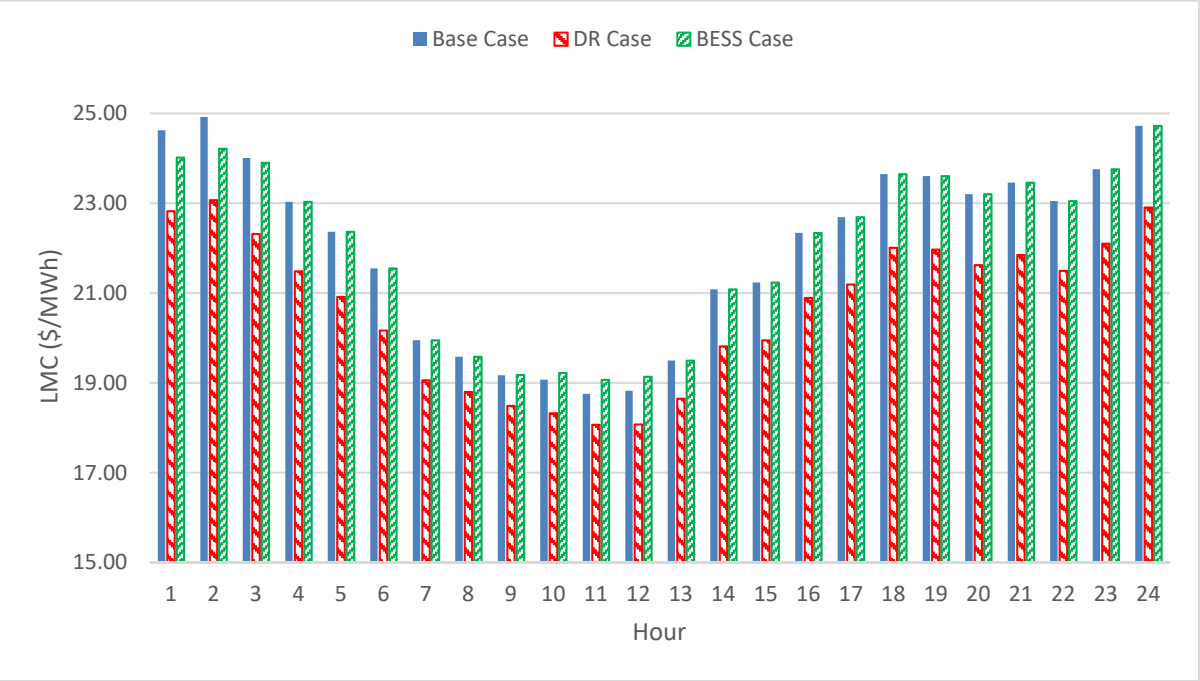

Figure 43 – LMCs at bus-2 (on the typical winter day)

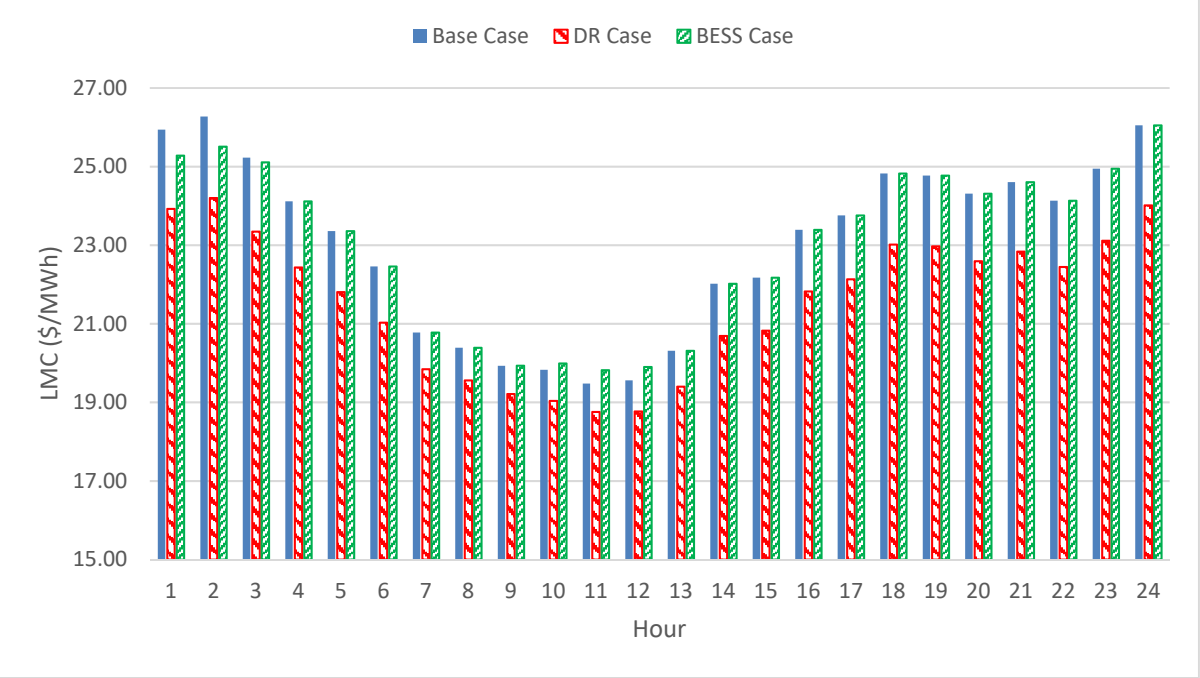

Figure 44 – LMCs at bus-3 (on the typical winter day)

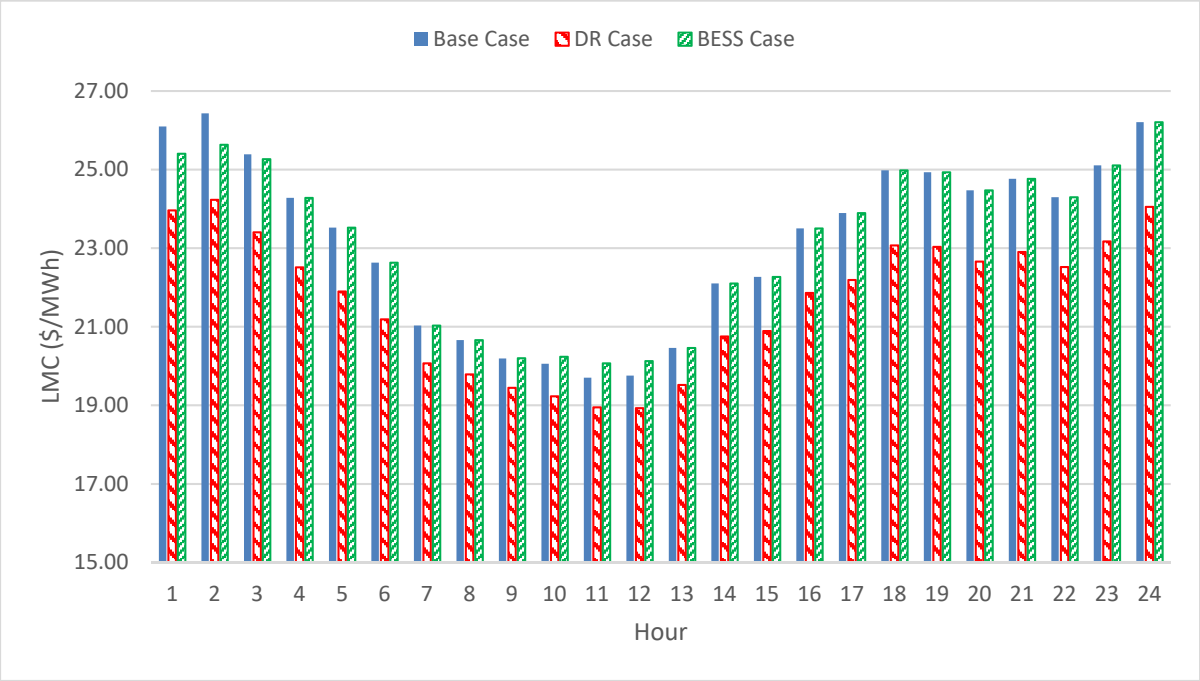

Figure 45 – LMCs at bus-4 (on the typical winter day)

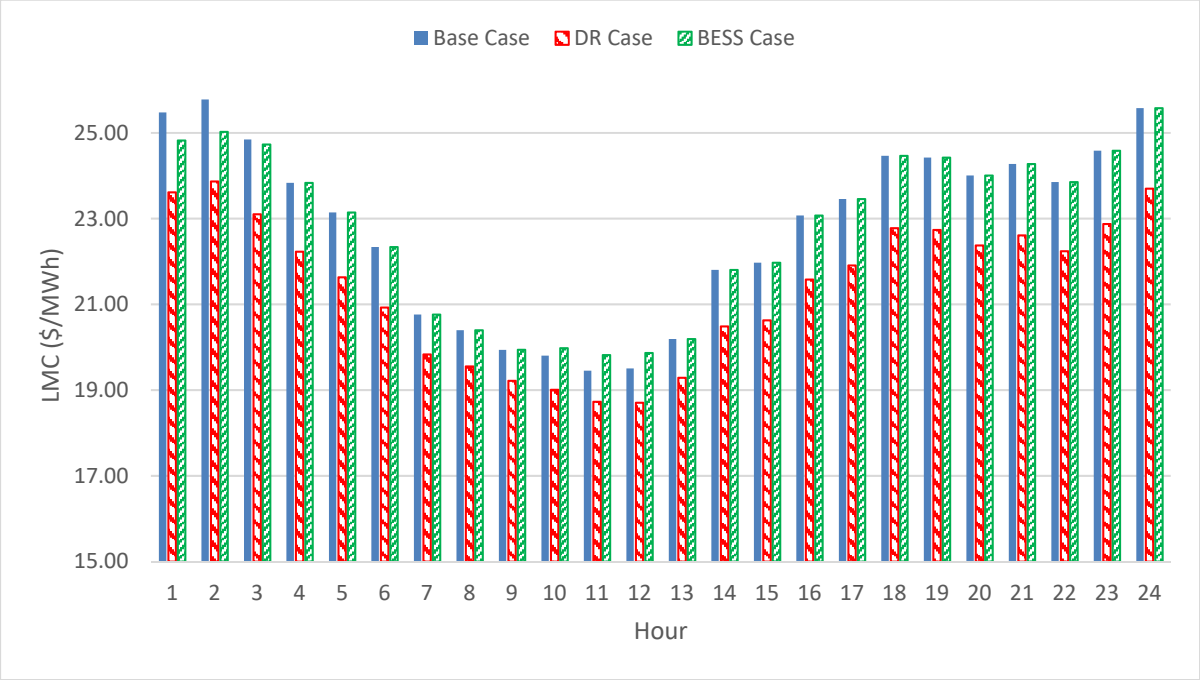

Figure 46 – LMCs at bus-5 (on the typical winter day)

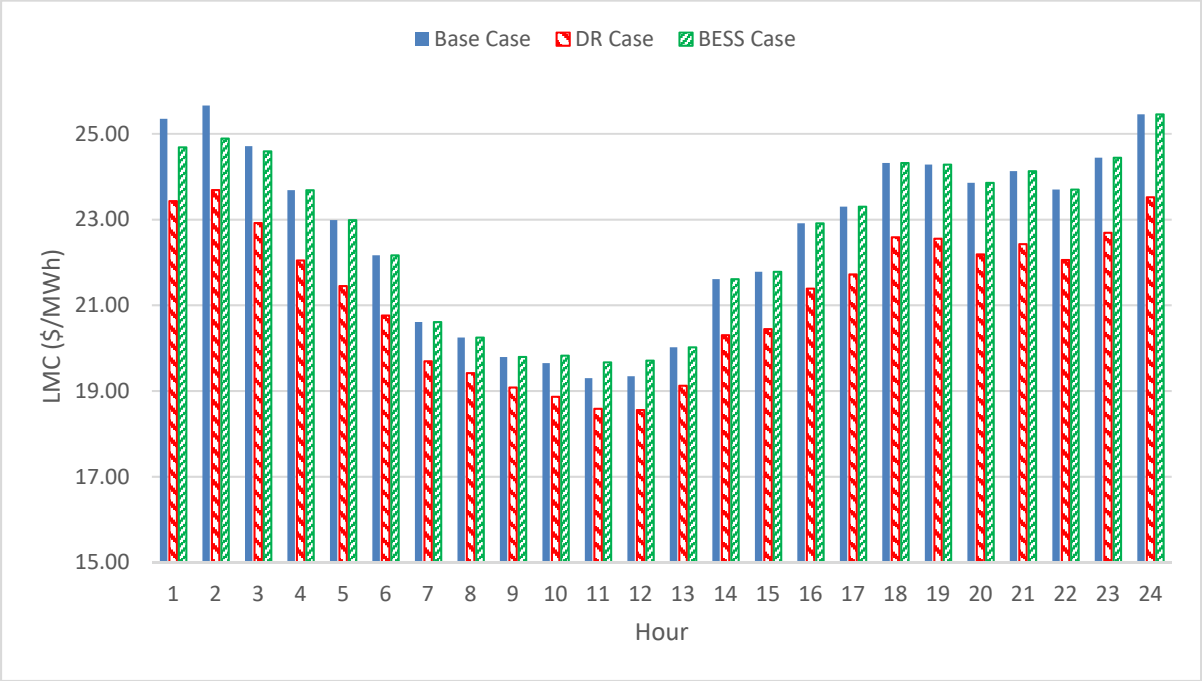

Figure 47 – LMCs at bus-6 (on the typical winter day)

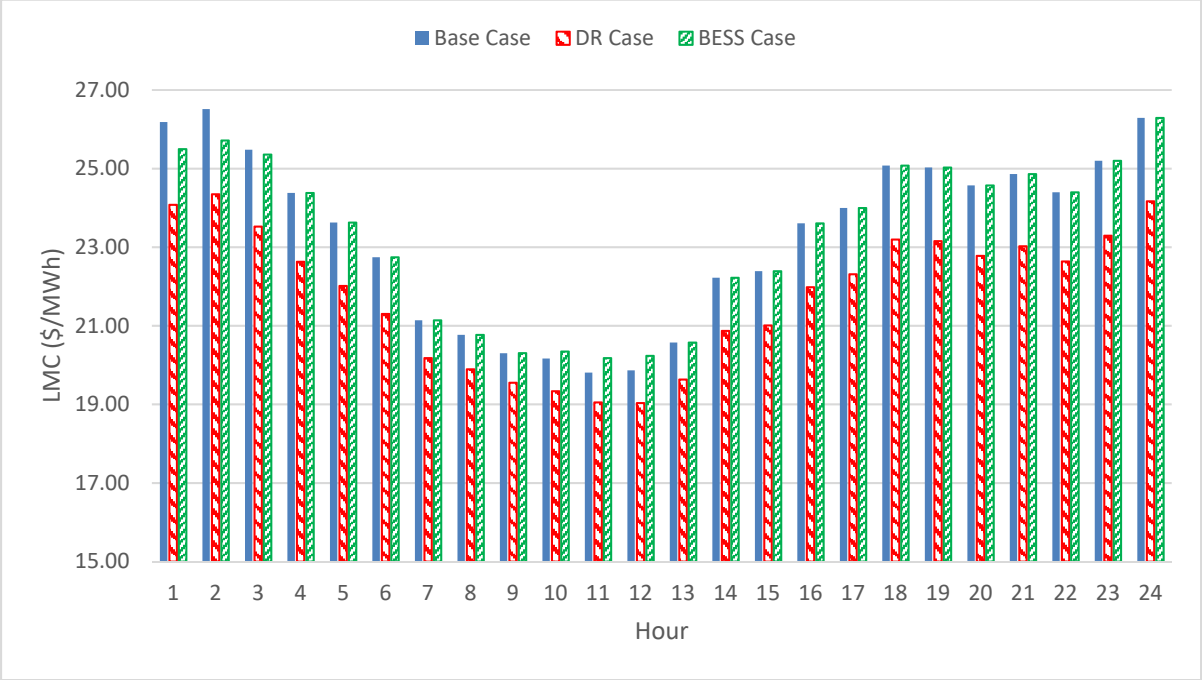

Figure 48 – LMCs at bus-8 (on the typical winter day)

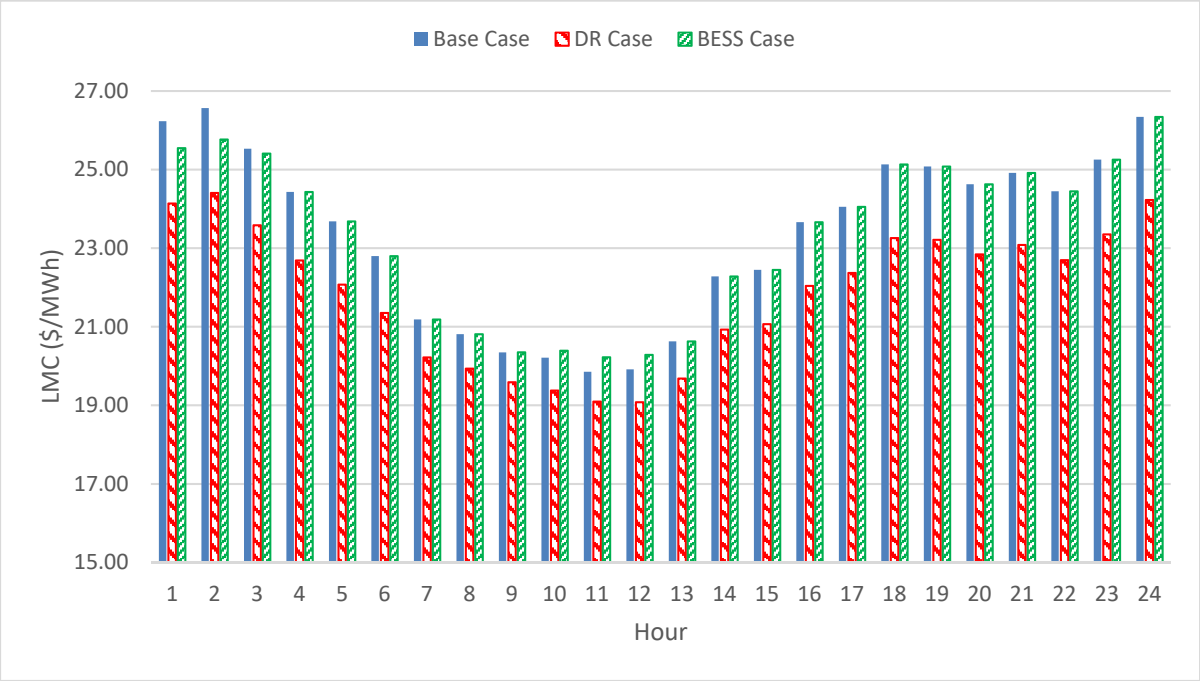

Figure 49 – LMCs at bus-9 (on the typical winter day)

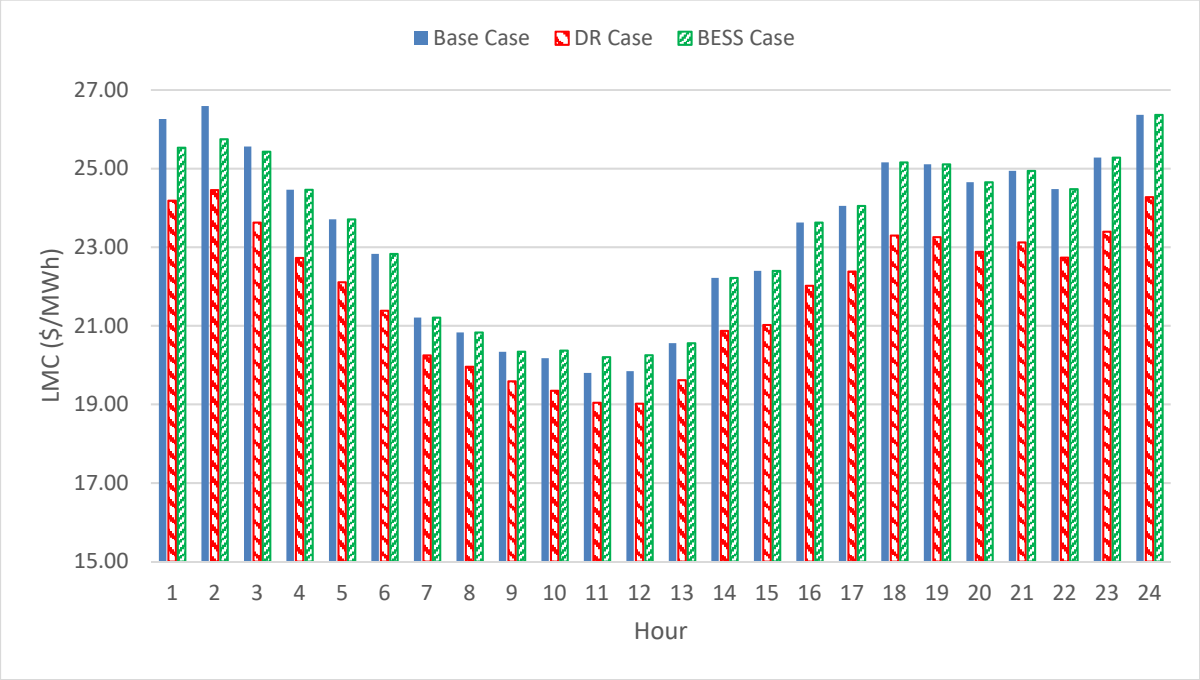

Figure 50 – LMCs at bus-10 (on the typical winter day)

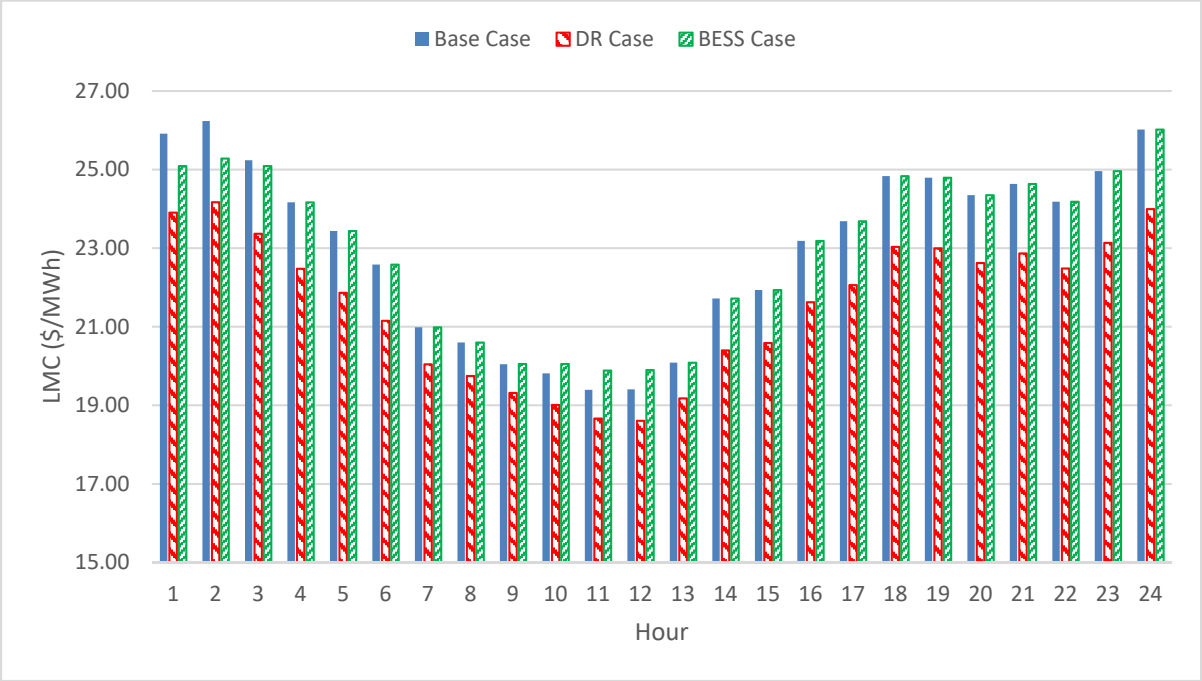

Figure 51 – LMCs at bus-11 (on the typical winter day)

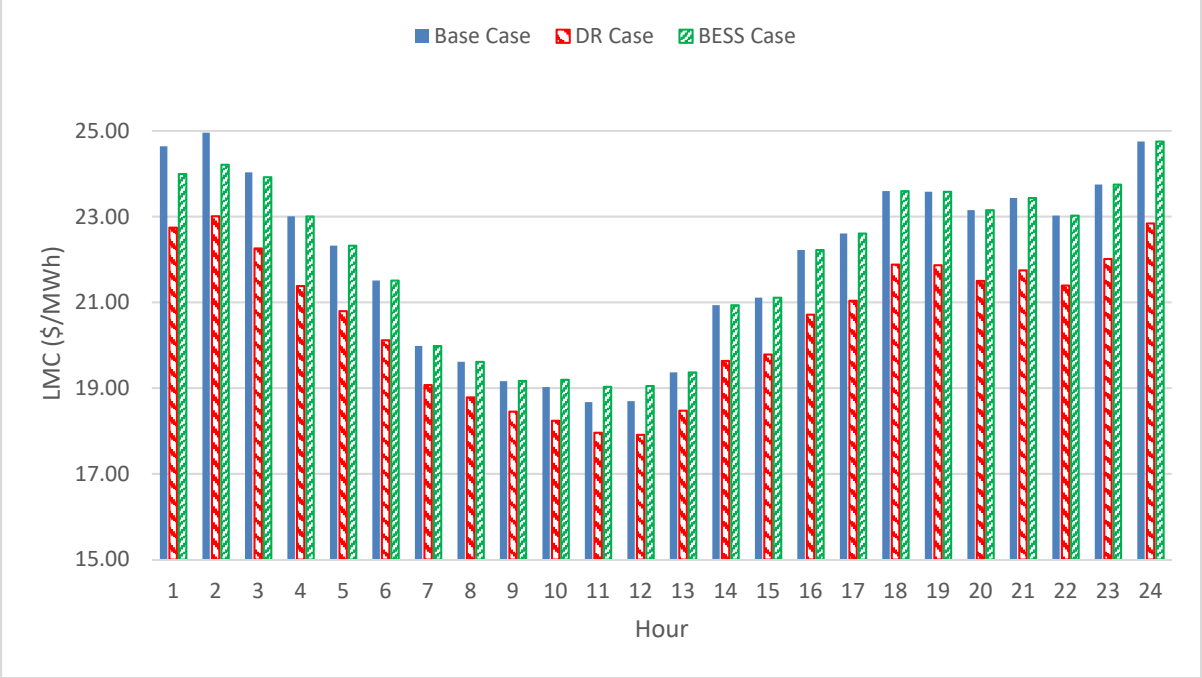

Figure 52 – LMCs at bus-12 (on the typical winter day)

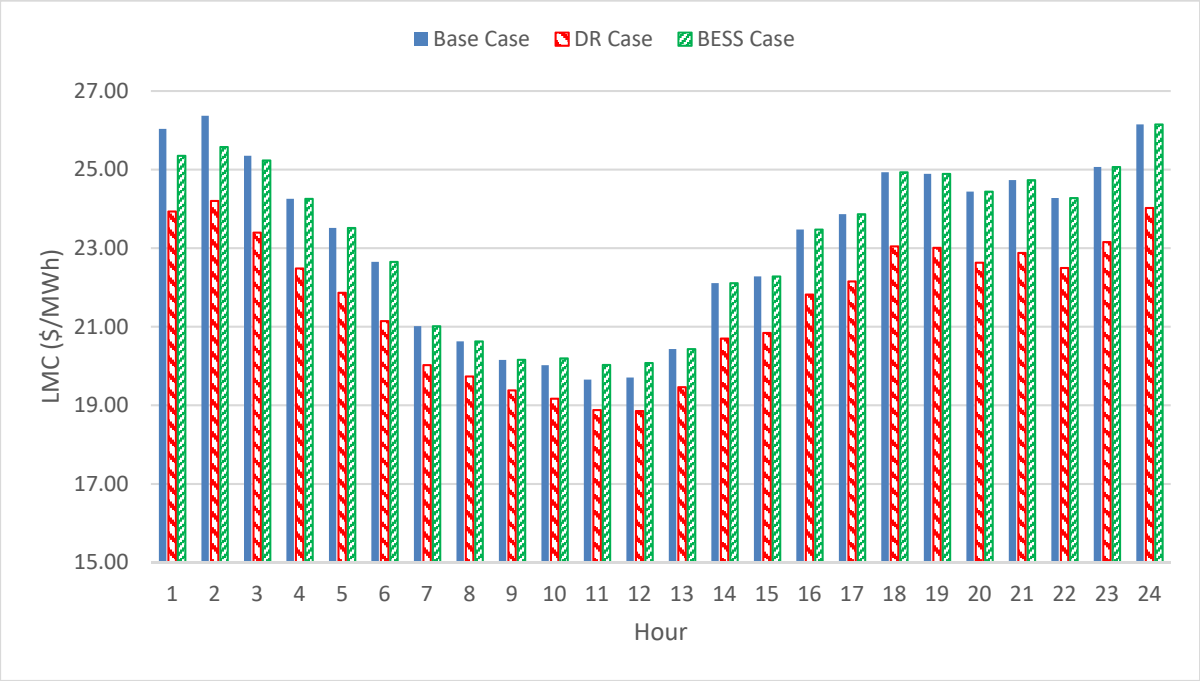

Figure 53 – LMCs at bus-13 (on the typical winter day)

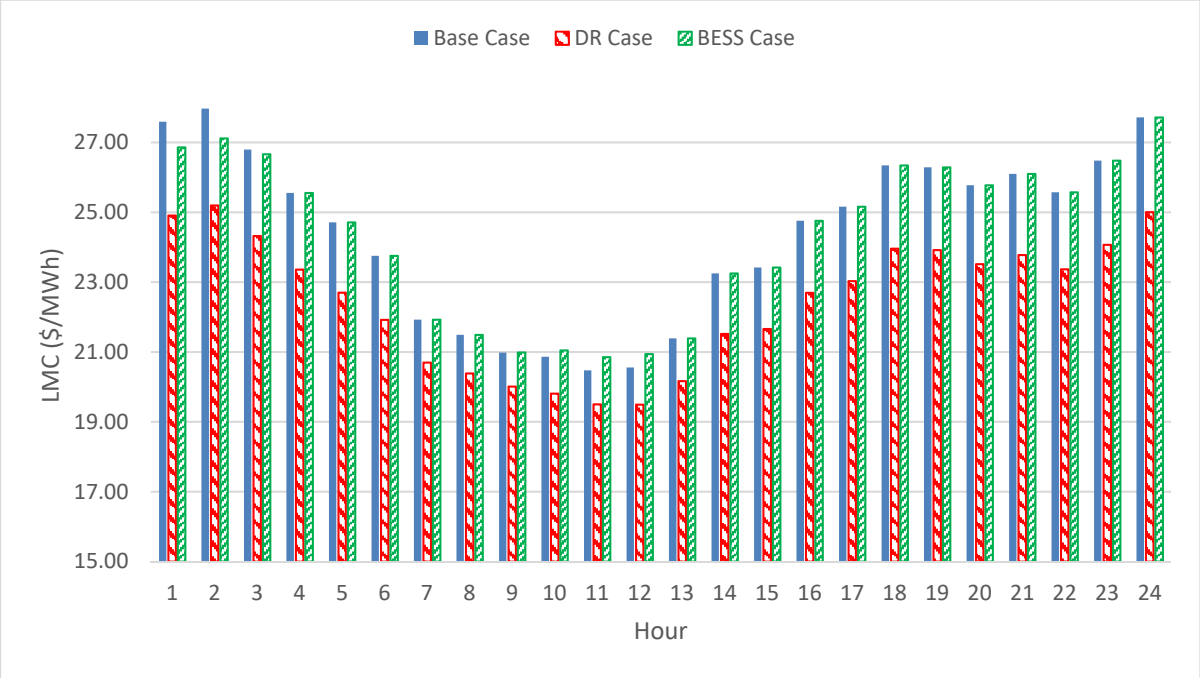

Figure 54 – LMCs at bus-14 (on the typical winter day)

Comparing the generators commitments in the Base Case and the DR Case from Figure 26-28 and 29-31, the utility savings from relieving the generators outweigh the costs incurred by the utility in the DR Case, and this is evident in the total costs in both cases. This results in making the LMCs in the DR Case lower than those of the Base Case as illustrated in Figures 42-54.

Furthermore, to compare the Base Case and the BESS Case, it can be split into two periods:

a. The battery is not operational (all day except hour 1-3 and 9-12): the generators commitments are the same in both cases (Figures 26-28 and 37-39). This means that the incurred costs are the same. Consequently, LMCs in both cases are the same in this period.

b. The battery is operational (discharging during hours 1-3 and charging during hours 9-12): the generator commitments will be different in both cases (Figures 26-28 and 37-39). So, the incurred costs will not be the same, and consequently, the LMCs will differ. On the one hand, during the discharging period (hours 1-3), the LMCs in the BESS Case are lower than those in the Base Case. On the other hand, during the charging hours (hours 9-12), the BESS Case LMCs are higher as the conventional generation commitments increase to supply the system demand and charge the battery.

   Also, charging the battery occurs during the interval with the lowest LMCs (hours 9-12) to achieve the objective of minimum operating costs (Figures 40 and 42-54).

4.5 Summary

In this chapter, the Optimal Power Flow (OPF) problem is formulated in three different cases that have different mathematical expressions of objective functions and mainly the same constraints. This is implemented in order to assess the impact of applying a DR program and utilizing an existing BESS on the total costs incurred by the utility and the locational marginal costs (LMCs) at different system buses. The results of Chapter-3 are used as inputs to the mathematical models developed in this chapter, and the following output quantities are obtained from three test cases:

1. Total incurred costs, conventional generation commitments and LMCs at each bus (All Cases).
2. Load Scaling Factors at each bus that represent DR at each bus (DR Case).
3. Battery Power and Stored Energy (BESS Case).

Chapter 5
Conclusion and Future Work

5.1 Summary of the Thesis

The deployment of renewable energy resources integration to the electrical power networks is expected to increase in the future. This is because of the recent trend to reduce the greenhouse gas emissions and the dependence on fossil fuels in generating electricity owing to their environmental impact which became apparent in climate change. The main obstacle to this spread is that these resources are not dispatchable and their coincidence with demand is not guaranteed. In other words, these energy sources are not reliable on their own owing to their intermittent nature which affects the system reliability. This is where energy storage means can play a major role. Also in the context of Smart Grid (SG), terms like Demand Side Management (DSM) emerged which promotes customers' interaction and response by using the load as an additional degree of freedom to guarantee supply/demand balance; one of the main categories of DSM is Demand Response (DR).

In this thesis, mathematical models that represent the stochastic nature of the solar and wind generation are developed. The models utilize historical data of solar irradiance, PV modules ambient temperatures, wind speed and system demand to calculate the most probable (expected) values of solar, wind and load powers by applying Monte Carlo Simulations on this available data. The profiles of the solar irradiance, wind speed and system demand for four typical days (representing the four seasons) are obtained.

These values are then used as inputs to an Optimal Power Flow (OPF) model in which three different cases are compared:

1. A Base Case Problem: a system with neither DR programs applied nor BESS utilized to fulfill the objective of cost minimization.
2. A DR Case Problem: a DR program is applied in which the participating customers receive incentives for the curtailed load.
3. A BESS Case Problem: an existing BESS is utilized with the objective of cost minimization.

Three different objective functions are formulated with their relevant constraints. Three test cases are introduced to represent each of the cases mentioned above, and the solutions are reached. The system under study is the IEEE 14-bus system.

5.2 Conclusion

The results of the three test cases show that the application of a DR program results in considerable cost savings from the utility point of view which has a direct influence on the LMCs at system buses. This -in turn- will result in lowering the prices of electricity at these buses (locational marginal prices).

Also, utilizing an existing BESS with the objective of cost minimization results in savings in total incurred costs depending on the maturity of the energy storage technology, and consequently the running costs of operating it. The overall operation pattern of the BESS results in cost savings as compared to a system with no BESS employed with the objective of operating cost minimization.

Moreover, comparing the results of DR Case and BESS Case, applying a DR program is more efficient in terms of total cost savings and LMCs. This is mainly because of the time frame of the model studied in this thesis. Therefore, a test case with both DR program and BESS was not studied in this model as it is evident from the results that DR will have the upper hand and the BESS will be slightly dispatched. Other models can be studied where BESS offers competitive cost savings as compared to DR. For example: a real-time (RT) model would present BESS as a superior technique owing to its fast response capability.

5.3 Future Work

The work of this thesis can be extended as follows:

1. Adopt a non-linear relationship between the incentives received by the DR program participating consumers and the curtailed load in the DR Case Problem.
2. Assess the impact of a BESS in a real-time (RT) model to evaluate the influence of fast response capability of such system on the problem solution.
3. Examine the impact of the BESS location / capacity on the overall cost savings.

Bibliography

[1] McLarnon, Frank R., and Elton J. Cairns. "Energy storage." Annual review of energy 14.1 (1989): 241-271.

[2] Ibrahim, Hussein, Adrian Ilinca, and Jean Perron. "Energy storage systems—characteristics and comparisons." Renewable and sustainable energy reviews 12.5 (2008): 1221-1250.

[3] Díaz-González, Francisco, et al. "A review of energy storage technologies for wind power applications." Renewable and sustainable energy reviews 16.4 (2012): 2154-2171.

[4] Fuchs, Georg, et al. "Technology overview on electricity storage." ISEA, Aachen, Juni (2012).

[5] Dekka, Apparao, et al. "A survey on energy storage technologies in power systems." Electrical Power and Energy Conference (EPEC), 2015 IEEE. IEEE, 2015.

[6] Palensky, Peter, and Dietmar Dietrich. "Demand side management: Demand response, intelligent energy systems, and smart loads." IEEE transactions on industrial informatics 7.3 (2011): 381-388.

[7] Qdr, Q. "Benefits of demand response in electricity markets and recommendations for achieving them." US Dept. Energy, Washington, DC, USA, Tech. Rep (2006).

[8] Albadi, Mohamed H., and Ehab F. El-Saadany. "A summary of demand response in electricity markets." Electric power systems research 78.11 (2008): 1989-1996.

[9] Elnashar, Mohab. "Enabling high wind penetration in electrical grids." (2012).

[10] Monticelli, A., M. V. F. Pereira, and S. Granville. "Security-constrained optimal power flow with post-contingency corrective rescheduling." IEEE Transactions on Power Systems 2.1 (1987): 175-180.

[11] Greening, Lorna A. "Demand response resources: Who is responsible for implementation in a deregulated market?." Energy35.4 (2010): 1518-1525.

[12] Aalami, H. A., M. Parsa Moghaddam, and G. R. Yousefi. "Demand response modeling considering interruptible/curtailable loads and capacity market programs." Applied Energy 87.1 (2010): 243-250.

[13] Evans, Annette, Vladimir Strezov, and Tim J. Evans. "Assessment of utility energy storage options for increased renewable energy penetration." Renewable and Sustainable Energy Reviews 16.6 (2012): 4141-4147.

[14] Luo, Xing, et al. "Overview of current development in electrical energy storage technologies and the application potential in power system operation." Applied Energy 137 (2015): 511-536.

[15] Cárdenas, Bruno, and Noel León. "High temperature latent heat thermal energy storage: Phase change materials, design considerations and performance enhancement techniques." Renewable and sustainable energy reviews 27 (2013): 724-737.

[16] Denholm, Paul, et al. "The role of energy storage with renewable electricity generation." (2010): 1.

[17] "Technology characterization." *Global CCS Institute*, [Online]. Available: https://hub.globalccsinstitute.com/publications/renewable-electricity-futures-study-volume-2-renewable-electricity-generation-and-storage-technologies/123-technology-characterization. Accessed: 2017-09-30.

[18] Christie, R. "Power systems test case archive, University of Washington." Electrical Engineering. https://www2.ee.washington.edu/research/pstca (2000).

[19] "*A Data Sheet for IEEE 14 Bus System.*", [Online]. Available: www.academia.edu/7781632/a_data_sheets_for_ieee_14_bus_system. Accessed: 2017-09-01.

[20] Billinton, Roy, et al. "A reliability test system for educational purposes-basic data." IEEE Transactions on Power Systems 4.3 (1989): 1238-1244.

[21] *SILIKEN - Innovation Experience*, [Online]. Available: www.siliken.com/ Accessed: 2017-07-18.

[22] Samsung Renewable Energy Inc., and Pattern Renewable Holdings Canada ULC. "10 Wind Turbine Specification Report for Armow Wind Project." (2012).

[23] *Natural Resources Canada*, [Online]. Available: www.nrcan.gc.ca/home. Accessed: 2017-08-05.

[24] *Alberta Electric System Operator*, [Online]. Available: www.aeso.ca/. Accessed: 2017-08-05.

[25] Abdelaziz, A. Y., et al. "Optimal allocation of stochastically dependent renewable energy based distributed generators in unbalanced distribution networks." Electric Power Systems Research 119 (2015): 34-44.

[26] Abdelaziz, A. Y., et al. "A novel Monte Carlo based modeling strategy for wind based renewable energy sources." Power Systems Conference (MEPCON), 2016 Eighteenth International Middle East. IEEE, 2016.

[27] Atwa, Y. M., et al. "Optimal renewable resources mix for distribution system energy loss minimization." IEEE Transactions on Power Systems 25.1 (2010): 360-370.

[28] Alotaibi, Majed. Modeling of renewable resources in distribution system planning and operation. MS thesis. University of Waterloo, 2014.

[29] Atwa, Yasser. "Distribution system planning and reliability assessment under high DG penetration." (2010).

[30] "GAMS-A User's Guide," 2008, New York.

[31] Awad, Ahmed SA, et al. "Impact of energy storage systems on electricity market equilibrium." IEEE Transactions on Sustainable Energy 5.3 (2014): 875-885.

Appendix A
System Data

IEEE 14-bus system is shown hereunder in Figure 55.

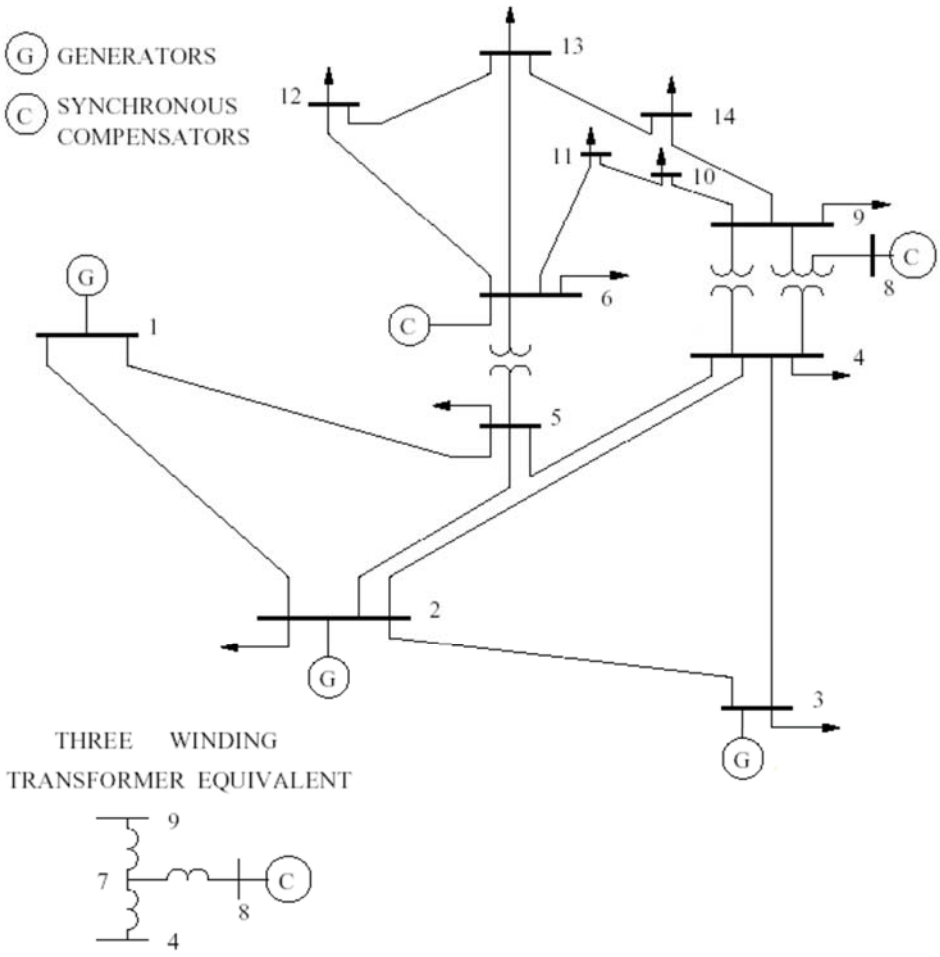

Figure 55 –IEEE 14-bus system

The system lines and transformer data is listed in Table 1. The data is given in per unit on a 100 MVA base. Also, the active and reactive power loads are given in Table 2 [18]. The generators data is listed in Table 3.

From bus no.	To bus no.	Resistance (pu)	Reactance (pu)	Line charging susceptance (pu)	Transformer tap ratio
1	2	0.01938	0.05917	0.0528	N/A
1	5	0.05403	0.22304	0.0492	N/A
2	3	0.04699	0.19797	0.0438	N/A
2	4	0.05811	0.17632	0.0340	N/A
2	5	0.05695	0.17388	0.0346	N/A
3	4	0.06701	0.17103	0.0128	N/A
4	5	0.01335	0.04211	0	N/A
4	7	0	0.20912	0	0.978
4	9	0	0.55618	0	0.969
5	6	0	0.25202	0	0.932
6	11	0.09498	0.19890	0	N/A
6	12	0.12291	0.25581	0	N/A
6	13	0.06615	0.13027	0	N/A
7	8	0	0.17615	0	N/A
7	9	0	0.11001	0	N/A
9	10	0.03181	0.08450	0	N/A
9	14	0.12711	0.27038	0	N/A
10	11	0.08205	0.19207	0	N/A
12	13	0.22092	0.19988	0	N/A
13	14	0.17093	0.34802	0	N/A

Table 1 – Lines and transformers data [18]

Bus no.	Active power load (MW)	Reactive power load (MVAR)
2	21.7	12.7
3	94.2	19.0
4	47.8	-3.9
5	7.6	1.6
6	11.2	7.5
9	29.5	16.6
10	9.0	5.8
11	3.5	1.8
12	6.1	1.6
13	13.5	5.8
14	14.9	5.0

Table 2 – Active and reactive power load data [18]

Generator at bus no.	P_{min} (MW)	P_{max} (MW)	Q_{min} (MVAR)	Q_{max} (MVAR)	a ($/(MW)^2.h)	b ($/MWh)	c ($/h)
1	10	160	0	0	0.05	11.50	105
2	20	80	-40	50	0.05	11.75	44.1
3	20	50	0	40	0.05	11.9375	40.6
6	-	-	-6	24	-	-	-
8	-	-	-6	24	-	-	-

Table 3 – Generators capacities and cost coefficients [20]

Appendix B
Solar Module Data Sheet

The solar module data sheet is in the next page. It includes the data used in the modeling the solar system in Chapter-3.

SLK60P6L SLV/WHT 220 W - 255 W

Poly-Crystalline Solar Modules

siliken

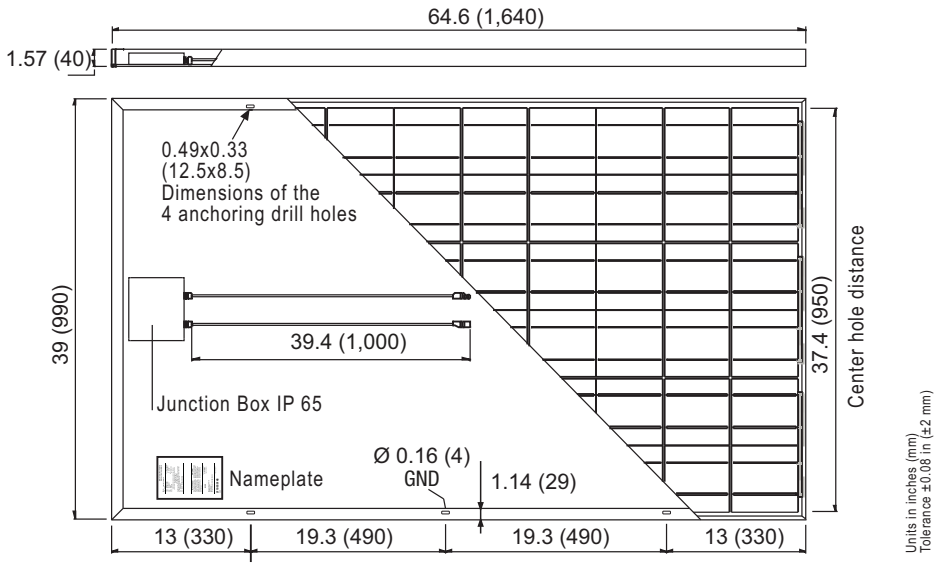

Construction Characteristics

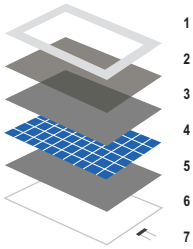

Frame Cross Section

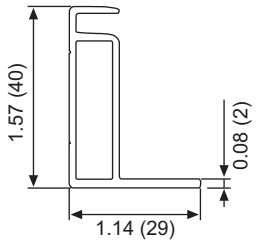

SLK60P6L - 225W
I-V and Pmax characteristics with a variety of radiation levels at 77ºF (25ºC)

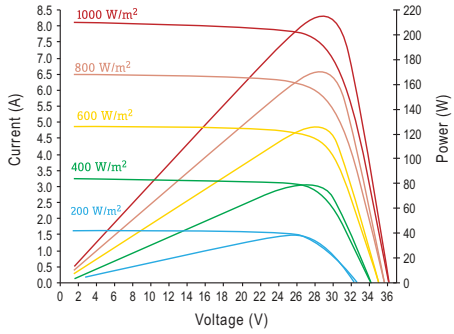

SLK60P6L - 225W
I-V characteristics with a variety of cell temperatures at 92.94W/ft² (1,000 W/m²)

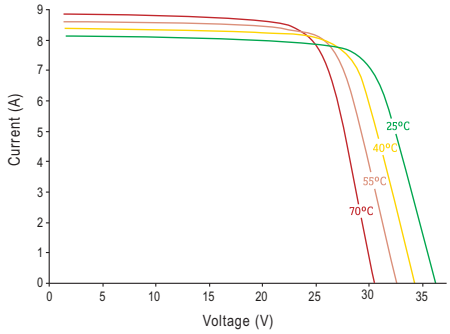

Weak light performance at Pmpp 77ºF (25ºC)
Siliken module's average

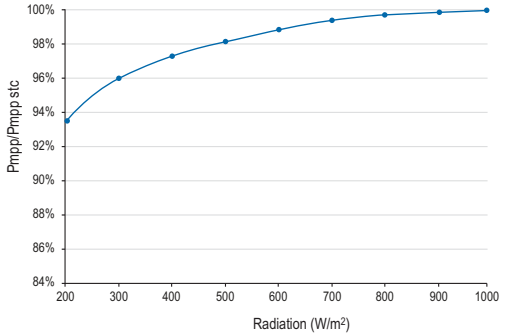

Mechanical Data

Dimensions (LxWxD)	64.6 x 39 x 1.57 in (1640 x 990 x 40 mm)
Weight	41.9 lbs (19 kg)
Output Cables	RHW-2 symmetrical length cable 39.4 in (1 m) Multi-Contact connectors (MC4)
Junction Box	IP-65 rated with bypass diodes
Frame	Anodized aluminum of 15 microns of thickness type 6063 T6
Front Glass	0.125 in (3.2 mm) low iron tempered glass with high transmissivity
Solar Cells	60 Poly-crystalline cells 6 x 6 in (156 x 156 mm)

Certifications

UL Listed	UL 1703
Fire Rating	Class C
TÜV Certified	IEC 61215 / IEC 61730 / 61701 Salt Mist Corrosion
EC Declaration of conformity (CE Mark)	
CEC (California Energy Commision) Program Registered	
FSEC (Florida Solar Energy Center) PV Module Certification	
MCS Mark (Microgeneration Certification Scheme)	

Electrical Data

Maximum power at STC (+3/0 %)	P_{mp} (W)	220	225	230	235	240	245	250*	255*
Efficiency at STC	η (%)	13.6	13.9	14.2	14.5	14.8	15.1	15.4	15.7
Power per Unit Area	P_{SqFt} (Wp/SqFt)	12.6	12.9	13.2	13.4	13.7	14.0	14.3	14.6
Voltage at Maximum Power	V_{mp} (V)	29.2	29.3	29.5	29.5	29.6	29.6	29.8	29.8
Current at Maximum Power	I_{mp} (A)	7.54	7.68	7.79	7.97	8.12	8.27	8.39	8.56
Open Circuit Voltage	V_{oc} (V)	36.7	36.8	36.9	36.9	37.0	37.0	37.1	37.1
Short Circuit Current	I_{sc} (A)	8.10	8.20	8.32	8.47	8.61	8.75	8.91	9.02
Maximum Voltage UL	V_{max} (V) UL	600							
Temperature Coefficient of Pmp	T_kP_{mp} (%/ºC)	-0.43							
Temperature Coefficient of Voc/Vmp	T_kV_{oc}/T_kV_{mp} (%/ºC)	-0.356 / -0.500							
Temperature Coefficient of Isc/Imp	T_kI_{sc}/T_kI_{mp} (%/ºC)	+0.062 / +0.030							
Normal Operating Cell Temperature	NOCT (ºF)/(ºC)	114.8±3.2 (46±2)							
Series Fuse Rating	A	15							
Bypass Diodes	A / V	15 / 40							
Reverse current test	A	15							

Test Operating Conditions

Temperature	-40 ºF to +185 ºF (-40 ºC to +85 ºC)
Static Load	50 psf (2400 Pa)
Max Load	112.8 psf (5400 Pa)
Impact Resistance	Hailstone impact Ø1 in at 52 mph (Ø25 mm at 23 m/s)

Product Warranty

10 year limited warranty on materials and workmanship

25 Year Linear Power Guarantee

Year 1: 97% of rated output

Years 2-25: 0.7% p.a. reduction

Values at Standard Test Conditions STC: Irradiance 92.94 W/ft² (1,000 W/m²), Air Mass AM 1.5 and cell temperature 77ºF (25ºC)

* Subject to availability.

WARNING: Read the instruction manual carefully before using this product. NOTE: Siliken Canada reserves the right to modify this product without prior notice

Siliken Canada · 1 Yonge Street, Suite 1801 · Toronto ON M5E 1W7 Canada · Tel.: +1 (416) 214-3655 · Fax: +1 (416) 369-0515 · www.siliken.com

April 2011

Appendix C

System Demand Modeling Results

The results of the active and reactive system demand at the load buses in the typical days of the four seasons are presented in Tables 4-11 as a result of the modeling performed in Chapter-3.

		Bus										
		N2	N3	N4	N5	N6	N9	N10	N11	N12	N13	N14
Hour	1	0.215	0.934	0.474	0.075	0.111	0.293	0.089	0.035	0.060	0.134	0.148
	2	0.217	0.942	0.478	0.076	0.112	0.295	0.090	0.035	0.061	0.135	0.149
	3	0.210	0.913	0.463	0.074	0.109	0.286	0.087	0.034	0.059	0.131	0.144
	4	0.204	0.885	0.449	0.071	0.105	0.277	0.085	0.033	0.057	0.127	0.140
	5	0.199	0.864	0.438	0.070	0.103	0.270	0.083	0.032	0.056	0.124	0.137
	6	0.193	0.839	0.426	0.068	0.100	0.263	0.080	0.031	0.054	0.120	0.133
	7	0.183	0.795	0.403	0.064	0.094	0.249	0.076	0.030	0.051	0.114	0.126
	8	0.180	0.782	0.397	0.063	0.093	0.245	0.075	0.029	0.051	0.112	0.124
	9	0.177	0.770	0.391	0.062	0.092	0.241	0.074	0.029	0.050	0.110	0.122
	10	0.180	0.779	0.396	0.063	0.093	0.244	0.074	0.029	0.050	0.112	0.123
	11	0.178	0.771	0.391	0.062	0.092	0.241	0.074	0.029	0.050	0.110	0.122
	12	0.181	0.784	0.398	0.063	0.093	0.246	0.075	0.029	0.051	0.112	0.124
	13	0.191	0.829	0.420	0.067	0.099	0.260	0.079	0.031	0.054	0.119	0.131
	14	0.203	0.881	0.447	0.071	0.105	0.276	0.084	0.033	0.057	0.126	0.139
	15	0.202	0.876	0.445	0.071	0.104	0.274	0.084	0.033	0.057	0.126	0.139
	16	0.206	0.896	0.455	0.072	0.107	0.281	0.086	0.033	0.058	0.128	0.142
	17	0.205	0.890	0.452	0.072	0.106	0.279	0.085	0.033	0.058	0.128	0.141
	18	0.209	0.907	0.460	0.073	0.108	0.284	0.087	0.034	0.059	0.130	0.143
	19	0.208	0.903	0.458	0.073	0.107	0.283	0.086	0.034	0.059	0.129	0.143
	20	0.205	0.892	0.452	0.072	0.106	0.279	0.085	0.033	0.058	0.128	0.141
	21	0.207	0.899	0.456	0.072	0.107	0.281	0.086	0.033	0.058	0.129	0.142
	22	0.204	0.885	0.449	0.071	0.105	0.277	0.085	0.033	0.057	0.127	0.140
	23	0.209	0.907	0.460	0.073	0.108	0.284	0.087	0.034	0.059	0.130	0.144
	24	0.216	0.936	0.475	0.076	0.111	0.293	0.089	0.035	0.061	0.134	0.148

Table 4 – Active power load at different buses on the typical winter day

		Bus										
		N2	N3	N4	N5	N6	N9	N10	N11	N12	N13	N14
Hour	1	0.126	0.188	-0.039	0.016	0.074	0.165	0.058	0.018	0.016	0.058	0.050
	2	0.127	0.190	-0.039	0.016	0.075	0.166	0.058	0.018	0.016	0.058	0.050
	3	0.123	0.184	-0.038	0.016	0.073	0.161	0.056	0.017	0.016	0.056	0.048
	4	0.119	0.178	-0.037	0.015	0.070	0.156	0.054	0.017	0.015	0.054	0.047
	5	0.116	0.174	-0.036	0.015	0.069	0.152	0.053	0.017	0.015	0.053	0.046
	6	0.113	0.169	-0.035	0.014	0.067	0.148	0.052	0.016	0.014	0.052	0.045
	7	0.107	0.160	-0.033	0.013	0.063	0.140	0.049	0.015	0.013	0.049	0.042
	8	0.105	0.158	-0.032	0.013	0.062	0.138	0.048	0.015	0.013	0.048	0.042
	9	0.104	0.155	-0.032	0.013	0.061	0.136	0.047	0.015	0.013	0.047	0.041
	10	0.105	0.157	-0.032	0.013	0.062	0.137	0.048	0.015	0.013	0.048	0.041
	11	0.104	0.155	-0.032	0.013	0.061	0.136	0.047	0.015	0.013	0.047	0.041
	12	0.106	0.158	-0.032	0.013	0.062	0.138	0.048	0.015	0.013	0.048	0.042
	13	0.112	0.167	-0.034	0.014	0.066	0.146	0.051	0.016	0.014	0.051	0.044
	14	0.119	0.178	-0.036	0.015	0.070	0.155	0.054	0.017	0.015	0.054	0.047
	15	0.118	0.177	-0.036	0.015	0.070	0.154	0.054	0.017	0.015	0.054	0.047
	16	0.121	0.181	-0.037	0.015	0.071	0.158	0.055	0.017	0.015	0.055	0.048
	17	0.120	0.179	-0.037	0.015	0.071	0.157	0.055	0.017	0.015	0.055	0.047
	18	0.122	0.183	-0.038	0.015	0.072	0.160	0.056	0.017	0.015	0.056	0.048
	19	0.122	0.182	-0.037	0.015	0.072	0.159	0.056	0.017	0.015	0.056	0.048
	20	0.120	0.180	-0.037	0.015	0.071	0.157	0.055	0.017	0.015	0.055	0.047
	21	0.121	0.181	-0.037	0.015	0.072	0.158	0.055	0.017	0.015	0.055	0.048
	22	0.119	0.178	-0.037	0.015	0.070	0.156	0.054	0.017	0.015	0.054	0.047
	23	0.122	0.183	-0.038	0.015	0.072	0.160	0.056	0.017	0.015	0.056	0.048
	24	0.126	0.189	-0.039	0.016	0.075	0.165	0.058	0.018	0.016	0.058	0.050

Table 5 – Reactive power load at different buses on the typical winter day

		Bus										
		N2	N3	N4	N5	N6	N9	N10	N11	N12	N13	N14
Hour	1	0.211	0.916	0.465	0.074	0.109	0.287	0.088	0.034	0.059	0.131	0.145
	2	0.215	0.932	0.473	0.075	0.111	0.292	0.089	0.035	0.060	0.134	0.147
	3	0.213	0.923	0.468	0.074	0.110	0.289	0.088	0.034	0.060	0.132	0.146
	4	0.203	0.880	0.447	0.071	0.105	0.276	0.084	0.033	0.057	0.126	0.139
	5	0.196	0.849	0.431	0.069	0.101	0.266	0.081	0.032	0.055	0.122	0.134
	6	0.186	0.807	0.409	0.065	0.096	0.253	0.077	0.030	0.052	0.116	0.128
	7	0.183	0.793	0.403	0.064	0.094	0.248	0.076	0.029	0.051	0.114	0.125
	8	0.178	0.771	0.391	0.062	0.092	0.241	0.074	0.029	0.050	0.111	0.122
	9	0.180	0.783	0.398	0.063	0.093	0.245	0.075	0.029	0.051	0.112	0.124
	10	0.179	0.777	0.394	0.063	0.092	0.243	0.074	0.029	0.050	0.111	0.123
	11	0.187	0.814	0.413	0.066	0.097	0.255	0.078	0.030	0.053	0.117	0.129
	12	0.192	0.833	0.423	0.067	0.099	0.261	0.080	0.031	0.054	0.119	0.132
	13	0.198	0.861	0.437	0.069	0.102	0.270	0.082	0.032	0.056	0.123	0.136
	14	0.209	0.907	0.460	0.073	0.108	0.284	0.087	0.034	0.059	0.130	0.143
	15	0.212	0.919	0.466	0.074	0.109	0.288	0.088	0.034	0.060	0.132	0.145
	16	0.216	0.938	0.476	0.076	0.112	0.294	0.090	0.035	0.061	0.134	0.148
	17	0.217	0.942	0.478	0.076	0.112	0.295	0.090	0.035	0.061	0.135	0.149
	18	0.212	0.920	0.467	0.074	0.109	0.288	0.088	0.034	0.060	0.132	0.146
	19	0.215	0.933	0.473	0.075	0.111	0.292	0.089	0.035	0.060	0.134	0.148
	20	0.215	0.935	0.475	0.075	0.111	0.293	0.089	0.035	0.061	0.134	0.148
	21	0.216	0.939	0.477	0.076	0.112	0.294	0.090	0.035	0.061	0.135	0.149
	22	0.215	0.932	0.473	0.075	0.111	0.292	0.089	0.035	0.060	0.134	0.147
	23	0.212	0.922	0.468	0.074	0.110	0.289	0.088	0.034	0.060	0.132	0.146
	24	0.214	0.928	0.471	0.075	0.110	0.291	0.089	0.034	0.060	0.133	0.147

Table 6 – Active power load at different buses on the typical spring day

		Bus										
		N2	N3	N4	N5	N6	N9	N10	N11	N12	N13	N14
Hour	1	0.124	0.185	-0.038	0.016	0.073	0.161	0.056	0.018	0.016	0.056	0.049
	2	0.126	0.188	-0.039	0.016	0.074	0.164	0.057	0.018	0.016	0.057	0.049
	3	0.124	0.186	-0.038	0.016	0.073	0.163	0.057	0.018	0.016	0.057	0.049
	4	0.119	0.178	-0.036	0.015	0.070	0.155	0.054	0.017	0.015	0.054	0.047
	5	0.114	0.171	-0.035	0.014	0.068	0.150	0.052	0.016	0.014	0.052	0.045
	6	0.109	0.163	-0.033	0.014	0.064	0.142	0.050	0.015	0.014	0.050	0.043
	7	0.107	0.160	-0.033	0.013	0.063	0.140	0.049	0.015	0.013	0.049	0.042
	8	0.104	0.156	-0.032	0.013	0.061	0.136	0.047	0.015	0.013	0.047	0.041
	9	0.106	0.158	-0.032	0.013	0.062	0.138	0.048	0.015	0.013	0.048	0.042
	10	0.105	0.157	-0.032	0.013	0.062	0.137	0.048	0.015	0.013	0.048	0.041
	11	0.110	0.164	-0.034	0.014	0.065	0.143	0.050	0.016	0.014	0.050	0.043
	12	0.112	0.168	-0.034	0.014	0.066	0.147	0.051	0.016	0.014	0.051	0.044
	13	0.116	0.174	-0.036	0.015	0.069	0.152	0.053	0.016	0.015	0.053	0.046
	14	0.122	0.183	-0.038	0.015	0.072	0.160	0.056	0.017	0.015	0.056	0.048
	15	0.124	0.185	-0.038	0.016	0.073	0.162	0.057	0.018	0.016	0.057	0.049
	16	0.126	0.189	-0.039	0.016	0.075	0.165	0.058	0.018	0.016	0.058	0.050
	17	0.127	0.190	-0.039	0.016	0.075	0.166	0.058	0.018	0.016	0.058	0.050
	18	0.124	0.186	-0.038	0.016	0.073	0.162	0.057	0.018	0.016	0.057	0.049
	19	0.126	0.188	-0.039	0.016	0.074	0.164	0.057	0.018	0.016	0.057	0.050
	20	0.126	0.189	-0.039	0.016	0.074	0.165	0.058	0.018	0.016	0.058	0.050
	21	0.127	0.189	-0.039	0.016	0.075	0.166	0.058	0.018	0.016	0.058	0.050
	22	0.126	0.188	-0.039	0.016	0.074	0.164	0.057	0.018	0.016	0.057	0.049
	23	0.124	0.186	-0.038	0.016	0.073	0.162	0.057	0.018	0.016	0.057	0.049
	24	0.125	0.187	-0.038	0.016	0.074	0.164	0.057	0.018	0.016	0.057	0.049

Table 7 – Reactive power load at different buses on the typical spring day

		Bus										
		N2	N3	N4	N5	N6	N9	N10	N11	N12	N13	N14
Hour	1	0.206	0.894	0.454	0.072	0.106	0.280	0.085	0.033	0.058	0.128	0.141
	2	0.209	0.907	0.460	0.073	0.108	0.284	0.087	0.034	0.059	0.130	0.143
	3	0.202	0.875	0.444	0.071	0.104	0.274	0.084	0.033	0.057	0.125	0.138
	4	0.200	0.870	0.441	0.070	0.103	0.272	0.083	0.032	0.056	0.125	0.138
	5	0.189	0.822	0.417	0.066	0.098	0.257	0.079	0.031	0.053	0.118	0.130
	6	0.180	0.781	0.396	0.063	0.093	0.245	0.075	0.029	0.051	0.112	0.124
	7	0.176	0.764	0.388	0.062	0.091	0.239	0.073	0.028	0.049	0.110	0.121
	8	0.171	0.741	0.376	0.060	0.088	0.232	0.071	0.028	0.048	0.106	0.117
	9	0.171	0.744	0.377	0.060	0.088	0.233	0.071	0.028	0.048	0.107	0.118
	10	0.171	0.740	0.376	0.060	0.088	0.232	0.071	0.028	0.048	0.106	0.117
	11	0.174	0.753	0.382	0.061	0.090	0.236	0.072	0.028	0.049	0.108	0.119
	12	0.178	0.771	0.391	0.062	0.092	0.241	0.074	0.029	0.050	0.110	0.122
	13	0.188	0.818	0.415	0.066	0.097	0.256	0.078	0.030	0.053	0.117	0.129
	14	0.195	0.846	0.429	0.068	0.101	0.265	0.081	0.031	0.055	0.121	0.134
	15	0.204	0.887	0.450	0.072	0.105	0.278	0.085	0.033	0.057	0.127	0.140
	16	0.210	0.911	0.462	0.074	0.108	0.285	0.087	0.034	0.059	0.131	0.144
	17	0.212	0.920	0.467	0.074	0.109	0.288	0.088	0.034	0.060	0.132	0.145
	18	0.217	0.942	0.478	0.076	0.112	0.295	0.090	0.035	0.061	0.135	0.149
	19	0.214	0.927	0.470	0.075	0.110	0.290	0.089	0.034	0.060	0.133	0.147
	20	0.216	0.939	0.476	0.076	0.112	0.294	0.090	0.035	0.061	0.135	0.149
	21	0.213	0.926	0.470	0.075	0.110	0.290	0.088	0.034	0.060	0.133	0.146
	22	0.214	0.927	0.471	0.075	0.110	0.290	0.089	0.034	0.060	0.133	0.147
	23	0.211	0.916	0.465	0.074	0.109	0.287	0.088	0.034	0.059	0.131	0.145
	24	0.207	0.900	0.456	0.073	0.107	0.282	0.086	0.033	0.058	0.129	0.142

Table 8 – Active power load at different buses on the typical summer day

		Bus										
		N2	N3	N4	N5	N6	N9	N10	N11	N12	N13	N14
Hour	1	0.121	0.180	-0.037	0.015	0.071	0.158	0.055	0.017	0.015	0.055	0.047
	2	0.122	0.183	-0.038	0.015	0.072	0.160	0.056	0.017	0.015	0.056	0.048
	3	0.118	0.176	-0.036	0.015	0.070	0.154	0.054	0.017	0.015	0.054	0.046
	4	0.117	0.175	-0.036	0.015	0.069	0.153	0.054	0.017	0.015	0.054	0.046
	5	0.111	0.166	-0.034	0.014	0.065	0.145	0.051	0.016	0.014	0.051	0.044
	6	0.105	0.158	-0.032	0.013	0.062	0.138	0.048	0.015	0.013	0.048	0.041
	7	0.103	0.154	-0.032	0.013	0.061	0.135	0.047	0.015	0.013	0.047	0.041
	8	0.100	0.150	-0.031	0.013	0.059	0.131	0.046	0.014	0.013	0.046	0.039
	9	0.100	0.150	-0.031	0.013	0.059	0.131	0.046	0.014	0.013	0.046	0.039
	10	0.100	0.149	-0.031	0.013	0.059	0.130	0.046	0.014	0.013	0.046	0.039
	11	0.102	0.152	-0.031	0.013	0.060	0.133	0.046	0.014	0.013	0.046	0.040
	12	0.104	0.155	-0.032	0.013	0.061	0.136	0.047	0.015	0.013	0.047	0.041
	13	0.110	0.165	-0.034	0.014	0.065	0.144	0.050	0.016	0.014	0.050	0.043
	14	0.114	0.171	-0.035	0.014	0.067	0.149	0.052	0.016	0.014	0.052	0.045
	15	0.120	0.179	-0.037	0.015	0.071	0.156	0.055	0.017	0.015	0.055	0.047
	16	0.123	0.184	-0.038	0.015	0.073	0.161	0.056	0.017	0.015	0.056	0.048
	17	0.124	0.186	-0.038	0.016	0.073	0.162	0.057	0.018	0.016	0.057	0.049
	18	0.127	0.190	-0.039	0.016	0.075	0.166	0.058	0.018	0.016	0.058	0.050
	19	0.125	0.187	-0.038	0.016	0.074	0.163	0.057	0.018	0.016	0.057	0.049
	20	0.127	0.189	-0.039	0.016	0.075	0.165	0.058	0.018	0.016	0.058	0.050
	21	0.125	0.187	-0.038	0.016	0.074	0.163	0.057	0.018	0.016	0.057	0.049
	22	0.125	0.187	-0.038	0.016	0.074	0.163	0.057	0.018	0.016	0.057	0.049
	23	0.123	0.185	-0.038	0.016	0.073	0.161	0.056	0.018	0.016	0.056	0.049
	24	0.121	0.181	-0.037	0.015	0.072	0.159	0.055	0.017	0.015	0.055	0.048

Table 9 – Reactive power load at different buses on the typical summer day

		Bus										
		N2	N3	N4	N5	N6	N9	N10	N11	N12	N13	N14
Hour	1	0.213	0.924	0.469	0.075	0.110	0.289	0.088	0.034	0.060	0.132	0.146
	2	0.210	0.911	0.462	0.073	0.108	0.285	0.087	0.034	0.059	0.131	0.144
	3	0.209	0.907	0.460	0.073	0.108	0.284	0.087	0.034	0.059	0.130	0.144
	4	0.202	0.878	0.445	0.071	0.104	0.275	0.084	0.033	0.057	0.126	0.139
	5	0.193	0.837	0.425	0.068	0.100	0.262	0.080	0.031	0.054	0.120	0.132
	6	0.181	0.787	0.399	0.064	0.094	0.246	0.075	0.029	0.051	0.113	0.124
	7	0.180	0.780	0.396	0.063	0.093	0.244	0.075	0.029	0.051	0.112	0.123
	8	0.178	0.774	0.393	0.062	0.092	0.243	0.074	0.029	0.050	0.111	0.122
	9	0.177	0.769	0.390	0.062	0.091	0.241	0.073	0.029	0.050	0.110	0.122
	10	0.178	0.771	0.391	0.062	0.092	0.241	0.074	0.029	0.050	0.110	0.122
	11	0.182	0.788	0.400	0.064	0.094	0.247	0.075	0.029	0.051	0.113	0.125
	12	0.192	0.833	0.423	0.067	0.099	0.261	0.080	0.031	0.054	0.119	0.132
	13	0.203	0.879	0.446	0.071	0.105	0.275	0.084	0.033	0.057	0.126	0.139
	14	0.203	0.881	0.447	0.071	0.105	0.276	0.084	0.033	0.057	0.126	0.139
	15	0.203	0.881	0.447	0.071	0.105	0.276	0.084	0.033	0.057	0.126	0.139
	16	0.213	0.923	0.468	0.074	0.110	0.289	0.088	0.034	0.060	0.132	0.146
	17	0.212	0.921	0.467	0.074	0.110	0.288	0.088	0.034	0.060	0.132	0.146
	18	0.210	0.913	0.463	0.074	0.109	0.286	0.087	0.034	0.059	0.131	0.144
	19	0.213	0.926	0.470	0.075	0.110	0.290	0.088	0.034	0.060	0.133	0.146
	20	0.212	0.921	0.467	0.074	0.109	0.288	0.088	0.034	0.060	0.132	0.146
	21	0.211	0.915	0.464	0.074	0.109	0.287	0.087	0.034	0.059	0.131	0.145
	22	0.215	0.932	0.473	0.075	0.111	0.292	0.089	0.035	0.060	0.134	0.147
	23	0.217	0.942	0.478	0.076	0.112	0.295	0.090	0.035	0.061	0.135	0.149
	24	0.215	0.931	0.473	0.075	0.111	0.292	0.089	0.035	0.060	0.133	0.147

Table 10 – Active power load at different buses on the typical fall day

		Bus										
		N2	N3	N4	N5	N6	N9	N10	N11	N12	N13	N14
Hour	1	0.125	0.186	-0.038	0.016	0.074	0.163	0.057	0.018	0.016	0.057	0.049
	2	0.123	0.184	-0.038	0.015	0.073	0.161	0.056	0.017	0.015	0.056	0.048
	3	0.122	0.183	-0.038	0.015	0.072	0.160	0.056	0.017	0.015	0.056	0.048
	4	0.118	0.177	-0.036	0.015	0.070	0.155	0.054	0.017	0.015	0.054	0.047
	5	0.113	0.169	-0.035	0.014	0.067	0.148	0.052	0.016	0.014	0.052	0.044
	6	0.106	0.159	-0.033	0.013	0.063	0.139	0.048	0.015	0.013	0.048	0.042
	7	0.105	0.157	-0.032	0.013	0.062	0.138	0.048	0.015	0.013	0.048	0.041
	8	0.104	0.156	-0.032	0.013	0.062	0.136	0.048	0.015	0.013	0.048	0.041
	9	0.104	0.155	-0.032	0.013	0.061	0.135	0.047	0.015	0.013	0.047	0.041
	10	0.104	0.155	-0.032	0.013	0.061	0.136	0.047	0.015	0.013	0.047	0.041
	11	0.106	0.159	-0.033	0.013	0.063	0.139	0.049	0.015	0.013	0.049	0.042
	12	0.112	0.168	-0.034	0.014	0.066	0.147	0.051	0.016	0.014	0.051	0.044
	13	0.119	0.177	-0.036	0.015	0.070	0.155	0.054	0.017	0.015	0.054	0.047
	14	0.119	0.178	-0.036	0.015	0.070	0.155	0.054	0.017	0.015	0.054	0.047
	15	0.119	0.178	-0.036	0.015	0.070	0.155	0.054	0.017	0.015	0.054	0.047
	16	0.124	0.186	-0.038	0.016	0.073	0.163	0.057	0.018	0.016	0.057	0.049
	17	0.124	0.186	-0.038	0.016	0.073	0.162	0.057	0.018	0.016	0.057	0.049
	18	0.123	0.184	-0.038	0.016	0.073	0.161	0.056	0.017	0.016	0.056	0.048
	19	0.125	0.187	-0.038	0.016	0.074	0.163	0.057	0.018	0.016	0.057	0.049
	20	0.124	0.186	-0.038	0.016	0.073	0.162	0.057	0.018	0.016	0.057	0.049
	21	0.123	0.185	-0.038	0.016	0.073	0.161	0.056	0.017	0.016	0.056	0.049
	22	0.126	0.188	-0.039	0.016	0.074	0.164	0.057	0.018	0.016	0.057	0.049
	23	0.127	0.190	-0.039	0.016	0.075	0.166	0.058	0.018	0.016	0.058	0.050
	24	0.126	0.188	-0.039	0.016	0.074	0.164	0.057	0.018	0.016	0.057	0.049

Table 11 – Reactive power load at different buses on the typical fall day